



**EFOMP**

EUROPEAN FEDERATION OF ORGANISATIONS FOR MEDICAL PHYSICS

# QUALITY CONTROL OF DYNAMIC X-RAY IMAGING SYSTEMS

**EFOMP PROTOCOL**

VERSION 01. 2024

This page intentionally left blank.

---

## Preface

This document was developed by an EFOMP Working Group with the aim of providing guidance on Acceptance, Commissioning and Constancy performance testing over the life of an x-ray imaging system. The main motivation for this document is to provide Medical Physics Experts (MPE) with unified guidance across Europe on the assessment of dynamic x-ray imaging systems, in an area that currently lacks such advice. Current testing practice is quite disparate, with specific and varied performance criteria being applied from country to country. It can be difficult for manufacturers to meet all of these different requirements and the introduction of a standardised protocol should simplify the situation, ensuring a consistent and comprehensive set of tests.

Image quality assessment of these systems has always been a challenge, given the dynamic nature of the images and the fact that a visual evaluation often had to be performed 'on the spot' by the MPE. There have been a number of developments in the area of image quality assessment using computational methods and a further aim was to provide information on this topic.

## Scope

This document provides guidance for testing dynamic x-ray systems. We will use the term 'dynamic x-ray imaging system' as a blanket term, covering simple mobile fluoroscopy to complex angiography devices. Not covered is the testing of cone beam computed tomography (CBCT) modes also referred to as 3D rotational angiography (3DRA) imaging. In these modes, the x-ray tube/detector assembly is rotated by at least 200° around the patient as a number of low dose projection images are acquired. These are then reconstructed to generate a volumetric dataset. Clinical applications include planning in stereotactic radio-surgery and angiography examinations such as imaging of aneurysms in neuroradiology and the evaluation of stent placement (Doerfler et al., 2015; Fahrig et al., 2021). Guidance on testing these systems is available in a separate EFOMP protocol (de las Heras Gala et al., 2017).

## Working Group

### Members

---

**Annalisa Trianni** (Italy)  
**Andy Rogers** (UK)  
**Marco Bertolini** (Italy)  
**Hilde Bosmans** (Belgium)  
**Nicholas Marshall** (Belgium)  
**Nicoletta Paruccini** (Italy)  
**Michael Sandborg** (Sweden)  
**Alexander Schegerer** (Switzerland)  
**Lucie Sukupova** (Czech Republic)  
**Diego Trevisan** (Italy)

### EFOMP Scientific Committee chairpersons

---

**Yolanda Prezado** (Spain)  
**Brendan McClean** (Ireland)  
**Eeva Boman** (Finland)

---

**Consultants:**

**Steve Balter** (US)  
**Jérémie Dabin** (Belgium)  
**Lynn Gaynor** (Ireland)  
**Jan Jans** (The Netherlands)  
**Shahed Khan** (UK)  
**Markus Lendl** (Germany)  
**Francoise Malchair** (Belgium)  
**Despina Papadopoulou** (Greece)  
**Kevin Wunderle** (US)

---

**Observers:**

**Carri Borrás** (US)  
**Richard Elek** (Hungary)  
**Pei-Jan Paul Lin** (US)  
**Desislava Kostova-Lefterova** (Bulgaria)  
**Ivan Lasic** (Bosnia and Herzegovina)  
**Sabina Strocchi** (Italy)  
**Giovanna Venturi** (Italy)  
**Raffaella Villa** (Italy)

# TABLE OF CONTENTS

<b>SECTION A - GENERAL BACKGROUND</b>	10
A.1. DYNAMIC X-RAY IMAGING SYSTEMS	10
A.2. TESTS AND CRITERIA	10
A.2.1 Tests	10
A.2.2 Criteria	12
A.3. MEDICAL PHYSICS EXPERT ROLE AND RESPONSIBILITIES	12
A.4. INSTRUMENTS	13
A.5. PROTOCOL OVERVIEW	13
A.5.1 Mechanical and geometrical parameters	15
A.5.2 X-ray tube and generator	15
A.5.3 Automatic Exposure Control (AEC)	15
A.5.4 Dose indicators	15
A.5.5 Skin Dose Map	16
A.5.6 Detector	17
A.5.7 Image Quality	19
A.6. SAFETY	28
A.7. OTHER GUIDANCE	29
<b>SECTION B - PROTOCOL</b>	30
B.1. MECHANICAL AND GEOMETRICAL PARAMETERS	30
B.1.1 Determination of source location and minimum source – skin distance	30
B.1.2 Minimum field size	30
B.1.3 Beam alignment	31
B.1.4 Correspondence between X-ray field and effective image receptor size	32
B.1.5 Verification of displayed distances	33
B.2. X-RAY TUBE AND GENERATOR	33
B.2.1 Tube voltage accuracy	33
B.2.2 Minimum HVL/filtration evaluation	34
B.2.3 Half value layer (HVL) evaluation for clinical spectra	35
B.2.4 Normalised air kerma	36
B.2.5 Leakage radiation	37
B.3. AUTOMATIC EXPOSURE CONTROL	37
B.3.1 AEC function	37
B.3.2 Comprehensive evaluation of AEC	39
B.4. DOSE INDICATORS	40
B.4.1 Air-kerma – Area product and rate display accuracy	40
B.4.2 Manufacturer specified Air-kerma rates	42
B.4.3 Measurement of table and mattress attenuation	42
B.4.4 Limiting Air Kerma Rate	43
B.5. SKIN DOSE MAPS	44
B.5.1 Skin dose map – Acceptance	44
B.5.2 Skin dose map – Commissioning	44
B.6. DETECTOR	45
B.6.1 Response Function	45
B.6.2 Detector presampling Modulation Transfer Function (MTF)	47

---

B.6.3	Image detector Brightness Non Uniformity (BNU)	48
B.6.4	Variance and SNR Image	49
B.6.5	Noise Decomposition using Variance	49
B.6.6	Noise Power Spectrum (NPS)	50
B.7.	IMAGE QUALITY	51
B.7.1	Signal-to-noise ratio rate, SNR <sup>2</sup> rate	51
B.7.2	Threshold-contrast detail detectability (TCDD) - Statistical method	52
B.7.3	Threshold-contrast detail detectability (TCDD) - CHO readout	54
B.7.4	Threshold-contrast detail detectability (TCDD) - Human visual scoring	55
B.7.5	Limiting spatial resolution (LSR)	56
<b>SECTION C - REFERENCES</b>		57
<b>SECTION D - APPENDICES</b>		63
D.1.	Appendix 1. Radiation Safety Procedures	63
D.2.	Appendix 2. Phantoms	65

## LIST OF ABBREVIATIONS

AAPM	American Association of Physicist in Medicine
AEC	Automatic Exposure Control
AIFM	Associazione Italiana di Fisica Medica - Italian Association of Physicist in Medicine
AP	AnteroPosterior
BNU	Brightness Uniformity
BSS	European Basic Safety Standards
CBCT	Cone Beam Computed Tomography
CDDISC	Contrast-Detail phantom with cylindrical holes
CDRAD	Contrast-Detail phantom for Radiography
CTSM	Threshold Contrast for the Statistical Method
CTPV	Threshold Contrast for the Statistical Method in terms of Pixel Values
CHO	Channelized Hotelling Observer
CT	Computed Tomography
CV	Coefficient of Variation
DMS	Dose Management System
DQE	Detective Quantum Efficiency
DICOM	Digital Imaging and Communication in Medicine
EFOMP	European Federation of Organizations For Medical Physics
ESAKR	Entrance Surface Air Kerma Rate
EU	European Union
FN	False Negative
FNF	False Negative Fraction
FoV	Field Of View
FP	False Positive
FPF	False Positive Fraction
FPD	Flat Panel Detector
HVL	Half Value Layer
IAEA	International Atomic Energy Agency
IBSS	International Basic Safety Standards
ICRU	International Commission on Radiation Units and measurements
IEC	International Electrotechnical Commission
IPEM	Institute of Physics and Engineering in Medicine
IR-IAK	Image Receptor Incident Air Kerma
KAP	Air Kerma Area Product
Ka,r	Reference Air Kerma
LCDD	Low-Contrast Detail Detectability
LSR	Limiting Spatial Resolution
MAFC	Multiple Alternative Forced Choice
MO	Model Observer
MPE	Medical Physics Expert
MPV	Mean Pixel Value
MTF	Modulation Transfer Function
NEMA	National Electrical Manufacturers Association
NPS	Noise Power Spectrum
PERP	Patient Entrance Reference Point
P <sub>KA</sub>	Air Kerma Area Product



$P(t)_{KA}$	Air Kerma Area Product Rate
PSD	Peak Skin Dose
PMMA	Polymethyl Methacrylate
PTB	Physikalisch Technische Bundesanstalt - German National Metrology Institute
PV	Pixel Value
QA	Quality Assurance
QC	Quality Control
RDSR	Radiation Dose Structured Report
ROI	Region Of Interest
ROC	Receiver Operating Characteristic
SDM	Skin Dose Mapping
SDNR	Signal Difference-to-Noise Ratio
SI	International System of Units
SID	Source to Image Detector Distance
SM	Statistical Method
SOD	Source to Object Distance
SNR	Signal-to-Noise Ratio
TCD	Threshold Contrast Detection
TCDD	Threshold Contrast Detail Detectability
TIQ	Technical Image Quality
TN	True Negative
TNF	True Negative Fraction
TO	Test Object
TP	True Positive
TPF	True Positive Fraction
VERIDIC	Validation and Estimation of Radiation Skin Dose in Interventional Cardiology
VGC	Visual Grading Characteristics
VGR	Visual Grading Regression
WHO	World Health Organization
XRII	X-Ray Image Intensifier

## SECTION A - GENERAL BACKGROUND

### A.1. DYNAMIC X-RAY IMAGING SYSTEMS

The dynamic x-ray imaging systems covered by this protocol generate a temporal sequence of images that may or may not be stored by the system. The term 'dynamic x-ray imaging system' covers a wide range of devices, and these can be broadly grouped as follows:

1. Complex C-arm systems used for the purpose of diagnosis and treatment/intervention. A broad range of applications is covered including abdominal radiology, cardiology, neuroradiology and peripheral angiography
2. Bi-plane devices, generally used for cardiac and neuroradiology examinations.
3. Radiography/fluoroscopy systems, typically with an overcoatch x-ray tube and tilting table, generally used for gastrointestinal examinations and contrast examinations in the radiology department
4. Mobile C-arm systems, for example used in operating theatres
5. Mini C-arms, used for the imaging of extremities
6. Radiography x-ray systems, with a fluoroscopy mode designated for patient positioning

The above is not an exclusive list and the protocol should be applied to all dynamic x-ray devices used at the clinical site.

Two main modes are used in dynamic x-ray systems. The term 'fluoroscopy' is applied to the mode where a sequence of images is generated and used as part of the examination. These images are not generally stored. Once the fluoroscopy sequence is stopped by the operator then the last frame or weighted combination of the last few frames is held on the display, as a 'last image hold' image. Many systems also allow images from the most recently performed fluoroscopy sequence to be stored or archived as an image sequence, using a function such as 'fluoroscopy store'. In addition to performing fluoroscopy, systems can acquire images that are stored as 'acquisition' images (sometimes called cineangiography). This can be single shot, or at some frame rate, typically ranging from 1 to 4 frame/s for radiology/angiography applications up to 10 or 15 frame/s even or higher for cardiac acquisitions.

### A.2. TESTS AND CRITERIA

#### A.2.1 Tests

The testing procedures applied by the MPE vary in scope and depth depending on the type and intention of the test and the equipment being evaluated. Before testing a system, the main clinical applications should be established along with the most commonly used fluoroscopy and acquisition modes. These will be the modes evaluated in the Constancy testing of the device and depend on the Acceptance and Commissioning testing. Tests should be relevant to clinical practice on the unit and should be able to uncover changes that can potentially affect the clinical performance of the system. Dose Management Systems (DMS) can also greatly help in establishing system usage and which fluoroscopy and acquisition modes are commonly used. This would aid the MPE to ensure the relevance of the tests. Simplified tests can be carried out by technologists/radiographers at frequencies determined by national guidance or recommended by the MPE.

Definitions of the various test types and how they fit in with the lifecycle of the equipment are largely consistent in the literature although some variations are seen (IPEM, 2005; European Commission, 2012; Dance et al., 2014; Jones et al., 2014). Note that there is likely to be some variation in test definitions and the person assigned with the duty of performing tests for the different national protocols already in place; these must be taken into consideration when applying this protocol. Focus in this protocol is on Acceptance, Commissioning and Constancy QC tests.

### **Acceptance Tests**

Acceptance tests ensure that new or replacement equipment complies with the specifications made at the tendering stage and performance meets that specified by the vendor for the system. When verifying aspects of system performance (including radiation safety assessments), measurements may have to be made using the methods specified by the equipment manufacturer/vendor. This will normally involve representatives of the vendor/installer and the MPE. These tests are performed to ensure that the system complies with acceptability requirements that may be in place at a regulatory (national) level and are required before the first use of the system on a patient. Acceptance tests are also required when new or replacement components or the installation/upgrade of software leads to a clinically important change in performance.

### **Commissioning Tests**

Commissioning tests follow Acceptance testing and clinical protocol development. They characterise the dose and image quality performance of the system. Clinical protocol development will involve inspection and possible adjustment of the default clinical protocols, pre-installed on the system, to meet the clinical requirements, and will be done in conjunction with the radiological practitioner, x-ray technologists/radiographer, the MPE and the installer's applications specialist. This can be an extended process that happens over a few weeks or months. Commissioning is the first stage in the optimisation process. The performance must be achieved whilst staying within regulatory limits that are in place.

It can be very helpful to record the values of various fluoroscopy and acquisition settings that influence dose and image quality delivered by a given imaging mode/protocol. This can help to avoid over testing by identifying modes that have different names but the same/similar underlying dose and image quality characteristics. Even if this can only be done to a limited extent, this will help the MPE's understanding of the system and improve the relevance of the tests.

A (sub)set of Commissioning tests should be performed after the Acceptance test of newly installed components, to establish whether or not new baselines for longitudinal testing are required.

If, subsequent to initial Commissioning, a change is made to an imaging protocol that substantially affects dose and image quality, then appropriate re-Commissioning should be undertaken and any affected baselines should be adjusted to reflect the results for the new protocols.

### **Constancy Tests**

These tests have variously been called 'quality control' tests or 'routine' tests.

They are a set of tests (normally a subset of the full Acceptance and Commissioning tests) performed at regular intervals, with the aim of confirming that selected performance parameters remain within their respective baseline values. Any changes in performance should be documented, and any corrective action should be reported to the department.

At Constancy testing the tester should record the parameter settings for the protocols as defined by the MPE during Commissioning. These can then be compared to values at previous visits and to those at Commissioning. After testing, it is important to ensure that the system is left in/returned to its standard clinical configuration. The x-ray tube port should be clear of any (metal) filters that were used for the tests.

### **User Quality Control Mode**

Tracking or auditing of protocol parameters is made much easier if the User Quality Control Mode, as described in NEMA standard (NEMA, 2018), is implemented on the system. This Standard enables the settings of all imaging protocols and modes to be exported to a spreadsheet for analysis. Changes in parameter settings are indicated, making the tracking of changes in protocols straightforward. When investigating changes in system performance, this can be separated into the identification of programmed (intentionally or unintentionally) changes in protocol settings (software) and actual changes in component (hardware) performance. Implementation of the NEMA User Quality Control Mode has additional advantages and it is hoped that more systems will include this. Manual control of the x-ray factors is possible, which makes tube and generator

testing and calibration of the kerma-area product ( $P_{KA}$ ) meter more straightforward and should improve reproducibility. Manual control of x-ray factors in conjunction with access to 'For Processing' images will allow the explicit assessment of x-ray detector performance. While detailed evaluation of the x-ray detector is not necessarily done at every routine visit, explicit testing of x-ray tube and detector is very helpful when trying to isolate or troubleshoot problems reported about the system in general by the operators.

### Daily Quality Control

As part of a comprehensive quality assurance system, it is important for the users (normally radiographers/technologists) to undertake a set of quick tests prior to first use of the day. The rationale for undertaking these tests, which take only a few minutes, is to ensure that the equipment is working before the first patient is prepped, i.e., to exclude the possibility of the patient being prepped unnecessarily. A list of suggested tests is:

1. Ensure all powered movements of the gantry work properly (where applicable)
2. Ensure that the table and detector powered movements work properly (where applicable)
3. Ensure that radiation can be emitted, and different fluoroscopy modes/magnifications can be selected (as applicable)
4. Ensure the collimators (and wedges where applicable) drive in and out
5. Disable x-rays then perform World Health Organisation type checklist tasks (see for example Appendix D.1)

If any of the above tests indicate a unit that is not working as usual, the user should seek advice to ascertain whether the unit may be used on patients.

### A.2.2 Criteria

A test is applied, and the results compared against Pass/Fail Criteria when available. These criteria can take different forms and are specified in the description of each test.

- Action level: corrective action is required if the value of the test parameter is out of the defined range for the test.
- Baseline value: a value of a parameter established in a Commissioning test and used for comparison in constancy testing. Often the percentage change in the value of the parameter from the baseline value is computed and if a subsequent measurement falls outside of test-specific tolerance levels then some form of corrective action is required.
- Limiting value: the maximum or minimum value of a parameter considered acceptable by either international standards or national regulations.

## A.3. MEDICAL PHYSICS EXPERT ROLE AND RESPONSIBILITIES

It is the responsibility of the Medical Physics Expert to ensure that the frequency and depth of testing is commensurate with the imaging applications undertaken on a particular system.

The goal is not just to apply a set of pass-fail tests and move on to the next system. The MPE should have some knowledge of the imaging tasks undertaken on the system, ensure that relevant Acceptance and Commissioning tests have been carried out and that the system is set up to perform the clinical tasks routinely undertaken on the system. Constancy testing can then take over, ensuring that the system remains within the baselines set at Commissioning. This should involve a regular audit of the system protocols.

Additionally, the duties of the MPE also include equipment specification and evaluation, which are important stages within the Quality Assurance (QA) framework (Dance et al., 2014), however the focus in this protocol is on Acceptance, Commissioning and Constancy tests.

## A.4. INSTRUMENTS

### Calibration

In order to obtain meaningful readings from your instrument you need to understand its response. This can be achieved through testing the instrument yourself under different circumstances or calibrating it for the quantities you intend to measure, e.g. air kerma, kVp, HVL etc. The manufacturer of your instrument should be able to give advice on where you can obtain a calibration certificate if one is not provided at purchase. The calibration is performed against a reference instrument (e.g., an air kerma detector, high voltage divider etc.), which in turn is traceable to a primary standards laboratory, e.g. PTB, Germany. The expanded uncertainty for the calibration factor is stated as the standard uncertainty multiplied with a coverage factor,  $k=2$ , which for a normal distribution corresponds to a coverage probability of 95% (true value lies within the coverage interval 95% of the time). If your instrument has been serviced, it is wise to have it calibrated or at least compare its reading with another calibrated instrument to make sure it is working properly.

### Accuracy and Precision

You also need to check the specification of your instrument with regards to the accuracy of any derived quantity so that you can draw the correct conclusion with regards to any measured change in the quantity of interest. For example, your multimeter estimates HVL with an uncertainty ( $k=2$ ) of  $\pm 10\%$  or  $\pm 0.2$  mm Al. When applying uncertainties to the limiting or baseline values against which the measurement will be compared, the MPE may wish to distinguish between performance metrics such as kV and limiting values set by standards, e.g. maximum air kerma rate. In the latter you may wish to subtract your instrument's uncertainty from the limiting value to ensure a high probability of conformance.

It is also useful to know the precise location of the instrument's reference point. The instrument specification is also useful as it will mention the range of, for example, air kerma rates when you can expect reliable readings. Measurement outside this specified range may reduce the precision. Ensure that you understand your dosimeter's response to backscattered radiation: add a back-scatter fraction when either adding or removing such effects from measured values, as appropriate.

### Energy dependence

Some instruments may have a significant so-called energy-dependence and therefore the calibration factor for the reference beam quality, e.g. RQR5 (70 kV, HVL=2.58 mmAl) at the calibration facility, may be different from the factor for the beam qualities used in your hospital. This can be an issue with air kerma area ion chambers ( $P_{KA}$  meters) that contain thin metallic conductive layers when you measure  $P_{KA}$  for an imaging system that uses varying filtration and tube voltages. Therefore, check your instruments' response to different beam qualities and, if possible, use instruments with minimal or at least known energy dependence. Useful information regarding dosimetry and use of dosimeters is given in various IAEA documents including IAEA TRS457 (IAEA 2007).

## A.5. PROTOCOL OVERVIEW

This protocol describes an extensive array of tests (Table 1), methods and test frequencies that can be applied by MPE to assess the performance of dynamic x-ray imaging systems used at a medical facility.

Tests are divided into 7 groups covering different aspects of the equipment:

- 1) Mechanical and geometrical
- 2) X-ray tube
- 3) Automatic Exposure Control
- 4) Dose indicators
- 5) Skin Dose Map

- 6) Detector
- 7) Image quality

In the following paragraphs the rationale and general introduction to the different tests are described where it is felt that some guidance is required. Not every test described in Section B [the protocol] has a corresponding description in Section A.

*Table 1 Tests and test frequencies reported in section B of the present document. The numbers in the Test column indicate the subsection of the protocol and the specific test, respectively. X = test to be performed.*

Test	Acceptance	Commissioning	Constancy
<b>B.1 MECHANICAL AND GEOMETRICAL PARAMETERS</b>			
B.1.1 Determination of source location and minimum source - skin distance	X		
B.1.2 Minimum field size	X		
B.1.3 Beam alignment	X		
B.1.4 Correspondence between X-ray field and effective image receptor size	X		X
B.1.5 Verification of displayed distances	X		
<b>B.2 X-RAY TUBE AND GENERATOR</b>			
B.2.1 Tube voltage accuracy	X		X
B.2.2 Minimum HVL/filtration evaluation	X		
B.2.3 Half value layer (HVL) evaluation for clinical spectra	X	X	
B.2.4 Normalised air kerma and air kerma rate			X
B.2.5 Leakage radiation	X		
<b>B.3 AUTOMATIC EXPOSURE CONTROL</b>			
B.3.1 AEC function	X		
B.3.2 Comprehensive evaluation of the functionality of AEC		X	X
<b>B.4 DOSE INDICATORS</b>			
B.4.1 Air-kerma - Area product and rate display accuracy	X		X
B.4.2 Manufacturer specified Air-kerma rates	X		X
B.4.3 Measurement of table and mattress attenuation	X		
B.4.3 Limiting air kerma rate	X		X
<b>B.5 SKIN DOSE MAPS</b>			
B.5.1 Skin dose map - Acceptance	X		
B.5.2 Skin dose map - Commissioning			X
<b>B.6 DETECTOR</b>			
B.6.1 Response Function			X
B.6.2 Detector presampling Modulation Transfer Function (MTF)	X		
B.6.3 Image detector Brightness Non Uniformity (BNU)		X	X
B.6.4 Variance and SNR Image			X
B.6.5 Noise Decomposition using Variance		X	X
B.6.6 Noise Power Spectrum (NPS)		X	X
<b>B.7. IMAGE QUALITY</b>			
B.7.1 Signal-to-noise ratio rate, SNR <sub>rate</sub>		X	X
B.7.2 Threshold-contrast detail detectability (TCDD) - Statistical method		X	X
B.7.3 Threshold-contrast detail detectability (TCDD) - CHO method		X	X
B.7.4 Threshold-contrast detail detectability (TCDD) - Human visual scoring		X	X
B.7.5 Limiting spatial resolution (LSR)		X	X

### A.5.1 Mechanical and geometrical parameters

An imaging system requires mechanical stability in order to achieve the intended operational performance. An assessment of mechanical and geometrical performance assures the MPE that the system is properly set up.

### A.5.2 X-ray tube and generator

The x-ray tube and generator are the first components in the production of known and stable X-ray beam. Therefore, characterization of the performance is a crucial element of the overall quality control programme. Moreover, tube and generator performance influences patient dose and image quality.

### A.5.3 Automatic Exposure Control (AEC)

The AEC system of the imaging equipment ideally maintains image quality or dose based upon the detector signal and potentially reduces patient skin entrance dose to a minimum regardless of selected protocol parameters and thickness as well as composition of the part of the patient's body that is being imaged. The AEC system may automatically control many imaging parameters (e.g., focal spot exposure time, tube voltage, tube current, filter, or/and pulse width), simultaneously, based upon the detector signal. Some recent units may adjust the detector dose as a function of attenuator thickness.

Given the multitude of protocols available on modern systems, a systematic method should be used to determine the protocols and modes to be included in the testing regime. This will require liaison with the clinical users to ascertain the primary clinical functions of the system, and the protocols and modes routinely used for this work – the testing regime should focus on these protocols. It is also important to test variations due to FoV changes and dose levels.

Abrupt changes in radiographic parameters due to thickness increments can happen and should be properly captured. Information on the AEC curve (see an example in Figure 1) can be obtained from the manufacturer prior to installation to establish which thicknesses should be used when characterising the curve.

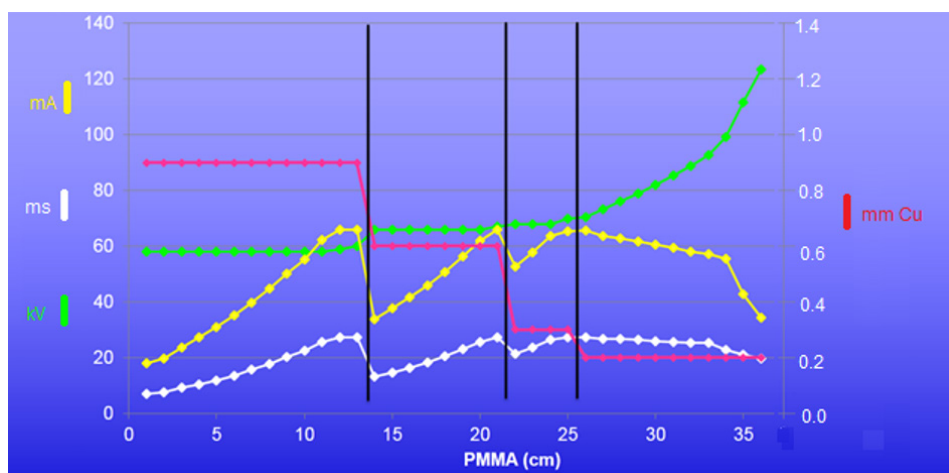


Figure 1: Exposure parameters as function of PMMA thickness. The illustration shows how four parameters vary with increasing PMMA-phantom thickness; green: tube voltage (kV), red: added copper filtration (mm), yellow: tube current (mA) and white: pulse width (ms).

### A.5.4 Dose indicators

The main dose indicators displayed by dynamic x-ray systems are Air Kerma-Area product ( $P_{KA}$ ), and  $P_{KA}$  rate, and Reference Air Kerma ( $K_{a,r}$ ) and  $K_{a,r}$  rate.

The  $P_{KA}$  display is derived either from an ionisation chamber integral to the collimator housing or is calculated by the x-ray unit using the field size and generator settings and can be displayed in many different units.  $P_{KA}$  is an important patient dose metric and therefore must be calibrated.



In interventional radiology or use of mobile c-arms in theatre, patient views may be taken in an anterior-posterior (AP) projection or in a lateral projection – clearly in one case a patient support will be in the beam and in the other no patient support will intercept the beam. The  $P_{KA}$  meter cannot be set-up to reflect both situations at the same time. Therefore, it is advised (AAPM TG190) that an ‘in-air’ calibration is performed for baseline metric determination and Acceptance testing reasons. To supplement this approach, knowledge of the table support and any mattress/pad support attenuation factors will be required to ascertain patient  $P_{KA}$  for projections that intercept the patient support/mattress. However, the MPE may decide to evaluate such systems with the table/mattress in the beam if they feel that this is more appropriate. For fixed fluoroscopy units with an integral undercouch tube the patient support will always intercept the radiation beam and so evaluation should be made with the patient support in situ. Knowledge of the manufacturer’s calibration method will aid the interpretation by the MPE of the results obtained.

The AAPM methodology presented here is not the only method to field calibrate a  $P_{KA}$  meter/calculation and attendant display. The IAEA TRS457 Code of Practice also mentions the tandem  $P_{KA}$  meter approach which is described in detail by Toroi et al (2008) and Malusek et al. (2014) This approach utilises a calibrated  $P_{KA}$  meter to directly compare the field  $P_{KA}$  meter and reference  $P_{KA}$  meter. If the user prefers the ‘tandem’ method, please refer to these references above.

For both approaches one may arrive at an average calibration coefficient across all clinically used beam areas and qualities or calibration curves depending upon beam area and beam quality. Which approach is used is dictated by the requirements locally for patient dosimetry precision (if any) and is beyond the scope of this protocol.

During the testing the displayed  $P(t)_{KA}$  must also be compared with that measured.

It should also be noted that some integral chambers measuring  $P_{KA}$  are not adjustable, nor is the  $P_{KA}$  determined by calculation within the fluoroscopy unit. For these situations it is unlikely that the  $P_{KA}$  relevant to a given procedure is the displayed  $P_{KA}$  and local decisions regarding adjustment must be made. For those  $P_{KA}$  meters that are adjustable, it may be prudent to adjust to have the closest possible agreement (i.e. calibration coefficient closest to 1.0) with the reference  $P_{KA}$  (beam area or tandem method) for the clinical field size and beam quality most often employed.

For constancy testing, any suitable, time-efficient arrangement will suffice.

#### A.5.5 Skin Dose Map

Monitoring the skin dose is an essential step for managing the risk of radiation induced tissue reactions. Due to the variability of the irradiation conditions during interventional procedures, predicting and estimating the distribution (or map) of skin dose and the maximum value (or peak skin dose) is challenging. Skin dose mapping (SDM) software products are available for that purpose.

The skin dose is defined as the absorbed energy to the patient skin. It should not be mistaken for the air kerma at the patient entrance reference point ( $K_{a,r}$ ), the position of which is defined in the manufacturer documentation. Although in some conditions the  $K_{a,r}$  displayed on the angiography unit might be a reasonable approximation of the skin dose, this is usually not the case (among other reasons, because the  $K_{a,r}$  does not take into account the x-ray tube position, the patient anatomy, the backscatter generated from the patient or the table movement). In addition, the skin dose should be reported as a dose to skin tissue while the  $K_{a,r}$  is calibrated in air. This is of limited effect for the beam qualities encountered in interventional procedures.

Some vendor-specific SDM software are integrated in the x-ray units informing the clinician as to the progression of the Peak Skin Dose (PSD) value and location in real time during the procedures. Other SDM applications generate a skin dose map offline, after completion of the procedure. These are either commercial products included in dose management software or stand-alone software. A review of numerous products is available in Malchair et al 2020. There is currently no regulatory requirement for x-ray systems to be equipped with SDM software in Europe as opposed to  $P_{KA}$  or  $K_{a,r}$ . However, the most recent version of IEC 60601-2-43: 2022 introduces the notion of a ‘Dose Map’ integral to the interventional x-ray unit.



Although most SDM software products available in clinics use similar analytical calculation algorithms (Jones, 2011; Bednarek et al; 2011; Bordier et al; 2015; Gardavaud et al, 2018; Habib Geryes et al, 2018), there exist significant differences in the implementation that can lead to discrepancies of several tens of percent in the dose estimates (Dabin, 2021). It is therefore of the utmost importance for the user to have knowledge of the SDM product calculation algorithm and the parameters customizable to the local use.

The dose map calculations, either online or offline, lend themselves to two types of testing.

The first test is analogous to Acceptance testing: it consists of verifying that, for a given set of input parameters (e.g., varying angulations), the SDM product gives results consistent with the manufacturer model. Some manufacturers may provide test procedures that should be followed if available. Otherwise, the user will have to establish their own testing protocol. The user should therefore have a sound knowledge of their SDM product in order to design the test methodology.

The second test is analogous to a Commissioning test and evaluates the agreement between the dose values as reported by the product and the actual PSD to the patient under consideration. The purpose of Commissioning SDM technology is to verify how the displayed values of skin dose relate to real-world patients. Accurate measurements of dose distribution and PSD are challenging and time-consuming. Radiochromic films can be used for assessing both the accuracy of the PSD and the dose map. However, film dosimetry can be subject to considerable uncertainty and demands considerable set-up and readout resources. The calibration for the energy range encountered in interventional procedures is cumbersome, and all elements from the dosimetry system (not only the films, but also the scanner/densitometer) need to be properly characterised. Point-like dosimeters might be a more accessible solution to most users, but they cannot be efficiently used if the position of the PSD is not known in advance (which is often the case on real patients), nor to verify the accuracy of the dose map.

These tests do not need to be performed as part of regular quality control checks unless stipulated by the manufacturer.

In the frame of the European-funded project VERIDIC (Validation and Estimation of Radiation Skin Dose in Interventional Cardiology), up to 10 SDM products were tested on four interventional X-ray systems following a common protocol composed of simple irradiation conditions and one more complex combination closer to clinical conditions (Dabin et. al., 2021). The PSD estimates generally agreed with the measurements within  $\pm 40\%$ . Furthermore, the accuracy of the PSD estimate for lateral irradiations could be very poor (up to 66% underestimation).

Although testing the accuracy of SDM products is challenging and the results should be considered with caution, this should not prevent MPEs from using SDM information in the daily clinical practice, as SDM software tools are still expected to be more efficient than only relying on the conventional dose metrics ( $P_{KA}$  and  $K_{a,r}$ ) as alert levels triggering patient follow-up for skin reaction.

### A.5.6 Detector

This section briefly describes the physical parameters used to characterise an x-ray imaging detector and the steps required for their measurement in the X-ray room. A standard evaluation includes the response function, the pre-sampling modulation transfer function (MTF), the noise power spectrum (NPS) and the detective quantum efficiency (DQE). There is a large body of literature describing the theory (Cunningham, 2000) and measurement (Dobbins et al. 1995; Samei et al., 2006; Dobbins et al., 2006) of these parameters. This can be explicitly for the image detector (IEC, 2008) or for the complete x-ray imaging system (Kyprianou et al., 2005), where aspects such as the focus size influence the system MTF and system DQE. The advantage of these physical characterization measurements is that performance characteristics of the image detector are assessed directly and can be tracked over time. This can be contrasted with a technical image quality measurement such as low contrast detectability, where image detector and x-ray tube performance are combined with many other system aspects including x-ray energy, AEC operating point, recursive temporal filtering and x-ray anti-scatter grid etc. Those unfamiliar with the theory and measurement should review the literature in order to understand the strengths and weaknesses of these methods before attempting measurements.

While it is not practical or even possible to apply the International Electrotechnical Commission (IEC) standard for dynamic imaging systems as a Constancy QC procedure (IEC, 2008), some brief discussion is instructive. The aim of these protocols is to standardise the evaluation of the imaging properties of image detectors, under carefully controlled imaging conditions. The x-ray energy and exposure at the image detector are set precisely in order to achieve this. Furthermore, for dynamic image detectors, the manufacturer will have full control over the many imaging modes available, which in turn will set important factors such as the pixel binning and the image detector gain. The fluoroscopy and acquisition programs on the system will utilise a specific image detector mode, chosen by the manufacturer, that is adapted to that specific clinical imaging program. The difficulty for MPEs responsible for Commissioning and QC tests lies in establishing the image detector modes being set for the tests/evaluation and also in setting these same modes for subsequent QC visits.

Application of these methods hinges upon the availability of images with fixed gain and minimal image processing (just the image detector gain and offset corrections applied, no clinical image processing set). If possible, at the Commissioning stage, the MPE should establish, with the aid of the engineer and/or application specialist, how these images ('For Processing' or equivalent) can be acquired routinely as part of the QC process. This may be via the User QC mode, or an alternative would be to copy a commonly used acquisition program or fluoroscopy mode and set minimal image processing – this would be done with the help of an engineer. An advantage of doing this is that the image detector will be assessed in a gain mode that is relevant to a commonly used imaging mode. A further requirement is that the user has some control over the x-ray parameters so that the energy can be set for the evaluation and the tube load (mAs) adjusted so that the x-ray exposure at the image detector can be varied. The extent of the characterization will depend on access to the different image detector gain modes, the range of FoVs and use of image detector binning, and the number of focus sizes available.

The image detector response function is a crucial measurement from which detector brightness uniformity, polynomial noise decomposition and noise power spectrum can be calculated.

As with all QC measurements, it is important that the same imaging conditions are set each time so that any changes can be isolated i.e., same energy, FoV (image detector binning) and focus. Ideally the same gain mode would be set at each QC visit, as the MPE would then know what magnitude of x-ray exposure to set in order to acquire an image set that gives relevant information on the image detector. A high gain mode with high x-ray exposure would lead to saturation of the image detector, while a low gain and low x-ray exposure could result in images that contain a lot of electronic noise. Neither of these scenarios would give much useful information on how the image detector is performing when used clinically. While MPEs have a reasonable amount of experience applying these methods to mammography and general radiography image detectors, implementing these methods in an efficient and relevant manner for fluoroscopy and angiography systems is a fresh challenge.

The IEC protocol (IEC, 2008) implements a lag effect correction factor that is used to correct the NPS and thus gives a lag-corrected DQE. This is considered outside the scope of this protocol and is therefore not discussed.

Other than for detector characterisation, these metrics could be used for system characterization using a different geometry. Imaging the edge at the patient position on the tabletop, instead of at the detector, will provide a system MTF.

It must be emphasised that although the parameters evaluated in this section have a major influence on the ability of the operator to perform a given imaging task, this is not an 'image quality' section. The MTF and NPS can be used to characterise the sharpness and the noise present in the images however many more parameters will determine the task performance, including the x-ray spectrum, the lag (recursive temporal filtering) and probably the final imaging processing set.

Physical image quality parameters provide insight into the signal to noise ratio transfer of the image detector, which is crucial in determining operator task performance. It is therefore assumed that using the MTF and NPS to track changes in detector or system performance is of value in QC measurements. Given

that the MTF and NPS have been measured, it is possible to calculate the DQE but the limitations of the evaluation must be recognized (i.e. the requirement to evaluate the lag, exact energy and incident air kerma at the detector surface). To track changes in detector performance it is sufficient just to measure/track the MTF and NPS (Mackenzie et al., 2010). The exact measurement conditions for the NPS and MTF must be noted carefully for a given QC visit, especially the applied recursive temporal filtering which can strongly influence the magnitude of noise in the image.

### A.5.7 Image Quality

The images generated by an imaging system are used to perform some specific imaging tasks and must therefore contain sufficient information for the operator to perform the task, within some level of confidence (ICRU Rep. No. 54., 1996). The degree to which an imaging system is delivering relevant and sufficient information to the user is established in a measurement of ‘image quality’. For this protocol, we distinguish between clinical and technical image quality evaluation: both relate to an assessment of the information contained within the images, but clearly have a different scope. This section also gives some background context for the different image quality methods.

#### Clinical image quality

##### Quantitative evaluation of task performance

To illustrate the evaluation of clinical image quality, then consider a classification task, where the observer is shown a set of images, some of which are normal, and some contain pathology. The observer has to assign each image to one of two classes: a normal case (signal absent) or abnormal case (signal present) (Metz, 1986; ‘ICRU Rep. No. 54.’, 1996). Binary classification of images in this way amounts to performing a detection task. In doing this, the observer is assumed to generate some internal response that is related to the presence or absence of the signal of interest; this is termed the ‘decision variable’ and is used to classify each image. The two samples of normal and abnormal images will produce a range of responses in the observer i.e., generate a range of decision variables, as seen in Figure 2. In general, the distributions of decision variables will overlap.

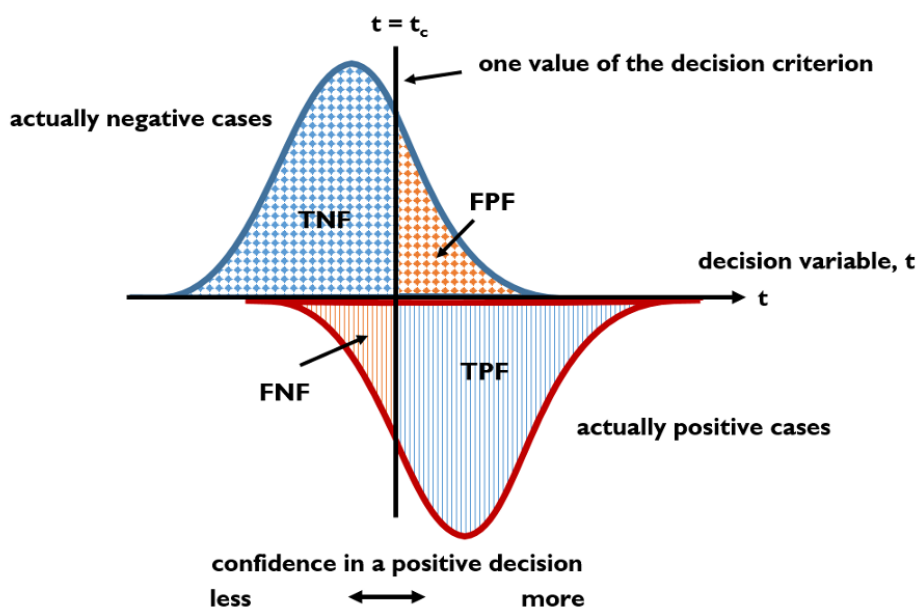


Figure 2. Probability density distributions of a radiologist's confidence in a positive decision for a given diagnostic task, for a set of images with and without pathology. The different shaded regions show the true positive (TP), true-negative (TN), false-positive (FP), false-negative (FN) region. The vertical line  $t$  shows a setting of the decision criterion; this separates ‘negative’ decisions from ‘positive’ decisions.

When making a decision, the observer adopts some value of the decision variable as a decision threshold; decision variables above this threshold are cases considered to be abnormal, while those below are considered normal by the observer. It is clear that unless there is complete separation of the two distributions, there will be instances where cases are declared abnormal when they are actually normal (the false positive fraction (FPF)) and cases said to be normal when in fact they are abnormal (the false negative fraction (FNF)). Correctly identified abnormal cases are given by the true positive fraction (TPF) while those correctly identified as negative are the true negative fraction (TNF), and are synonymous with sensitivity and specificity, respectively. Specifying system performance must be done using at least one (sensitivity, specificity) pair, as just using the TPF does not characterise the system performance with respect to actually negative patients (Metz, 1986). In fact, during the reading study, the observer is asked to give a rating reflecting their confidence that a given case is normal or abnormal. This generates sets of (sensitivity, specificity) pairs which can be plotted to give the receiver operating characteristic (ROC) curve. The different points on the curve are effectively obtained by the observer varying their “decision criterion”. The ROC curve clearly depicts the trade-off between sensitivity and specificity. Depending on the overlap and spread of the distributions, increasing the decision threshold to increase sensitivity generally comes at the expense of more false positive decisions. ROC analysis is often applied to studies involving detection tasks, where a ground truth regarding the presence or absence of a lesion can be established by another means, for example using histopathology of lesions, where cases can be collected and used retrospectively in the ROC study. However, applying this method to angiography or fluoroscopy tasks is particularly challenging. Examinations may, for example, involve detection of some stenosis or bleeding within a vessel, along with an estimation of the severity of the case. Active therapeutic intervention will follow, with the placement of a device such as a stent or balloon. Retrospective use of these image sequences in an ROC study is not possible and hence even quantifying clinical image quality for dynamic imaging exams using standard methods remains a challenge. The enormous range of tasks for which dynamic x-ray imaging systems are used further compounds the problem. In effect, clinical image quality is indirectly measured all the time, during the imaging of patients. Formal quantification of clinical image quality in studies involving fluoroscopy/angiography will only be rarely done but this should not prevent the MPE from discussing the clinician’s impression of image quality when problems arise, reviewing cases together and noting which are considered problematic. The MPE can then take steps to investigate some specific aspects of technical image quality, generally using test objects to identify the point(s) within the imaging chain that are limiting clinical quality.

The following sections describe some of the methods available to MPEs for use in Constancy measurement of technical image quality, along with some historical background information and a word on the strengths and weaknesses of each method.

### **Subjective evaluation using visual grading methods**

The use of image criteria to evaluate the quality of image sequences in image guided interventions is rare, compared to their usage in computed tomography, and projection radiography examinations, which has been formalised in EU publications (Carmichael et al., 1996; Menzel, Schibilla and Teunen, 1999). The lack of published task-specific image criteria for the large number of different procedures performed using dynamic imaging may be a reason, further compounded by the complexity of the procedures. There are some practical advantages of using image criteria evaluation compared to ROC-type evaluation in that the ground truth need not to be known and therefore basically any stored patient examination can be used in the evaluation. The task is to assess the visibility of relevant anatomy rather than subtle pathology. However, the validity of image criteria evaluation, i.e., visual grading methods, relies on a positive correlation between the visibilities of such criteria and detection of pathology or the ability to safely perform the procedure. Since the image criteria are often assessed using a graded scale (e.g., 5-point Likert-type) it is important that the correct statistical methods are used in the analysis. This includes Visual Grading Characteristics (VGC) (Båth and Månsson, 2007) or Visual Grading Regression (VGR) (Smedby and Fredrikson, 2010) where the ordinal properties of the dependent variable (graded quality score) are considered rather than performing parametric tests of means of pseudo-interval Likert-type scores e.g., 1-5.

Attempts to optimise the quality of the images of an image guided intervention by dividing the whole procedure into stages (Lundh et al., 2021) have been made, where each imaging event is linked to a medical task (e.g., location of stent graft or visualise graft and vessels etc.) and an imaging purpose. Assigning specific image criteria to each stage with its specific imaging purpose may be a way forward to optimise these complex procedures.

### **Technical image quality, TIQ**

Technical image quality tests are important for the evaluation of radiological equipment and use phantoms to represent the patient.

Four methods have been selected and described in this protocol. Three methods are quantitative methods: Signal-to-noise ratio rate (SNR<sub>2rate</sub>) using model observer analysis, threshold-contrast detail detectability (TCDD) based on a statistical method and TCDD using model observer analysis. Before implementing any specific method, the reader is strongly recommended to study the references (see specific protocol sections). The last method is based on visual scoring, because medical physics services may not have experience in using quantitative methods. In the long term, a switch to quantitative methods calculated from images is recommended, as this is more reproducible and more readily compared against a TIQ standard. In general, the system generates and stores images with a given clinical image processing set applied and these are usually referred as ‘For Presentation’ images. The characteristics of the image processing will depend on the acquisition or fluoroscopy program used. When evaluating or discussing clinical image quality then clearly ‘For Presentation’ images will be used. For the evaluation of technical image quality with one of the four methods described in this protocol, then physicists will, in general, only have access to ‘For Presentation’ images from the system. Technical image quality will therefore be routinely assessed from ‘For Presentation’ images, and physicists must exercise some caution when interpreting these results. Furthermore, it may also be possible to use ‘For Presentation’ images when calculating Fourier metrics as a means of tracking detector or system performance over time. The use of image quality metrics calculated from ‘For Presentation’ fluoroscopy and angiography images for QC purposes is still in its infancy. It will be some time before sufficient data are available for a broad range of systems and imaging applications to determine whether the results are sensitive and reproducible. When explicitly assessing detector performance using Fourier methods, access to ‘For Processing’ images is required i.e. images without the clinical image processing set applied. Access to these image types will generally be via the XR27 user QC mode, or by a program set up to have fixed gain (no auto-ranging) and minimal clinical processing.

Before applying any of the methods, discuss the procedures performed on the system with the relevant clinical staff in order to establish the TIQ test settings (e.g., commonly used imaging protocol(s), dose modes and FoV).

If protocols are amended such that TIQ would be affected, then re-commissioning is required, and new baseline values established. Situations where the protocols are amended include clinician requests, software and/or hardware updates, and new clinical applications.

### **Detector vs system evaluation: influence of geometry**

Broadly speaking, two geometries are used for TIQ testing, depending on the focus of the evaluation. These are depicted in Figure 3. The detector geometry is easily applied to mobile C-arm type systems used in operating theatres where access to a table needed to support the scattering material can sometimes be difficult. The x-ray detector is one of the basic determinants of the quality of the images produced by an imaging system, setting a fundamental limit on the sharpness and noise of the images that can be produced. For many years, there was considerable focus on a direct assessment of the x-ray detector in fluoroscopy (Hay et al., 1985), reflecting the use of x-ray image intensifiers (XRII) coupled to a television camera and QC testing with a ‘detector’ geometry (Figure 3a). These are vacuum electro-optical devices and can suffer from a gradual reduction in gain over time, which could be quantified via the conversion factor (Holm and Moseley, 1964). There could also be a loss of sharpness, due to changes in the focusing voltages and therefore QC methods tended to focus on detecting changes in the detector (i.e., the XRII-TV system) over time (Hay et al., 1985). XRII devices have since been largely superseded by digital flat panel x-ray detectors

in fluoroscopy and angiography systems that do not have active electrostatic focusing, although many QC programs have not adapted to this change. As far as we have been able to, this protocol tries to adapt to these technological changes as far as practical.

The two principal means of evaluating x-ray detector imaging performance are via Fourier metrics and using low scatter planar test objects imaged at the detector input plane (Hay et al., 1985; Cowen, Haywood, et al., 1987) (Figure 3a). In both cases, an appropriate metal filtration is positioned at the x-ray tube port, to reduce the quantity of scattered radiation produced and giving a defined x-ray beam energy distribution for the evaluation. Detector input exposure levels can be quantified and the influence of geometric blurring from the x-ray focus is reduced by positioning the test tools at the detector input plane. As a result, a clear picture of x-ray detector sharpness, noise and efficiency is obtained, and these can be compared against reference data and also used to track detector performance over time. However, many important system parameters which influence clinical image quality and task performance are ignored by this kind of detector-centric evaluation.

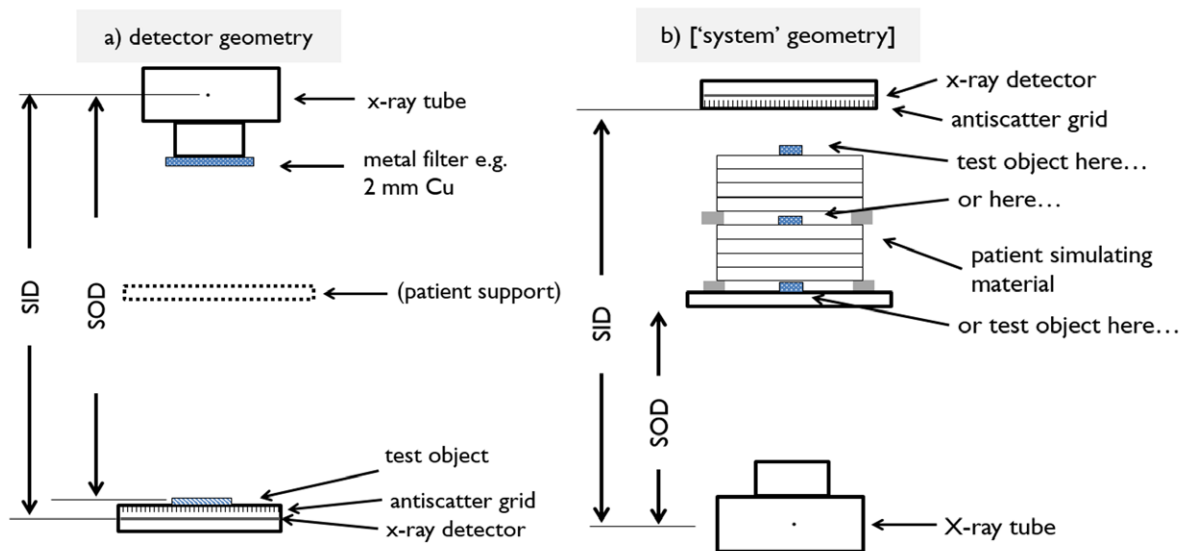


Figure 3. a) geometry for explicit evaluation of the x-ray detector (can also be orientated with x-ray at the bottom/detector at the top). The anti-scatter grid has to be removed (if possible). b) geometry for measurement of x-ray system performance

If an overall system performance test is required, a 'system geometry' has to be used. Many more system parameters will influence the TIQ score in this geometry, including geometric focus blurring, scattered radiation and the influence of the anti-scatter grid and the x-ray energy. A detailed evaluation of the x-ray detector could be made at the Commissioning stage and explicit detector evaluations only made if problems with the x-ray detector are suspected at some point during the lifetime of the detector. Constancy TIQ testing of the overall system would be made using test objects in a system geometry. Table 2 lists the expected PMMA thickness ranges for four common clinical applications and the FoVs used. At Commissioning, TIQ can be assessed for a number of patient thicknesses and FoV. Longitudinal testing should track the commonly used imaging protocol and the associated fluoroscopy mode and acquisition program (series imaging). This should be done at a relevant phantom thickness for one FoV. It is important to have a relevant dosimetry measurement to accompany the TIQ measurement. The entrance surface air kerma rate (ESAKR) should already have been measured at the corresponding phantom thickness(s) in the AEC tests and these values can be used with the TIQ data, provided the phantoms do not change the beam load/dose.



*Table 2. Ranges of patient equivalent thicknesses (PMMA) and field of view (FoV) for different clinical applications. Also angulated positions are considered.*

Clinical application	PMMA Thickness (cm)	Field of View (cm)
Head	16 cm	16-22 cm
Abdomen	20,25,30 cm	32-42 cm
Cardiac	20,25,30,40 cm	20-25 cm
Paediatric	5-20 cm	FoVs vary widely depending upon size and application

### Phantoms

An overview of phantoms used in clinical practice is discussed in Appendix 2. Often these phantoms bear little resemblance to patients and should therefore not be used to optimise procedures since they provide a too simplistic image representation (e.g., no anatomical varying background). Image processing, which is an important component of dynamic imaging systems, is likely to have a different response to current TIQ test objects compared to scenes containing anatomical information.

Current test objects are still typically formed from circular details arranged in a geometric pattern, set within a homogeneous background and are usually static when imaged. Extrapolation of the TIQ measurement to clinical image quality is therefore difficult. A good example of this occurs when using static test objects to assess cardiac imaging modes, where clinical image processing will be set up for good temporal resolution but at the expense of increased quantum noise in the images. The use of a static phantom in this situation would give a misleading result. Note that the implementation of advanced analysis methods would not resolve the problem in this case. Test object composition and the method used for imaging can also give potentially misleading results. Using copper attenuation at the x-ray tube to mimic patient attenuation may distort the measured technical image quality performance compared to using a more realistic attenuator such as PMMA. A test object containing iodine could produce higher SDNR results at higher tube voltages when imaged with copper, while the use of PMMA attenuation would produce higher SDNR at lower tube voltages. Furthermore, the use of materials such as aluminium in test objects to optimise protocol selection must be done with caution. Aluminium will not correctly indicate the optimal setup for objects containing iodine, steel (stents or guidewires) or any of the higher atomic number materials often used to increase device visibility. However, these simple test objects form a controlled input that is suitable for constancy testing and can be used to detect deviations from the imaging performance established at Commissioning.

### Signal-to-noise ratio rate - Model Observer

Several papers have described technical image quality evaluation in the spatial domain using statistical model observers for fluoroscopy or dynamic imaging systems (Tapiovaara, 1993; Tapiovaara and Wagner, 1993; Favazza et al., 2015; Bertolini et al., 2019; Villa et al., 2019). There has been strong growth in the development and application of these methods in recent years; further information on model observer methods is available in many papers or reference books (Barrett et al., 1993; Eckstein, Abbey and Bochud, 2000; Abbey and Barrett, 2001; Barrett and Myers, 2003; He and Park, 2013).

A model observer method is a means of applying a mathematical model, usually developed using signal detection theory, to a set of images with the aim of estimating task performance for some theoretical ('model') observer (Barrett et al., 1993). While estimation tasks can be modelled, much of the literature focuses on detection tasks i.e., classification into signal present or signal absent images. This clearly has parallels with the measurement of clinical image quality using ROC analysis with human readers. The SNR resulting from these methods is a measure of the image quality: a well set up system will generate a large separation between the distribution means and/or reduce the standard deviation on the distributions.

A Model Observer called the DC-suppressing observer (DCS) has been applied to fluoroscopic data (Tapiovaara, 1993; Tapiovaara and Wagner, 1993). Its advantages in terms of precision compared to visual threshold contrast tests or alternative forced choice tests are described in Tapiovaara and Sandborg (2004) in a direct comparison. This model observer excludes the DC-component (average image brightness) and is constructed by averaging a large number of images (e.g., 1024) with and without the test object (e.g., a small disc) being

$$D_{DCS}(g) = \sum_{i,j} \left[ \Delta g_{i,j} - \frac{1}{P} \sum_{k,l} \Delta g_{k,l} \right] g_{i,j}$$

present. The difference of these averaged images  $\Delta g$  is used in computing the decision variable  $D_{DCS}(g)$  where  $g_{i,j}$  is the pixel values of each analysed image with the test object and  $P$  is the number of pixels in the imaged area (Tapiovaara, 2003). The model observer template  $\Delta g$  is then cross-correlated with each image frame separately with and without the test object to form the observer’s decision variable. The SNR is calculated from the conditional distributions:

$$SNR = \frac{\overline{D(g | signal)} - \overline{D(g | background)}}{\sigma_D}$$

where:

- $D(g|signal)$  and  $D(g|background)$  are the decision variables
- ‘background’ represents the situation without the test object (see Figure 4)
- $\Delta D$  is the standard deviation of the distributions.

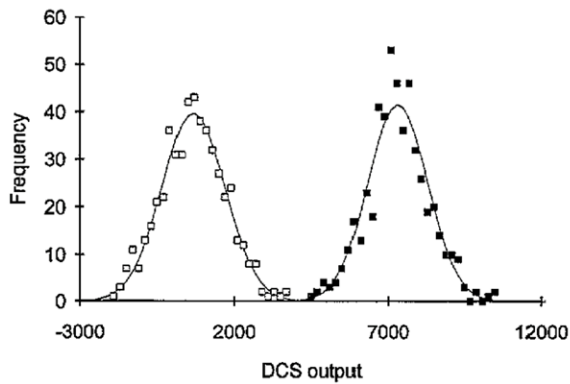


Figure 4 An example of the experimental distributions of DDCS for the signal-present (•) and absent (◻) cases (from Tapiovaara 1993). The Gaussian fits are shown as full curves. The  $SNR_{single\ frame}$  in this example is 6.6 and the experimental conditions are 30 cm acrylic phantom, 65 kV, total filtration 2.5 mm Al, no grid, air kerma rate at phantom surface 3.8 mGy min<sup>-1</sup>.

It is, however, the accumulation rate of  $SNR^2$ , i.e.,  $SNR^2_{rate}$  which is of interest in fluoroscopy. Neighbouring frames in a sequence are not independent, and hence a lag-factor,  $F$ , is calculated from the spatial-temporal noise power spectrum to account for the number of independent frames per second such that  $SNR^2_{rate} = SNR * F$ , for details see (Tapiovaara, 2003).

Application of  $SNR^2_{rate}$  in Constancy QC is described in (Elgström, Tesselaar and Sandborg, 2021) and in (Tesselaar and Sandborg, 2016). Longitudinal testing of a fluoroscopy system in a simple QC setup over 4 months showed that uncertainty in  $SNR^2_{rate}$  was  $\pm 14\%$  ( $\pm 2$  standard deviations).

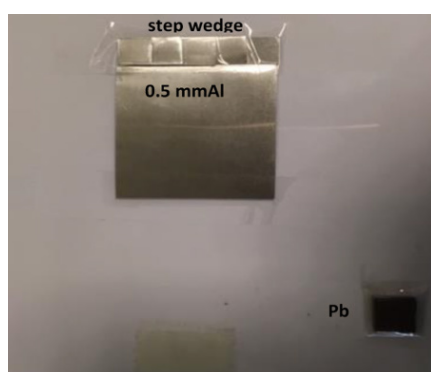
### Threshold-contrast detail detectability (TCDD) – Statistical method

Recent work by the AIFM (Associazione Italiana di Fisica Medica) describes the use of the statistical method (SM) for the QC of fluoroscopy and angiography systems (Paruccini et al., 2021). The method was initially presented by (Chao et al., 2000) for CT imaging, and is closely related to the model developed by (Rose, 1948). The approach is based around the extraction of  $n$  ROIs of identical size in pixels (e.g.,  $d \times d$  pixels) from a homogeneous image region. The mean pixel value of each ROI is calculated ( $\bar{x}$ ) and the standard deviation of these means ( $\sigma_x$ ) is used to determine threshold contrast. The distribution of means is assumed to follow a normal distribution and the threshold contrast for the statistical method ( $C_{TSM}$ ) defined for the 95% confidence level:



$$C_{TSM}(d) = 3.29 \sigma_x(d)$$

This effectively states that there must be some separation between adjacent distributions for an object of a given ROI size for an object to be considered visible, similar to the threshold visibility condition applied in the Rose model (Rose, 1948). The size of the ROI has some influence on the correlation of the noise present within the ROIs. Minimum ROI size is 2x2 pixels, which is of the order of 0.3 mm for a typical detector pixel spacing of 0.15 mm. The minimum number of ROIs used to estimate  $\sigma_x$  is taken to be 25 (Paruccini et al., 2021). Furthermore, the uncertainty of the method depends on the insert size: for smaller inserts, the coefficient of variation (CV) of  $C_{TSM}$  is 2-3%, whilst for the larger inserts (25 subROIs) it may reach 10% or greater. Repeating this process for a range of sizes generates a contrast-detail curve. An important part of the method is the use of an aluminium step wedge that allows the influence of x-ray energy on the c-d curve to be included, by converting pixel value to millimetres of aluminium (see Figure 5).



*Figure 5. Statistical Method test object: central homogenous region, aluminium step wedge and lead insert to estimate scatter and veiling glare effects and image offset.*

The method has been adapted to include the influence of temporal integration of the human visual system, which temporally integrates over ~200 ms, depending on scene luminance. This results in an averaging of uncorrelated noise in different images and a blurring or temporal smearing of moving signals. To include this effect on the noise, groups of images that correspond to the approximate eye integration time of 200 ms, e.g., 3 images @ 15 fps, 6 images @ 30 fps are averaged before extracting the ROIs for the  $C_{TSM}$  calculation (Villa et al., 2019).

Implementation requires fewer images compared to model observer methods (Villa et al., 2019). The test object is inexpensive and robust and can be used standalone, in scatter-free conditions, or with tissue simulating materials such as PMMA. The method has been applied to both 'For Processing' and 'For Presentation' images. It should be noted that this method only uses data extracted from homogenous image regions containing noise. No detail objects are present and therefore this method cannot assess the influence of geometric blurring due to the x-ray focus on system spatial resolution, even if the object is positioned at isocenter. This effect is especially noticeable for small size details (< 1 mm).

### **Threshold-contrast detail detectability (TCDD) - Model Observer**

In order to overcome computational constraints related to spatial model observer methods, many authors implement a linear observer model called the channelized Hotelling observer (CHO). At the heart of the CHO method is a template that is typically built and applied as follows:

- Image patches (ROIs) of many images of the expected target (e.g., a disc in a uniform background, a guidewire or a lesion) are extracted from the set of signal present images along with ROIs containing signal absent (background) areas.
- These ROIs are multiplied by a set of 2D functions (the 'channels') that reduce the dimensions of the data. The number (n) and shape/type of channels is generally chosen to reflect characteristics of the target.

- Each channel is the size of an ROI and the dot product of the ROI and channel function (e.g.,  $n=1$ ) gives a scalar value. These scalar values are stacked to form a vector with  $n$  elements. The difference between the signal present and signal absent channelized vectors is defined as the expected signal.
- The covariance matrix is also calculated from the channelized signal present and signal absent vectors.
- The expected signal and covariance matrix are combined to give the CHO template.
- This template is built using a set of signal present and signal absent images in the ‘training’ stage.

Once built, the template (a vector of  $n$  values) is applied in the ‘reading’ or ‘testing’ stage, to a fresh set of signal present and signal absent images. Signal present and signal absent ROIs are extracted, ‘channelized’ i.e., multiplied by the channel set, and then multiplied by the template. This generates a ‘decision variable’ ( $t$ ), analogous to those assumed for a human reader in an ROC study. Applying the template to many signal present and signal absent images produces two distributions of decision values (figure 6).

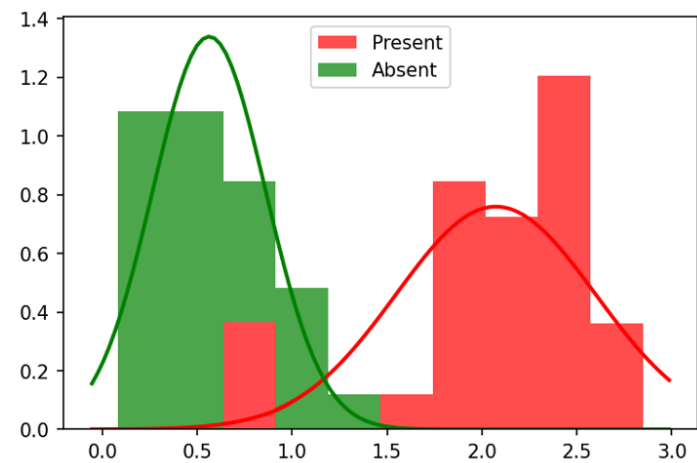


Figure 6. Distributions of decision variables calculated for signal present and signal absent image sets

The signal to noise ratio (SNR) can be calculated using a model observer from the distributions in figure 6 as follows:

$$SNR = d' = \frac{|t_1 - t_0|}{\sigma_{t_1 t_2}}$$

where  $t_1$  and  $t_0$  are the mean value of decision variables for the signal present and absent images, respectively, and  $\sigma_{t_1 t_2}$  is the averaged standard deviation for these distributions.

One of the drawbacks of CHO implementation is the number of images required to obtain a reliable estimate of the covariance matrix. The rank of the standard covariance matrix is less than or equal to the number of samples used to estimate the matrix (Gallas and Barrett, 2003), meaning for example that at least 96 images are needed to form a covariance matrix that can be inverted in a 96 channel CHO template. To obtain an accurate covariance matrix, the number of training images is between 10 and 100 times the number of channels (Gallas and Barrett, 2003), with a factor of 10 (Favazza et al., 2015) being a typical value. Reducing the number of channels helps in this respect but comes at the cost of reduced flexibility when modelling different targets. Spatial domain model observers can be used to produce an objective, quantitative measurement of either TCDD or low contrast-detail detectability (LCDD) i.e., not at the threshold condition. This is an alternative to visual scoring of c-d test objects. In the CHO applied by Bertolini (Bertolini et al., 2019), images of the Leeds TO10 are used, and the output is converted to threshold contrast values. These are then compared against human reader results generated using a 2-AFC method. Internal noise was added to the CHO results to obtain a good match between the model and human reader results.

### Threshold-contrast detail detectability (TCDD) – Human visual scoring

Until the implementation of analogue to digital converters and digital storage in these systems, it was not possible to store fluoroscopy images for analysis. TCDD test objects were therefore designed for subjective (visual) scoring by human readers. As discussed, the arrangement of the discs within the test object determines how the test object is read out. Figure 2a in Appendix 2 shows an image of the Leeds TO12 test object and when scoring this test object, the reader has to count to the last disc considered visible. This type of readout is quick, which is important when testing live fluoroscopy, however there are a number of drawbacks. TCDD scoring suffers from lack of precision which makes the identification of significant changes in CT difficult in longitudinal testing (Cohen, McDaniel and Wagner, 1984; Marshall et al., 1992; Launders et al., 1995; Tapiovaara, 1997; Tapiovaara and Sandborg, 2004). There is no way of knowing the percentage correct scores for the readers in this type of readout, making this method unsuitable for estimating observer efficiency (Burgess, 2011). Perhaps the biggest drawback is the difficulty in defining and communicating a common detectability criterion among the scorers i.e. what is considered actually visible. As a result, it is particularly difficult to set standards in terms of CT derived this way and for observers to compare their scores against this standard.

MAFC is an alternative readout method that requires a different arrangement of discs, where the observer typically has to state which corner contains the disc, which is then compared against the ground truth disc position (see Figure 2b in Green and Swets, 1966). The observer has to read several test object images, enabling  $C_T$  to be defined at a known percentage correct level. Unfortunately, MAFC scoring is time consuming (10 or 15 minutes per image, depending on test object). The determination of a threshold value ( $C_T$ ) i.e., a signal at the limit of detectability inevitably limits the precision that can be achieved, which is an important consideration in QC testing (Tapiovaara and Sandborg, 2004). Although suffering from several weaknesses, visual assessment of test objects using TCDD with ‘count to the last disc’ scoring remains widely used in fluoroscopy QC programs, largely because of the speed with which the object can be scored.

### Limiting spatial resolution (LSR)

The ability of an imaging system to resolve fine details (often termed ‘spatial resolution’) is an important system attribute for some imaging tasks. The spatial resolution of an imaging system is determined by the x-ray detector properties and by geometric blurring. In fluoroscopy and angiography applications, geometric blurring depends on x-ray focus size, the geometric magnification, and any motion between the anatomy or devices being imaged and the ray focus/detector axis.

The flat panel detectors used in current fluoroscopy and angiography systems are indirect detection devices, with a needle-like CsI scintillation phosphor coupled to an array of light sensitive detector elements, usually referred to as pixels. Assuming square pixels, then the pixel pitch ( $p$ ) can be defined as the distance between the centre of adjacent pixels in a given detector row. This pitch determines the Nyquist frequency,  $f_N$ , of the detector:

$$f_N = \frac{1}{2p}$$

which is the maximum spatial frequency that can be reproduced by the pixel array without aliasing of the signal. Ideally, limiting spatial resolution should be assessed with a test object that produces a sinusoidally varying x-ray signal over a range of spatial frequencies. Practically, a line pair or bar pattern test object is used to perform this measurement that contains groups of lines each with a specific spatial separation corresponding to a spatial frequency. Groups of rectangular lines are cut into a thin lead sheet and these generate square waves at a given spatial frequency; a typical line pair test object for fluoroscopy and angiography systems covers frequencies from  $0.5 \text{ mm}^{-1}$  to  $5.0 \text{ mm}^{-1}$ .

In use, the line pair test object is imaged at a low tube voltage to give a high contrast and at a kerma rate that limits the amount of x-ray quantum noise in the image (although some noise will be present). The observer counts to the last linepair group that is clearly imaged and that does not have disturbing patterns (aliasing) running at some angle across a given linepair group (Albert et al., 2002). This is defined as the

limiting spatial resolution of the system. If the line pair test object is positioned on the x-ray detector then this result will be close to the Nyquist frequency of the x-ray detector. If the linepair test object is positioned on the x-ray table then the limiting resolution will be limited by the combined effect of the x-ray geometric blurring and x-ray detector. Note that if the test object is positioned on the x-ray table, then the spatial frequencies within each bar group are magnified by the geometric magnification ( $m$ ) i.e. each spatial frequency is reduced by a factor  $1/m$ .

## A.6. SAFETY

Any new fluoroscopic installation must undergo a comprehensive safety assessment. Including radiation protection aspects, to ensure the facility is safe for both staff and patients. The assessment includes facility aspects such as a verification of the shielding of the walls and design layout, as well as procedural approaches such as radiation risk assessments and optimization of protocols for patient imaging. A comprehensive description of these tasks is beyond the scope of a report dealing with fluoroscopic equipment performance. However, as part of the initial equipment checks there are a number of safety assessments one may carry out. The performance evaluation of fluoroscopic systems should include also a radiation safety survey to determine whether the radiological medical equipment, the practical techniques and the ancillary equipment are complying with the national radiation control regulations, based on the European Basic Safety Standards (BSS) (Official Journal of the European Union;2014). Also, relevant publications are the IEC 60601-2-54, last updated in 2022 (IEC 60601-2-54; 2009), and the IEC 60601-2-43, last updated in 2022 (IEC 60601-2-43; 2010). Practical guidance, especially regarding radiation protection optimization, has been given by the International Atomic Energy Agency in a 2018 Specific Safety Guide on Radiation Protection and Safety in Medical Uses of Ionizing Radiation (IAEA; 2018). In many European countries, these checks will form part of national regulations. Some of these checks are already covered in detail in the relevant equipment section (e.g., leakage is covered in the 'X-Ray Tube' section).

For the staff performing the fluoroscopy procedure in the room, the most important aspect from the radiation safety point of view is the stray radiation (leakage plus scatter) from the patient, the tube, the image detector and peripheral devices close to the patient. Measurements of stray radiation around the fluoroscope, using the maximum air kerma rate and the largest field size and with a phantom in the beam (NCRP, 2010), should be performed before the system is used clinically and after changes in hardware or software affecting the patient dose (ACR; 2016). Results can be compared with manufactured supplied isokerma plots.

Details about radiation safety tests are given in Appendix 1.

A succinct list of potential equipment-based radiation protection checks is shown in table 3.

Assessment	Potential Methodology
Equipment warning lights	Check for: - Power on lights - Exposure on lights
Equipment alarms	Check against national & IEC standards such as: - Warning alarm after a certain level is reached e.g., 5 min of fluoroscopy - Sound when high dose-rate fluoroscopy is used - Collision avoidance warnings
UPS functionality	Can table be driven to cardiopulmonary resuscitation position with mains failure
Exposure switch/footswitch	Check for: - Correct operation (e.g., 'dead man' mode) - Can exposure be made on leaving the footswitch up-side down?

X-Ray Tube	Assess leakage radiation, labelling of focal spot position and minimum focus-skin distance. Assess minimum filtration meets national or IEC guidelines/regulations
Collimator	Ensure all blades are just visible and close symmetrically to the centre of the FoV.
Alignment	Check that the x-ray field and displayed field are aligned within national or IEC tolerances.
Pb equivalence of tableside and ceiling shields	Assess Pb equivalence and marking meets national standards and specification.

## A.7. OTHER GUIDANCE

A number of reports providing guidance on the performance testing and quality control of fluoroscopy systems have been published over the years. The paper by Boone et al., (1993) reports fluoroscopy exposure rate measurement methods and results from AAPM Task Group No. 11. More general advice on QC of fluoroscopy equipment by AAPM Task Group No. 12 is given in AAPM Report 74 (Shepard, 2002). More recent publications are available from the AAPM. Estimation of patient skin dose in fluoroscopy is described in a joint report by AAPM TG357 and by EFOMP (Andersson et al., 2021). AAPM Task Group Report 272 gives guidance on Acceptance Testing and Evaluation of fluoroscopy systems (Lin et al., 2022).

Fluoroscopy systems are included in the Institute of Physics and Engineering and Medicine (IPEM) Report No 91 that lists standards for diagnostic x-ray system performance testing (IPEM, 2005). IPEM Topic Group Report 32 Part II provides specific information on the technology and testing of image intensifier TV systems (Hiles and Starritt, 1996). This has been updated in the IPEM-IOP series report entitled 'Dynamic X-ray Imaging Systems Used in Medicine' (Stevens, 2021). Analysis of fluoroscopy QC results acquired by MPEs across the UK using methods described in IPEM Report 91 and IPEM Report 32 Part II is described by (Worrall et al., 2020).

The European Commission has published report No 162 (European Commission, 2012), which provides an extensive set of non-binding criteria that assesses the acceptability of imaging equipment and advises on appropriate remedial action, where indicated. These are acceptability criteria and should be seen as minimum standards rather than remedial levels to be applied to modern, well-adjusted and well-functioning imaging equipment. The excellent review paper by Jones (Jones et al., 2014) summarises lectures given at the AAPM summer school in 2012 and covers equipment specification, Acceptance and QC testing plus information on dose measurement and radiation effects.

The International Electrotechnical Commission (IEC) publishes international standards applicable to fluoroscopy systems. These include those that address safety and essential performance (IEC 60601-2-54 & 60601-2-43) and the newly published IEC61223-3-8 (2024) addressing acceptance and constancy testing for radiography and radioscopy.

## SECTION B - PROTOCOL

This section contains the detailed description of the suggested tests. The background to some tests is included in Section A.

### B.1. MECHANICAL AND GEOMETRICAL PARAMETERS

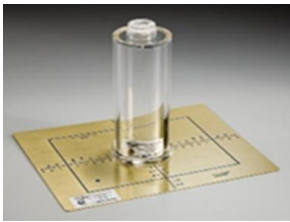
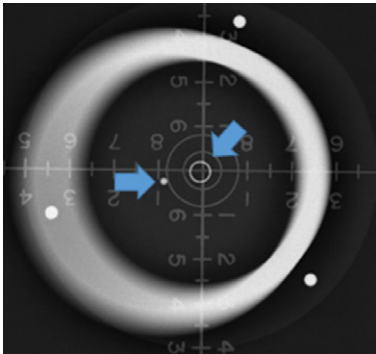
#### B.1.1 Determination of source location and minimum source – skin distance

Reference	<ol style="list-style-type: none"> <li>1. IEC 60601-2-43 Medical electrical equipment - Part 2-43: Particular requirements for the basic safety and essential performance of X-ray equipment for interventional procedures, 2022</li> <li>2. Accuracy and calibration of integrated radiation output indicators in diagnostic radiology: A report of the AAPM Imaging Physics Committee Task Group 190 Med. Phys. 42 (12), December 2015</li> <li>3. IEC 60601-2-54 Medical electrical equipment Part 2: Particular requirements for the basic safety and essential performance of X-ray equipment for radiography and radioscopy</li> </ol>
Instrumentation	<p>Tape measure</p> <p>Two square test objects, the side of one object is twice the length of the side of the other object</p>
Procedure	<p>The first action is to ensure that the focal spot position is marked. If it isn't, ask the engineer to correctly mark the position of the focal spot on the x-ray tube housing.</p> <p>If the engineer is not present or cannot do this, undertake the following procedure to determine the focal spot position:</p> <ul style="list-style-type: none"> <li>-Use two square test objects, the side of one object is twice the length of the side of the other object.</li> <li>-Place the smallest on the tabletop and attach the largest to the front face of the image detector.</li> <li>-During fluoroscopy, with the x-ray beam vertical, modify the height of the tabletop or the focus-to-image detector distance until the two test objects coincide in the image. This will place the smallest object exactly halfway between the focal spot and the largest object.</li> <li>-Measure the distance between the two objects. The focal spot position is at the same distance from the smallest test object.</li> <li>-Mark permanently on the x-ray tube housing surface for future reference.</li> </ul>
Evaluation	Compare the measured distance with the reference value
Pass/Fail Criteria	<p>Minimum focal spot - skin distance:</p> <ul style="list-style-type: none"> <li>-20 cm for surgery application</li> <li>-30 cm for other application</li> </ul>
Frequency	Acceptance test

#### B.1.2 Minimum field size

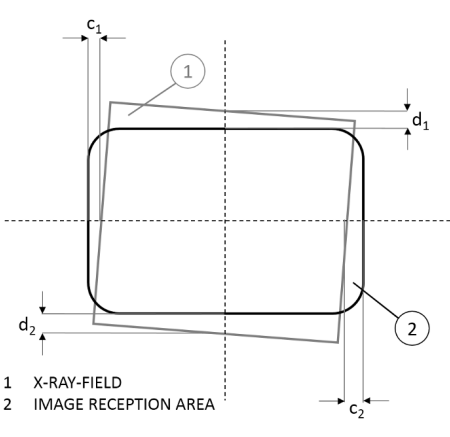
Instrumentation	<p>Tape measure</p> <p>Field size test object (e.g. radio-opaque ruler)</p>
Procedure	<p>Close the collimators as far as possible.</p> <p>Place the field size test object in the beam and record the focal spot-to-test object distance.</p> <p>Acquire an image of the field size test object using a few seconds of fluoroscopy.</p>
Evaluation	<p>Measure both sides of the image obtained.</p> <p>Rescale the distances to 1 m from the source.</p>
Pass/Fail Criteria	The minimum field size, measured at 1 m from the focus in a plane normal to the reference axis, shall not exceed 5 x 5 cm <sup>2</sup>
Frequency	Acceptance test

### B.1.3 Beam alignment

Reference	<ol style="list-style-type: none"> <li>IEC 60601-2-43 Medical electrical equipment - Part 2-43: Particular requirements for the basic safety and essential performance of X-ray equipment for interventional procedures, 2022</li> <li>Radiation Protection n. 162, 2012 "Criteria for acceptability of Medical Radiological Equipment used in Diagnostic Radiology, Nuclear Medicine and Radiotherapy" 2010</li> </ol>
Instrumentation	Spirit level Beam alignment test tool (plate and PMMA cylinder with two lead marks)
Procedure	<p>If possible, inspect engineers' tests results for perpendicularity          If this is not possible, one of the two following methods can be used          Method a):          Rotate the C-arm to a lateral position (90° or 270°)          Select a source detector distance (SID) of 100 cm          Position the test object at the centre of the detector          Acquire an image of the field size test object using few seconds of fluoroscopy</p>  <p><i>Figure 7. The beam alignment test tool consists of a plate and a cylinder with two radiopaque marks, placed at its top and at its bottom, respectively.</i></p> <p>Method b):          Place the test object on the couch          Move the couch until the two ball bearings in the cylindrical TO are overlaid on the image (Video showing positioning of alignment test object)</p>  <p><i>Figure 8. X-ray misalignment measured in terms of distance between the two radiopaque marks..</i></p>
Evaluation	<p>Method a):          Evaluate the alignment of the two radio opaque marks</p> <p>Method b):          Allowing for magnification effects calculate the focal offset from centre and convert the offset into an angle deviation at 100 cm SID</p>
Pass/Fail Criteria	Achievable $\leq 1.5^\circ$ Acceptable $\leq 3^\circ$
Frequency	Acceptance test



### B.1.4 Correspondence between X-ray field and effective image receptor size

Reference	<ol style="list-style-type: none"> <li>IEC 60601-2-54 Medical electrical equipment - Part 2-54: Particular requirements for the basic safety and essential performance of X-ray equipment for radiography and radioscopy', 2022</li> <li>Radiation Protection n. 162, 2012 "Criteria for acceptability of Medical Radiological Equipment used in Diagnostic Radiology, Nuclear Medicine and Radiotherapy" 2010</li> </ol>
Instrumentation	Tape measure External image device (e.g., radiochromic film or CR plate)
Procedure	<p>Position the external image device in the beam at a known distance to the source (as close as possible to the source).</p> <p>Set a FoV and acquire an image using sufficient radiation to produce an adequate image on the external image. Make the measurements with the reference axis normal to the image detector plane within three degrees.</p> <p>Repeat for all the available FoVs, minimum and maximum SID, vertical (0°) and lateral (90°) positions.</p>
Evaluation	<p>Correct the image size recorded on the external image device to the SID used for the test. Verify the correspondence between the nominal FoV and measured x-ray beam size. For rectangular fields, as shown in the figure 9, the measured discrepancies in the image detector plane are represented by <math>c_1</math> and <math>c_2</math> on one axis and by <math>d_1</math> and <math>d_2</math> on the other.</p>  <p><b>Figure 9. <math>c_1</math>, <math>c_2</math>, <math>d_1</math> and <math>d_2</math> assess the correspondence between X-ray and effective image receptor size.</b></p>
Pass/Fail Criteria	<p>If the image receptor area is circular, the x-ray field shall coincide with the image receptor area as required in 1) and 2).</p> <ol style="list-style-type: none"> <li>The x-ray field measured along a diameter in the direction of greatest misalignment with the image receptor area shall not extend beyond the boundary of the effective image receptor area by more than 2 cm;</li> <li>At least 80 % of the area of the x-ray field shall overlap the effective image receptor area. Effective image receptor areas smaller than 10 cm in diameter are exempted.</li> </ol> <p>If the image receptor area is rectangular:</p> <ol style="list-style-type: none"> <li>Along each of the two major axes of the image receptor area, the total of the discrepancies between the edges of the x-ray field and the corresponding edges of the image receptor area shall not exceed 3 % of the indicated focal spot to image detector distance when the image detector plane is normal to the x-ray beam axis:  <math> c_1  +  c_2  \leq 0.03 \times \text{SID}</math>  <math> d_1  +  d_2  \leq 0.03 \times \text{SID}</math> </li> <li>The sum of the discrepancies on both axes shall not exceed 4 % of the indicated source to image detector distance (SID):  <math> c_1  +  c_2  +  d_1  +  d_2  \leq 4\% \text{ SID}</math> </li> </ol>
Frequency	Acceptance (SID = min, max and 100cm) Annual test (All FoVs, both angulations and SID = 100cm)



### B.1.5 Verification of displayed distances

Reference	1. IPEM Report 91 “Recommended Standards for the Routine Performance Testing of Diagnostic X-ray Imaging Systems” (2005)
Instrumentation	Tape measure Two square test objects, with one object’s sides twice as long as the other
Procedure	Vary the SID between the maximum and minimum values (ideally 3 values in total), noting that the display of SID is equal to the measured value as determined with a tape measure 1) Adjust the table height from the lowest to the highest position and note that the display tracks the difference in height. 2) Record the focus-tabletop distance at zero displayed height and compare with the manufacturer’s reference value.
Evaluation	Compare the measured distances with the displayed data taking into account the nominal distance between the accessible surface of the detector and the detector (as stated by the manufacturer)
Pass/Fail Criteria	The measured distances shall not differ from the nominal distances more than 1.5%
Frequency	Acceptance

## B.2. X-RAY TUBE AND GENERATOR

### B.2.1 Tube voltage accuracy

Aim	To quantify accuracy of the set tube voltage on the imaging system
Reference	1. IPEM Report 91 “Recommended Standards for the Routine Performance Testing of Diagnostic X-ray Imaging Systems” (2005) 2. AAPM report 14 “Performance specifications and acceptance testing for x-ray generators and automatic exposure control devices” (1985) 3. IEC 60601-2-54 Medical electrical equipment Part 2: Particular requirements for the basic safety and essential performance of X-ray equipment for radiography and radioscopy (2022)
Instrumentation	Attenuation layers to ensure the tube voltage is set at an appropriate level Calibrated multimeter or tube voltage divider
Procedure	1a. For systems where x-ray factors can be set manually (including user QC mode), set the tube voltage to a value of approximately 70% of maximum tube voltage achievable e.g., 80 kV and set a typical loading (mAs) value. 1b. For systems with only AEC mode available, where the tube voltage cannot be set by the operator, vary the thickness of attenuator positioned between the multimeter and the image detector such that a value of approximately 70% of maximum tube voltage is achieved e.g. 80 kV. 2. Record the tube voltage, tube load, focus size and spectral pre-filtration 3. Repeat this for at least two other tube voltages, at 90% (~110kV) and at 50% (~60 kV) of maximum tube voltage value
Evaluation	The measured kVp’s shall not differ from the displayed values by more than 8%
Pass/Fail Criteria	Calculate the difference between the measured and displayed tube voltage.
Frequency	Acceptance test Annual test (at least 3 kVp points spread across appropriate clinical range)

## B.2.2 Minimum HVL/filtration evaluation

Aim	<p>To establish the minimum filtration on the imaging system</p> <p>Note: The minimum HVL or filtration assessment is carried out for regulatory reasons and the approach will be determined by the national regulations. For instance, in some jurisdictions the limit may be given in terms of HVL in which case the measurement may be directly compared with the requirement. However, in some jurisdictions the limit may be given in 'mm Al equivalent' in which case the HVL value measured must be converted into a 'mm Al equivalent' value, taking into account the generator waveform, anode angle and kVp.</p>
References	<ol style="list-style-type: none"> <li>1. Radiation Protection n. 162, 2012 "Criteria for acceptability of Medical Radiological Equipment used in Diagnostic Radiology, Nuclear Medicine and Radiotherapy" 2010</li> <li>2. IEC 60601-2-54 Medical electrical equipment Part 2: Particular requirements for the basic safety and essential performance of X-ray equipment for radiography and radioscopy (2022)</li> </ol>
Instrumentation	<p>Al sheets of purity <math>\geq 99\%</math>, typically 1 mm thickness</p> <p>Attenuation layers to ensure the kV is approximately set at 70% of maximum tube voltage achievable</p> <p>Dosimeter or multimeter</p>
Procedure	<ol style="list-style-type: none"> <li>1) For systems where x-ray factors can be set manually (including user QC mode), set the tube voltage to a value of approximately 70% of the maximum tube voltage achievable, e.g. 80kVp, and set a typical loading (i.e. mAs) value. (Follow manufacturer recommendations to protect the detector from excessive irradiation)</li> <li>2) For systems with only AEC mode available, and the tube voltage cannot be set by the operator, vary the thickness of attenuator positioned between the dosimeter and the image detector such that a value of approximately 70% of maximum tube voltage achievable e.g. 80 kV.</li> <li>3) Position the dosimeter centrally in the x-ray beam and collimate to the dosimeter and do not change its position during the test</li> <li>4) Use an acquisition protocol with minimum filtration (i.e. no added spectral filtration)</li> <li>5) For systems where x-ray factors can be set manually:             <ol style="list-style-type: none"> <li>a. Record the air kerma for no added Al filter</li> <li>b. Introduce Al sheets into the x-ray beam, between the x-ray source and dosimeter, recording Al thickness and air kerma each time</li> </ol> </li> <li>6) For systems with only AEC mode:             <ol style="list-style-type: none"> <li>a. position all the Al sheets in the x-ray beam, between the exit side of the dosimeter and the image detector</li> <li>b. record the air kerma for no added Al filter</li> <li>c. successively remove All sheets from the exit side of the dosimeter to the entrance side i.e., between the x-ray source and dosimeter, recording Al thickness and air kerma each time</li> </ol> </li> <li>7) Alternatively, record the half value layer (HVL) and estimated tube filtration given by the multimeter.</li> </ol>
Evaluation	<p>For both system configurations (AEC or manual), determine the HVL using the equation:</p> $HVL = \frac{X_1 \cdot \ln\left(\frac{2 \cdot Y_2}{Y_0}\right) - X_2 \cdot \ln\left(\frac{2 \cdot Y_1}{Y_0}\right)}{\ln\left(\frac{Y_2}{Y_1}\right)},$ <p>where <math>Y_0</math> is the air kerma reading without additional attenuation. <math>Y_1</math> and <math>Y_2</math> are the air kerma readings with added aluminium filters thickness of <math>X_1</math> and <math>X_2</math>, respectively.</p> <p>If needed, estimate the x-ray filtration from the measured tube voltage and HVL. This can be done using a spectral model, for example, the Boone model, the SpekCalc or SpekPy models or IPEM Report 78. For greater accuracy - if the model implementation allows - the target angle and waveform ripple can be included in the estimate.</p> <p>Boone Model:  <a href="https://bps.healthcare.siemens-healthineers.com/booneweb/index.html">https://bps.healthcare.siemens-healthineers.com/booneweb/index.html</a>            SPEKTR 3.0 (Boone Model): <a href="https://istar.jhu.edu/downloads/">https://istar.jhu.edu/downloads/</a>            SpekCalc Model: <a href="http://spekcalc.weebly.com/">http://spekcalc.weebly.com/</a>            SpekPy Model: <a href="https://bitbucket.org/spekpy/spekpy_release/wiki/Home">https://bitbucket.org/spekpy/spekpy_release/wiki/Home</a></p>

Pass/Fail Criteria	Minimum half value layer value shall not be less than the values in the table below.		
	First half value layer		
	kV	HVL*	HVL **
	50	1.8	1.5
	60	2.2	1.8
	70	2.5	2.1
	80	2.9	2.3
	90	3.2	2.5
	100	3.6	2.7
	110	3.9	3
	120	4.3	3.2
	130	4.7	3.5
	140	5.0	3.8
	150	5.4	4.1
	HVL*: Reference values for systems CE marked after 2012 IEC 60601-1-3 2008		
	HVL**: Reference values for systems CE marked before 2012 IEC 60601-1-3		
	The minimum filtration must be $\geq 2.5$ mm Al or the relevant regulatory limit in place		
Frequency	Acceptance test)		

### B.2.3 Half value layer (HVL) evaluation for clinical spectra

Aim	To establish the HVL for all the available clinical spectra
Reference	<ol style="list-style-type: none"> <li>1. Radiation Protection n. 162, 2012 "Criteria for acceptability of Medical Radiological Equipment used in Diagnostic Radiology, Nuclear Medicine and Radiotherapy" 2010 IEC 60601-2-54 (2011)</li> <li>2. IEC 60601-2-54 Medical electrical equipment Part 2: Particular requirements for the basic safety and essential performance of X-ray equipment for radiography and radioscopy (2022)</li> <li>3. IEC 61223-3-1 (2001)</li> </ol>
Instrumentation	<p>Al sheets of purity <math>\geq 99\%</math>, typically 1 mm thickness</p> <p>Attenuation layers to ensure the kV is approximately set at 70% of maximum tube voltage achievable</p> <p>Dosimeter or multimeter</p>

Procedure	<ol style="list-style-type: none"> <li>1) For systems where x-ray factors can be set manually (including user QC mode), set the tube voltage to a value of approximately 70% of maximum tube voltage achievable e.g., 80 kV and set a typical loading (mAs) value. (Follow manufacturer recommendations to protect the detector from excessive irradiation).</li> <li>2) For systems with only AEC mode available, and the tube voltage cannot be set by the operator, vary the thickness of attenuator positioned between the dosimeter and the image detector such that a value of approximately 70% of maximum tube voltage achievable e.g., 80 kV.</li> <li>3) Position the dosimeter centrally in the x-ray beam and collimate to the dosimeter.</li> <li>4) Select the first spectral prefilter to be assessed</li> <li>5) Set this manually if possible</li> <li>6) Alternatively, use an acquisition mode that gives this filter setting</li> <li>7) For systems where x-ray factors can be set manually: <ol style="list-style-type: none"> <li>a. record the air kerma for no added Al filter</li> <li>b. successively introduce Al sheets into the x-ray beam, between the x-ray source and dosimeter, recording Al thickness and air kerma each time</li> </ol> </li> <li>8) For systems with only AEC mode: <ol style="list-style-type: none"> <li>a. position all the Al sheets in the x-ray beam, between the exit side of the dosimeter and the image detector</li> <li>b. record the air kerma for no added Al filter</li> <li>c. successively remove Al sheets from the exit side of the dosimeter to the entrance side i.e., between the x-ray source and dosimeter, recording Al thickness and air kerma each time</li> </ol> </li> <li>9) Alternatively, record the half value layer (HVL) and estimated tube filtration given by the multimeter.</li> <li>10) Repeat for all available pre-filtrations</li> </ol>
Evaluation	<p>Calculate the HVL for each spectrum</p> <p>Estimate spectrum prefiltration</p>
Pass/Fail Criteria	The measured HVL must be consistent with the spectral prefiltration. Possible filtrations shall be assessed against the manufacturer's stated values.
Frequency	Acceptance

#### B.2.4 Normalised air kerma

Aim	To quantify the Air Kerma normalised to mAs at 1 metre from the x-ray source
Reference	<ol style="list-style-type: none"> <li>1. IPEM Report 32 "Measurement of the performance characteristics of diagnostic x-ray systems used in medicine" (1996)</li> <li>2. AAPM report 14 "Performance specifications and acceptance testing for x-ray generators and automatic exposure control devices" (1985)</li> </ol>
Instrumentation	<p>Attenuation layers</p> <p>Dosimeter or multimeter</p> <p>Tape measure</p>
Procedure	<ol style="list-style-type: none"> <li>1a) For systems where x-ray factors can be set manually (including user QC mode), set the tube voltage to a value of approximately 70% of maximum tube voltage achievable (about 80 kV) and set a typical loading (mAs) value with no added filtration. (Follow manufacturer recommendations to protect the detector from excessive irradiation).</li> <li>1b) For systems with only AEC mode available, where the tube voltage cannot be set by the operator, vary the thickness of attenuator positioned between the dosimeter and the image detector such that a value of approximately 70% of maximum tube voltage achievable is achieved e.g., 80 kV with no added filtration.</li> <li>2) Position the dosimeter centrally in the x-ray beam and collimate to the dosimeter.</li> <li>3) Remove the couch whenever possible, otherwise assess the reduction in the air-kerma.</li> <li>3) Measure the source-to-dosimeter distance.</li> <li>4) Record the air kerma, the tube voltage, tube load, focus size and spectral pre-filtration.</li> </ol>
Evaluation	Calculate the Air Kerma normalised to mAs at a source-to- dosimeter distance of 1 meter.

Pass/Fail Criteria	Air Kerma normalised to mAs at a source-to-detector distance of 1 meter, 80 kV and approximately 2.5 mm Al filtration shall measure between 25 and 80 $\mu\text{Gy}/\text{mAs}$ .
Frequency	Acceptance test

### B.2.5 Leakage radiation

Aim	To quantify the Air Kerma normalised to mAs at 1 metre from the x-ray source
Reference	1. IEC 60601-1-3: Medical electrical equipment – Part 1-3: General requirements for basic safety and essential performance – collateral standard: Radiation protection in diagnostic X-ray equipment. (2021)
Instrumentation	Tape measure Air kerma rate meter with appropriate cross-section area Attenuating sheets of Pb (lead)  Note: If an air kerma rate meter of reasonably large size is not available, a dose rate survey meter (ambient dose rate) sensitive enough and able to respond quickly to changes in the dose rate could be used.
Procedure	1) Consult the manufacturer’s test data on leakage radiation and evaluate the content. If this is not deemed to be sufficient, do the measurement described below. 2) Minimise the x-ray beam and place Pb attenuating layers, e.g., 5 mm, close to the X-ray tube’s collimator to block the primary beam. 3) Select the suitable mode (e.g., high kV) and start x-rays. 4) Move your dosimeter slowly approximately 50 cm from the focal spot and note the dose rate readings. Measure in all directions and identify the direction with the highest dose rate. (If your survey dosimeter did not measure air kerma rate (but ambient dose rate), measure air kerma rate in this direction with a calibrated dosimeter).
Evaluation	Estimate the maximum leakage radiation in terms of air kerma rate at 1 meter from the focal spot in fluoroscopy mode.
Pass/Fail Criteria	Measured maximum values shall match manufacturer specifications. When the tube is operating at maximum rating in fluoroscopy mode, the air kerma rate at 1 meter distance from the focal spot must be less than 1 mGy/h. If the maximum measured air kerma rate at 1 meter is higher than 1mGy/h the clinical activity shall be suspended. Estimate the position of the possible gap in the shielding and contact the manufacturer.
Frequency	Acceptance test

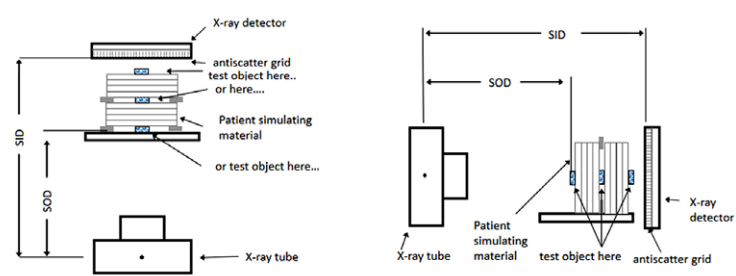
## B.3. AUTOMATIC EXPOSURE CONTROL

### B.3.1 AEC function

Aim	To test the response of the AEC to varying thicknesses of PMMA in comparison with manufacturer’s data
Reference	1. AAPM TG 125 “Functionality and Operation of Fluoroscopic Automatic Brightness Control/Automatic Dose Rate Control Logic in Modern Cardiovascular and Interventional Angiography Systems”, (2012)
Instrumentation	Tape measure 35 cm to 40 cm slabs of PMMA 30 cm x 30 cm with thicknesses to allow increment of 1 cm between 5 cm and 40 cm

<p>Procedure</p>	<p>Select a clinically relevant imaging mode for which the manufacturer has supplied data. Verify if the manufacturer dictates a geometrical set-up for the test and if so follow it. Otherwise follow the described procedure:</p> <p>For units with an integrated patient support</p> <ol style="list-style-type: none"> <li>1) Position the tube underneath the table.</li> <li>2) Remove the mattress.</li> <li>3) Set the table height in order to have the entrance surface of the PMMA phantom at the reference point [if ESAK/ESAKR is measured simultaneously, support blocks should be used to support the PMMA in order to be able to introduce the dosimeter below the stack].</li> <li>4) Lower the image detector as much as possible.</li> <li>5) Select a clinically relevant protocol, FoV and mode that you have manufacturer's data for. For all thicknesses of attenuator, the relevant exposure parameters that change as a function of attenuator thickness must be recorded - depending upon the manufacturer and model these may include the following: kV, mA(s), pulse width, spectral shaping filter, focal spot and entrance exposure to the detector. If the detector entrance air kerma is to be measured, ensure the detector is positioned on the detector as per manufacturer's instructions or outside the measuring field for the mode in question]. Do for both fluoroscopy and acquisition.</li> <li>6) Starting with 15 cm PMMA, add 1 cm each time, repeating the procedure, and once the exit surface of the PMMA block is within 5 cm from the detector housing entrance, start raising the detector to keep 5 cm between the exit surface of the stack and entrance of the detector housing. For all thicknesses keep the table height fixed.</li> <li>7) Keep adding PMMA until you reach the tube loading limits for your system. You may wish to exceed this thickness to ascertain what happens for extremely thick patients.</li> <li>8) Remember to ensure that during fluoroscopy the factors have stabilised prior to recording, and also undertake a short amount of fluoroscopy before each acquisition to ensure factors start at the correct value for the thickness in the beam.</li> </ol> <p>For mobile units</p> <ol style="list-style-type: none"> <li>1) To support the PMMA either use a patient support similar to that used clinically or position the mobile in a lateral angulation and support the PMMA with a trolley.</li> <li>2) If you are working laterally, take care to position yourself on the detector side of the set-up, to limit exposure to scattered radiation.</li> </ol> <p>Additional Notes</p> <ul style="list-style-type: none"> <li>- For units that undertake paediatric procedures, start at 5 cm thickness.</li> <li>- For mini C-arms start at 1cm and stop at 10 cm thickness. Repeat the above procedure for all clinically relevant modes (use the appropriate FoV for the clinical mode).</li> <li>- If you attempt to measure phantom exit air kerma or detector air kerma, be aware that this is highly scatter and geometry dependent so repeated measurements may vary greatly unless extreme care is made to ensure your set-up is exactly the same if retested</li> <li>- When testing against a manufacturer's curve, you should sample at smaller PMMA steps (e.g. 1 cm) across discontinuities in defined parameters. Where parameters are slowly changing, a 5 cm increment in PMMA thickness may be more efficient.</li> </ul>
<p>Evaluation</p>	<p>For Acceptance testing, the functioning of the AEC system should be tested for all the clinically relevant imaging modes (e.g., fluoroscopic, acquisition mode) as advised by the MPE.</p>
<p>Pass/Fail Criteria</p>	<p>Where manufacturer data exists, compare the results with those of the manufacturer. Raise with the manufacturer any deviations that, in the judgement of the MPE, are significant.</p>
<p>Frequency</p>	<p>Acceptance test</p>

### B.3.2 Comprehensive evaluation of AEC

Aim	To characterise the performance of the AEC for Commissioning and optimisation, and to ensure continued acceptable performance.
Reference	1. AAPM TG 125 “Functionality and Operation of Fluoroscopic Automatic Brightness Control/Automatic Dose Rate Control Logic in Modern Cardiovascular and Interventional Angiography Systems”, (2012)
Instrumentation	Dosimeter (two if also trying to measure detector air kerma) Tape measure 35 cm to 40 cm slabs of PMMA 30 x30 cm
Procedure	<p>For units with an integrated patient support</p> <ol style="list-style-type: none"> <li>1) Set the x-ray unit, remove the mattress, position the dosimeter(s) and phantom as depicted in the figure below (Courtesy of AAPM). If you are trying to also simultaneously measure the phantom exit air kerma or detector entrance air kerma, position an additional dosimeter in a way that is easily repeatable from year to year.</li> <li>2) Set the table height in order to have the entrance surface of the PMMA phantom at the patient entrance reference point (if ESAK/ESAKR is measured simultaneously, support blocks should be used to support the PMMA in order to be able to introduce the dosimeter below the stack).</li> <li>3) Lower the image detector as much as possible.</li> <li>4) Select a clinically relevant protocol, FoV and mode as advised by the MPE. Acquire an image and record the exposure parameters: kV, mA(s), pulse width, spectral shaping filter and entrance exposure to the detector has to be recorded as a function of the attenuator thickness.</li> <li>5) Starting with 15 cm PMMA, add 1 cm each time (see note in Frequency below to see how it changes in annual checks), repeating the procedure, and once the exit surface of the PMMA block is within 5 cm from the detector housing entrance, start raising the detector to keep 5 cm between the exit surface of the stack and entrance of the detector housing.</li> <li>6) Keep adding PMMA until you reach the tube loading limits for your system.</li> </ol> <p>For mobile units</p> <ol style="list-style-type: none"> <li>1) To support the PMMA either use a patient support similar to that used clinically or position the mobile in a lateral angulation and support the PMMA with a trolley.</li> <li>2) If working laterally, take care to work on the detector side of the set-up.</li> <li>3) The fluoroscopic imaging parameters kVp, mA, pulse width, spectral shaping filter as well as entrance surface kerma/entrance surface kerma rate at the phantom (and the exit phantom air kerma/detector air kerma if measured) shall be recorded and measured as a function of the attenuator thickness</li> </ol> <div data-bbox="487 1423 1218 1699">  <p>The figure contains two diagrams illustrating X-ray system verification geometries. The top diagram shows a vertical setup where an X-ray tube is positioned below a stack of PMMA blocks. An X-ray detector is positioned above the stack. Labels include 'X-ray detector', 'antiscatter grid', 'test object here.. or here...', 'Patient simulating material', and 'or test object here...'. Distances are marked as SID (Source-to-Image Distance) and SOD (Source-to-Object Distance). The bottom diagram shows a lateral setup where an X-ray tube is positioned to the left of a stack of PMMA blocks. An X-ray detector is positioned to the right of the stack. Labels include 'X-ray tube', 'Patient simulating material', 'test object here', and 'antiscatter grid'. Distances are marked as SID and SOD.</p> </div> <p><i>Figure 10. Typical geometries used for system verifications. The vertical one is suitable in case of units with an integrated patient support (up). The lateral geometry is used for mobile units (down).</i></p> <p>Note</p> <ul style="list-style-type: none"> <li>- For units that undertake paediatric procedures, use 5 cm thickness.</li> <li>- For mini C-arms start at 1 cm and stop at 10 cm thickness.</li> <li>- Repeat the above procedure for all clinically relevant modes (including varying the FoV) for both fluoroscopy and acquisition.</li> <li>- When solid state dosimeters are used apply the factor 1.35 to take into account the backscatter.</li> </ul>

Evaluation	Upon completion of the data acquisition, the fluoroscopic imaging parameters and entrance (and exit) air kermas should be plotted against the PMMA thickness. The graphs thus obtained reveal how the imaging system responds to changes in PMMA thickness.
Pass/Fail Criteria	The results obtained are to be used as a baseline following Commissioning and to aid optimisation decisions. For constancy tests, the deviations from the baseline shall be within 20%.
Frequency	Commissioning Annual reduced set of tests (dependent upon MPE judgement and clinical usage) <ul style="list-style-type: none"> <li>- Fix the PMMA thickness and vary the mode and FoV</li> <li>- Fix the mode and FoV and vary the PMMA thickness [e.g., 10 cm, 20 cm, 30 cm]</li> <li>- Ensure high usage clinical set-ups are covered.</li> </ul>

## B.4. DOSE INDICATORS

### B.4.1 Air-kerma – Area product and rate display accuracy

Aim	To determine the accuracy of the displayed air kerma-area product, $P_{KA}$ and displayed air kerma-product rate, $P(t)_{k,a}$
Reference	<ol style="list-style-type: none"> <li>1. AAPM TG 190 “Accuracy and calibration of integrated radiation output indicators in diagnostic radiology” (2015)</li> <li>2. IEC 60601-2-54 “Particular requirements for the basic safety and essential performance of X-ray equipment for radiography and radioscopy” (2022)</li> <li>3. IEC 60580 – Dose Area Product Meters (2019)</li> <li>4. IAEA TRS457 – Dosimetry in Diagnostic Radiology: An International Code of Practice (2007)</li> <li>5. Toroi P et al, A tandem calibration method for kerma-air product meters, Physics in Medicine &amp; Biology 53 (2008) 4941-58</li> <li>6. Malusek A et al, In-situ calibration of clinical built-in KAP meters with traceability to a primary standard using a reference KAP meter, Physics in Medicine &amp; Biology 59 (2014) 7195-210</li> <li>7. Accompanying documentation and Instructions for Use for the system under test</li> </ol>
Instrumentation	Attenuating layer Dosimeter Tape measure Field-size measurement plate (FSMP)



Procedure	<p>For interventional and mobile systems in air</p> <ol style="list-style-type: none"> <li>1) Set maximum SID</li> <li>2) Adjust the table height so that it is approximately 50% distance between tube focus and detector</li> <li>3) Mount the FSMP in the beam</li> <li>4) Image the FSMP and adjust the collimators to achieve an imaged field size of approximately 10 x 10 cm</li> <li>5) Remove the FSMP and place the dosimeter on the central axis of the x-ray beam, without changing the collimation. The dosimeter can be placed at another point, different from the FSMP, and then the measured air kerma corrected to the FSMP distance through the inverse square law</li> <li>6) Place the attenuators as close to the image detector as possible, ensuring that they fully intercept the beam, to ensure the operating tube voltage is between 80-90 kVp</li> <li>7) Noting the <math>P_{KA}</math> display pre- and post-exposure, irradiate the dosimeter in both fluoroscopy and acquisition mode. Aim for an integrated air kerma in the range 10-100 mGy. Where relevant, note the air kerma rate during exposure and the displayed <math>P(t)_{KA}</math>.</li> <li>8) Multiply the integrated air kerma by the area to calculate the measured <math>P_{KA}</math> and <math>P(t)_{KA}</math> and compare with the displayed <math>P_{KA}</math> and <math>P(t)_{KA}</math>.</li> <li>9) For Acceptance testing, repeat steps 3-8 for the following variable conditions: <ol style="list-style-type: none"> <li>a. Repeat the initial set-up 3 times and determine the coefficient of variation</li> <li>b. Adjust the attenuator thickness to drive the x-ray system to 50-60 kVp and 100-110 kVp and repeat the measurements to verify the energy dependence</li> <li>c. For 80-90 kVp set a field size of approximately 5 x 5 cm and repeat the measurement to verify the field size dependence</li> </ol> </li> </ol> <p>Note: this test may also be conducted in a lateral beam projection. Systems with non-removable integral patient support</p> <ol style="list-style-type: none"> <li>1) Set maximum SID</li> <li>2) Remove the mattress</li> <li>3) Position the FSMP on the patient support</li> <li>4) Image the FSMP and adjust the collimators to achieve an imaged field size of approximately 10 x 10 cm</li> <li>5) Remove the FSMP and place the dosimeter at the same position on the central axis of the x-ray beam.</li> <li>6) Place the attenuator as close to the image detector as possible, ensuring that they fully intercept the beam, to ensure the operating tube voltage is between 80-90 kVp</li> <li>7) Noting the <math>P_{KA}</math> display pre- and post-exposure, irradiate the dosimeter in both fluoroscopy and acquisition and/or radiographic mode. Aim to achieve an integrated air kerma of approximately 10 mGy. Where relevant, note also the displayed <math>P_{KA}</math> rate and air kerma rate given by the dosimeter.</li> <li>8) Multiply the integrated dose by the area to calculate the measured <math>P_{KA}</math> and compare with the displayed <math>P_{KA}</math>. Repeat for the <math>P(t)_{KA}</math>.</li> <li>9) For Acceptance testing, repeat steps 3-8 for the following variable conditions: <ol style="list-style-type: none"> <li>a. Repeat the initial set-up 3 times and determine the coefficient of variation</li> <li>b. Adjust the attenuator thickness to drive the x-ray system to 50-60 kVp and 100-110 kVp and repeat the measurements to verify the energy dependence</li> <li>c. For 80-90 kVp set a field size of approximately 5 x 5 cm and repeat the measurement to verify the field size dependence</li> </ol> </li> </ol>
Evaluation	<p>Use the ratio of the measured to displayed values to ascertain a calibration factor. Following successful Acceptance, the MPE should assess whether or not a calibration factor should be applied to patient <math>P_{KA}</math> values, based upon the calibration factor measured. For constancy checking, if the calibration value differs from the baseline test an MPE decision should be made regarding further adjustment of patient dose values using <math>P_{KA}</math>.</p> <p><i>Note: For systems with non-removable integral patient support, attenuation of the couch has to be considered.</i></p>
Pass/Fail Criteria	<p>At Acceptance the <math>P_{KA}</math> value measured shall be within 35% of that displayed across all parameter variations. For consecutive tests, the calibration factor should not change by more than 5%.</p>
Frequency	<p>Acceptance testing Annual test (single point)</p>

#### B.4.2 Manufacturer specified Air-kerma rates

Aim	To determine the manufacturer specified air kerma rate and compare to the manufacturer's specification. To check display values
Reference	1. IEC 60601-2-54 "Particular requirements for the basic safety and essential performance of X-ray equipment for radiography and radioscopy" (2022) 2. Accompanying documentation and Instructions for Use for the system under test
Instrumentation	30 cm x 30cm slabs of PMMA up to at least 20 cm (check manufacturer's specification) Dosimeter
Procedure	1) Set up the attenuating layer, geometry and dosimeter position as instructed in the manufacturer's documents 2) Utilise an attenuating layer of 20cm PMMA or as instructed by the manufacturer if different from 20cm PMMA 3) Initiate fluoroscopy at the specified equipment settings and geometry 4) Measure the air kerma-rate and compare with the manufacturer's specification 5) If the manufacturer specifies target Air Kerma per frame for acquisition, at the manufacturer recommended equipment settings, measure the cumulative air kerma and the number of frames or measure the air kerma-rate and the frame-rate, then divide one by the other to get air kerma / frame and compare results with manufacturer's specification 6) Repeat the above procedure for all clinically relevant modes and FoV's where manufacturer's reference air kermas are provided. 7) If your dosimeter allows for simultaneous air kerma and air kerma rate recording, use the integrated air kerma from the above tests, adjusted to the Patient Entrance Reference Point, to compare with the displayed reference air kerma metric.
Evaluation	Compare against manufacturer's specification Compare to displayed values
Pass/Fail Criteria	Acceptance - within +/-50% of manufacturer's specification Constancy - remedial +/- 20% from baseline  $K_{a,ref}$ value measured shall be within 35% of that displayed across all parameter variations. Note: In practice, many units will perform with a constancy such that a 20% deviation from baseline may be viewed as excessive, in which case a local decision could be made to reduce the remedial level. It has been set at 20% as the minimum dose change likely to lead to a clinically detected image quality change.
Frequency	Acceptance test Annual test for displayed values only

#### B.4.3 Measurement of table and mattress attenuation

Aim	To determine, at acceptance, the attenuation of the manufacturer supplied tabletop and mattress and to compare with manufacturer supplied values. (This only applies to systems with integrated tables, not mobiles, although the MPE may wish to determine the attenuation of non-manufacturer supplied tables etc using a similar method)
Reference	Manufacturer specifications 1. IEC 60601-2-54 "Particular requirements for the basic safety and essential performance of X-ray equipment for radiography and radioscopy" (2022)
Instrumentation	Dosimeter Tape measure Attenuators (if using the x-ray equipment in a clinical mode)

Procedure	<p><u>Manual/Service Mode</u></p> <ol style="list-style-type: none"> <li>1) Set kV to 100 kV and ensure a beam HVL of approximately 3.6 mm Al</li> <li>2) Set for a single exposure of approximately 20 mAs</li> <li>3) Position the dosimeter such that the tabletop may be moved either between the dosimeter and the beam or such that it does not intercept the beam</li> <li>4) Measure the air kerma with no attenuators in the beam</li> <li>5) Measure the air kerma with the tabletop in the beam</li> <li>6) Measure the air kerma with either both the tabletop and mattress in the beam or the mattress in the beam on its own</li> <li>7) Calculate the attenuation for both the tabletop and mattress separately and, using a suitable spectrum generator, calculate the AI equivalence</li> </ol> <p><u>Clinical Mode</u></p> <ol style="list-style-type: none"> <li>1) Select a low filtration fluoroscopy mode</li> <li>2) Add attenuators to achieve the desired tube voltage [between about 80-100 kVp]</li> <li>3) Position the tabletop in the primary beam (without the mattress) and place the dosimeter on the beam entry side of the table in the centre of the primary beam - measure the air kerma rate from fluoroscopy and the focus-dosimeter distance.</li> <li>4) Keep the tabletop in the beam and move the dosimeter to the beam exit side of the table - measure the air kerma rate and the focus-dosimeter distance.</li> <li>5) Repeat steps 3 and 4 with the mattress on the tabletop</li> <li>6) Calculate the attenuation for both tabletop and mattress separately and, using a suitable spectrum generator, calculate the AI equivalence.</li> </ol> <p><i>Note: for the clinical mode remember to use the inverse square law to adjust the air kerma rates to a single distance before calculating the attenuation.</i></p>
Evaluation	<p>Compare the AI equivalence derived for both the tabletop and mattress to the manufacturers supplied figures.</p> <p>Ensure that the manufacturers supplied figures are less than or equal to the values in IEC 60601-2-54 Table 203.104.</p>
Pass/Fail Criteria	<p>At acceptance the derived AI equivalence should be within 20% of the manufacturer supplied figures and less than or equal to the values in IEC 60601-2-54 Table 203.104</p>
Frequency	<p>Acceptance test</p>

#### B.4.4 Limiting Air Kerma Rate

Aim	<p>To determine the manufacturer specified limiting air kerma rate and compare to the manufacturer's specification.</p>
Reference	<ol style="list-style-type: none"> <li>1. National regulations (where such exist)</li> <li>2. IEC 60601-2-54 "Particular requirements for the basic safety and essential performance of X-ray equipment for radiography and radioscopy" (2022)</li> <li>3. Local Protocol Set-up</li> </ol>
Instrumentation	<p>30 cm x 30 cm slabs of PMMA up to at least 20 cm (check manufacturer's specification) Dosimeter</p>
Procedure	<ol style="list-style-type: none"> <li>1) Set up the test as per B.4.2 (acceptance) or B.3.2 (constancy)</li> <li>2) Add a Pb apron or similar attenuating layer to the existing PMMA</li> <li>3) Initiate fluoroscopy at the normal and High Level Control (HLC) fluoroscopy modes, ensuring the radiographic factors have reached maximum value.</li> <li>4) Measure the dose-rate and adjust the values using the inverse square law to 30cm in front of the accessible entrance of the detector.</li> </ol>
Evaluation	<p>Compare against manufacturer's set-up and IEC limits.</p> <p><i>Note: some equipment may be locally set to have a lower limiting air kerma than the IEC limits - if so, compare your results to these local values.</i></p>

Pass/Fail Criteria	Acceptance: $\leq$ manufacturer set-up or 88 mGy/min for normal fluoroscopy or 176 mGy/min HLC fluoroscopy mode. Constancy: as above
Frequency	Acceptance test Annual test

## B.5. SKIN DOSE MAPS

### B.5.1 Skin dose map – Acceptance

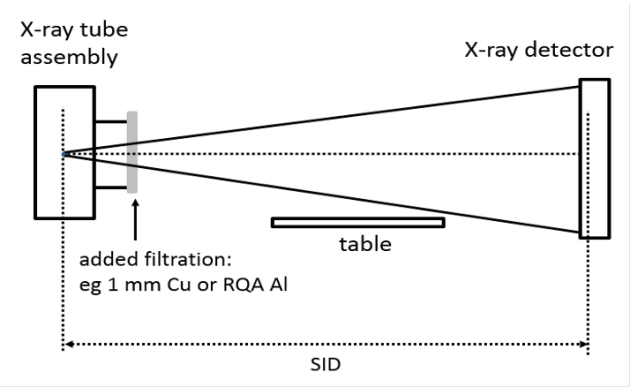
Aim	To verify that the SDM software gives results that are consistent with the model employed by the software
Reference	Manufacturer specifications
Instrumentation	Manufacturer model Phantom to simulate a patient
Procedure	<p>2) Place the phantom on the table.</p> <p>3) Irradiate the phantom using the following conditions and for each step record the level of exposure (<math>K_a, r</math>) that is displayed on the system, as well as all the other parameters used by the SDM software:</p> <ol style="list-style-type: none"> <li>A few simple angulations.</li> <li>Angulations that generate beam overlap.</li> <li>Vary table height and lateral/longitudinal positions.</li> <li>Vary beam quality (kV/filtration)</li> <li>Vary FoV.</li> </ol>
Evaluation	For each step, calculate what the system would give using the method implemented by the SDM software and compare with the SDM software display.
Pass/Fail Criteria	NA
Frequency	Acceptance test

### B.5.2 Skin dose map – Commissioning

Aim	To evaluate the agreement between the dose values reported by the SDM software and the actual PSD
Reference	Not Available
Instrumentation	Real patients or phantom to simulate a patient Dosimeter (e.g., radiochromic films, point detector, grid of point detectors)
Procedure	<p>Verification of patient dose</p> <p>1) Place the dosimeter in the area of the patient skin that will be exposed during the procedure</p> <p>Verification of phantom dose</p> <p>1) Place the phantom on the table.</p> <p>2) Place a suitable dosimeter on the phantom's surface that will be most irradiated during the evaluation.</p> <p>3) Irradiate the phantom using the following conditions:</p> <ol style="list-style-type: none"> <li>Angulations that generate beam overlap.</li> <li>Vary table height and lateral/longitudinal positions.</li> <li>Vary beam quality (kV/filtration)</li> <li>Vary FoV.</li> </ol>
Evaluation	Compare measured results with calculated results by the SDM software.
Pass/Fail Criteria	NA
Frequency	Acceptance test

## B.6. DETECTOR

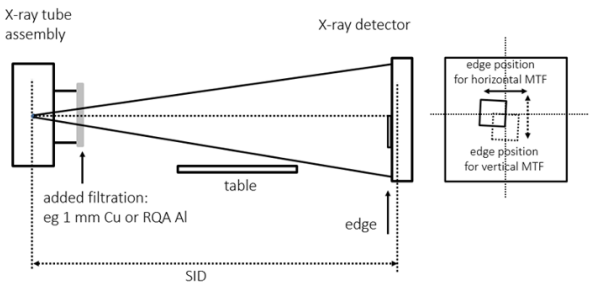
### B.6.1 Response Function

Aim	To assess the response of the X-ray image detector in terms of output pixel value as incident air kerma/image at the detector entrance is varied.
Reference	<ol style="list-style-type: none"> <li>1. IEC 62220-1-1. Medical electrical equipment - Characteristics of digital X-ray imaging devices - Part 1-1: Determination of the detective quantum efficiency - Detectors used in radiographic imaging; 2015</li> <li>2. IEC 62220-1-3. Medical electrical equipment - Characteristics of digital X-ray imaging devices - Part 1-3: Determination of the detective quantum efficiency - Detectors used in dynamic imaging. Geneva, Switzerland; 2008.</li> <li>3. Mackenzie A, Doshi S, Doyle P, Hill A, Honey I, Marshall NW, et al. IPEM Report 32 (Part VII) Measurement of the performance characteristics of diagnostic x-ray systems: digital imaging systems. York, UK; 2010.</li> </ol>
Instrumentation	Dosimeter Validated software for calculation of parameters Filters (1 mm or 2mm Cu or 21 mm Al)
Procedure	<ol style="list-style-type: none"> <li>1) Set a suitable mode for physical image quality measurements (e.g., User Quality Control Mode, or a clinical mode with no clinical image processing applied). The mode must give the user control over the tube load (mAs) and the tube voltage; the mode must acquire and store images without clinical image processing ('For Processing' or equivalent) and without compression or resizing the images.</li> <li>2) Note the imaging mode (Fluoroscopy, Cardiac or Series Mode) and detector gain mode if known.</li> <li>3) Set the geometry for the physical image quality measurements. Figure 11 shows a lateral arrangement suitable for measurement of the detector response function and NNPS</li> <li>4) Set the SID to represent clinical practice - use the same SID as was used for image receptor incident air-kerma (IR-IAK) rate measurements. Be consistent with the previously performed detector response test</li> </ol> <div data-bbox="503 1320 1128 1710" style="border: 1px solid black; padding: 10px; margin: 10px 0;">  </div> <p><i>Figure 11. Typical setup geometry used for detector verifications.</i></p> <ol style="list-style-type: none"> <li>5) Open the collimators fully and ensure the beam shaping filters are not visible in the image.</li> <li>6) Position the dosimeter on axis, record the source-to-dosimeter distance and calculate the inverse square correction to the detector input plane</li> </ol>

Procedure	7) Remove the anti-scatter grid if possible					
	8) Set the beam quality for the evaluation:					
	Radiation Quality	kV	Additional filtration	Approx mean energy (keV)	HVL (mm Al)	Photons (mm <sup>-2</sup> μGy <sup>-1</sup> ) i.e., SNR <sub>in</sub> <sup>2</sup>
	RQA 3	50	10.0 mm Al	40.3	4.0	21759
	RQA 5	70	21.0 mm Al	53.3	7.1	30174
	RQA 7	90	30.0 mm Al	64.0	9.1	32362
	RQA 9	120	40.0 mm Al	77.0	11.5	31077
	IPEM 70	70	1.0 mm Cu	56.6	-7.9	-32300
	IPEM 70	70	2.0 mm Cu	60.1	-9.0	-33820
	9) Establish the tube current and pulse length settings required for the “normal” level for the Imaging Mode and also to cover the image detector incident air kerma/image range:					
		Fluoroscopy (Imaging Mode 1)	Cardiac imaging (Imaging Mode 2)	Series Imaging/DSA (Imaging Mode 3)		
“normal” level		20 nGy/im	200 nGy/im	2000 nGy/im		
IR-IAK/image range for detector response		0 (dark); 5 to 80 nGy/im	0 (dark); 50 to 800 nGy/im	0 (dark); 500 to 8000 nGy/im		
IR-IAK /image for NPS and lag		6 nGy, 20 nGy and 64 nGy	60 nGy, 200 nGy and 640 nGy	600 nGy, 2000 nGy and 6400 nGy		
IR-IAK /image for MTF		64 nGy	640 nGy	6400 nGy		
Tot No. of consecutive images		≥128	≥128	approximately 12		
10) Remove the dosimeter.						
11) At each IR-IAK /image level (tube current and pulse length setting), acquire the required number of images.						
12) Store the images after each fluoroscopy sequence.						
13) Repeat i.e., change the mAs and acquire series until the IR-IAK /image range is covered						
14) Repeat for the other imaging modes if evaluating them e.g., Cardiac Mode, Series Mode)						
15) Transfer the series for analysis (e.g., USB drive or network).						
Evaluation:	1) For each imaging mode evaluated, there will be a series of images for the response function, acquired at the IR-IAK /image levels relevant to that mode.					
	2) Calculate mean and variance of pixel values in a 5x5 mm ROI at the image centre for the whole sequence to see where the pixel values and variance have stabilised/plateaued. Select the images(s) for analysis from a stable part of the sequence (as a guide, the first 10 images should be skipped).					
	3) Measure the mean pixel value (MPV) in a region of interest (ROI) of 5 x 5 mm at the centre of the irradiated field.					
	4) Do this for all the series acquired i.e., all the IR-IAK /image levels					
	5) Plot MPV versus IR-IAK/image and fit the model function (typically linear, logarithmic or power). For example, versus air kerma (IR-IAK /image): MPV = A + B × K, or MPV = A + B × exp(K) or MPV = A + B <sup>C</sup>					
	6) Record the fit coefficients (A, B, C etc) and the correlation coefficient for the curve fit (R <sup>2</sup> ). Track these over the lifetime of the image detector					

Pass/Fail Criteria	There should be a simple, monotonic relationship between IR-IAK/image and output pixel value. Expect $R^2 > 0.99$
Frequency	Commissioning: if possible, assess response function for one example each of Fluoroscopy, Cardiac and Series imaging. Annual: evaluate response function for one fluoroscopy mode (either in User QC Mode, or for a commonly used fluoroscopy mode).

### B.6.2 Detector presampling Modulation Transfer Function (MTF)

Aim	To assess sharpness of images produced by the image detector using the pre-sampling MTF
Reference	<ol style="list-style-type: none"> <li>Cunningham IA. Applied Linear-Systems Theory. In: Jacob Beutel, editor. Medical Imaging Volume 1 Physics and Psychophysics. Bellingham: SPIE - The International Society for Optical Engineering; 2000. p. 79-156</li> <li>Samei E, Ranger NT, Dobbins JT, Chen Y. Intercomparison of methods for image quality characterization. I. Modulation transfer function. Med Phys. 2006;33(5):1454-65</li> </ol>
Instrumentation	Dosimeter, validated software for calculation of parameters, filters (1 mm or 2mm Cu or 21 mm Al), radio-opaque edge of dimension $\geq 5 \times 5$ cm, with straight, sharp edges.
Procedure	<ol style="list-style-type: none"> <li>Set a suitable mode for physical image quality measurements (e.g., User Quality Control Mode, or a clinical mode with no clinical image processing applied).</li> <li>Note the imaging mode (Fluoroscopy, Cardiac or Series Mode) and detector mode if known.</li> <li>Set the geometry for the MTF measurements</li> <li>Set SID to represent clinical practice (be consistent with previous year).</li> </ol> <div style="text-align: center;">  </div> <p><b>Figure 12. Typical setup geometry used for modulation transfer function assessment.</b></p> <ol style="list-style-type: none"> <li>Remove the anti-scatter grid if possible.</li> <li>Set the beam quality for the evaluation (see B.6.1)</li> <li>Set the tube current and pulse width settings required for MTF evaluation IR-IAK /image level (see B.6.1).</li> <li>Position the edge test device to measure the horizontal or vertical MTF, as desired. Rotate the edge to give an angle of <math>1.5^\circ</math> to <math>3.0^\circ</math> between the edge and the pixel matrix columns or rows.</li> <li>If possible, set the smallest focus.</li> <li>Set largest FoV.</li> <li>Acquire the sequence of images.</li> <li>Store the images after each fluoroscopy sequence.</li> <li>Reposition the edge to measure the MTF in the orthogonal direction.</li> <li>Acquire the sequence of images.</li> <li>Repeat for all other FoVs.</li> </ol>

Evaluation	<ol style="list-style-type: none"> <li>1) Linearize the images containing the edge image using the response function (section B.6.1).</li> <li>2) Calculate the horizontal and vertical MTF curves. It may be necessary to average a number of MTF curves calculated from different images in the sequence if image noise is high</li> <li>3) Record spatial frequencies at which the MTF has fallen to 0.5 (MTF<sub>0.5</sub>) and 0.1 (MTF<sub>0.1</sub>).</li> <li>4) Repeat calculations for all FoV.</li> </ol>
Pass/Fail Criteria	The measured MTF for the image detector should correspond to reference MTF data provided by the manufacturer, for a given FOV and Imaging Mode. MTF <sup>0.5</sup> and MTF <sup>0.1</sup> should be within $\pm 0.2 \text{ mm}^{-1}$ of the baseline value.
Frequency	Acceptance test(all FoVs).

### B.6.3 Image detector Brightness Non Uniformity (BNU)

Aim	To assess the uniformity of brightness across the image detector and check for presence of artefacts
Reference	<ol style="list-style-type: none"> <li>1. Mackenzie A, Doshi S, Doyle P, Hill A, Honey I, Marshall NW, et al. IPEM Report 32 (Part VII) Measurement of the performance characteristics of diagnostic x-ray systems: digital imaging systems. York, UK; 2010</li> <li>2. Marshall NW, Mackenzie A, Honey ID. Quality control measurements for digital x-ray detectors. Phys Med Biol. 2011; 56(4).</li> </ol>
Instrumentation	Dosimeter, validated software for calculation of parameters, filters (1 mm or 2mm Cu or 21 mm Al)
Procedure	<ol style="list-style-type: none"> <li>1) Acquire a sequence using the setup for the response function but using the largest FoV. If doing this, use a clinically relevant IR-IAK/image. Alternatively, use a sequence obtained for the response function measurement that has a clinically relevant IR-IAK/image for the BNU calculation.</li> <li>2) This IR-IAK/image level should be used for the BNU evaluation throughout the lifetime of the detector unless there is a large change in the set (target) IR-IAK /image.</li> </ol>
Evaluation	<ol style="list-style-type: none"> <li>1) Linearize the image to air kerma using the response function.</li> <li>2) Extract a centrally positioned ROI from the image. The ROI should cover most of the FoV, leaving a gap of ~1 cm at the image edge.</li> <li>3) From this large ROI, extract 20 x 20 mm half-overlapping small ROIs.</li> <li>4) Within each small ROI, calculate the mean pixel value (<math>\bar{S}</math>) of the pixel values.</li> <li>5) Record the value of (<math>\bar{S}</math>) at the ROI position and repeat for all ROIs extracted from the large ROI.</li> <li>6) Calculate the maximum (<math>\bar{S}_{max}</math>), minimum (<math>\bar{S}_{min}</math>) and average (<math>\bar{S}_{avg}</math>) value of the small ROIs and then calculate the BNU: <math display="block">BNU = \frac{\bar{S}_{max} - \bar{S}_{min}}{\bar{S}_{avg}} \times 100\%</math> </li> <li>7) Examine the image for artefacts, especially for signs of flat-fielding artefacts.</li> </ol>
Pass/Fail Criteria	Signal brightness should be uniform across the image; BNU should be <10%. No artefacts visible.
Frequency	Commissioning: all FoVs for systems with FoV-specific flat field correction, else only largest FoV Annual test: Largest FoV



#### B.6.4 Variance and SNR Image

Aim	To assess the global uniformity of the image noise and check for presence of artefacts
Reference	<ol style="list-style-type: none"> <li>1. Mackenzie A, Doshi S, Doyle P, Hill A, Honey I, Marshall NW, et al. IPEM Report 32 (Part VII) Measurement of the performance characteristics of diagnostic x-ray systems: digital imaging systems. York, UK; 2010</li> <li>2. Marshall NW, Mackenzie A, Honey ID. Quality control measurements for digital x-ray detectors. Phys Med Biol. 2011;56(4).</li> <li>3. Monnin P, Bosmans H, Verdun FR, Marshall NW. Comparison of the polynomial model against explicit measurements of noise components for different mammography systems. Phys Med Biol. 2014;59(19)</li> </ol>
Instrumentation	Dosimeter, validated software for calculation of parameters, filters (1 mm or 2 mm Cu or 21 mm Al)
Procedure	Use the image sequence acquired for the BNU test.
Evaluation	<ol style="list-style-type: none"> <li>1) Linearize the image to air kerma using the response function.</li> <li>2) Extract a centrally positioned ROI from the image. The ROI should cover most of the FoV, i.e., leaving a gap of ~1 cm at the image edge.</li> <li>3) From this large ROI, extract 2 x 2 mm half-overlapping small ROIs.</li> <li>4) Within each small ROI, calculate the mean pixel value (<math>\bar{S}</math>), variance (<math>\sigma^2</math>) and standard deviation (<math>\sigma</math>) of the pixel values.</li> <li>5) Record the value of <math>\sigma^2</math> and <math>SNR = \bar{S}/\sigma</math> at the ROI position and repeat for all small ROIs extracted from the large ROI, to generate the variance and SNR images.</li> <li>6) Examine the variance image for signs of artefacts; regions with reduced variance that could indicate blurring in the X-ray converter; regions with increased variance that could indicate regions with increased electronic noise or artefacts.</li> </ol>
Pass/Fail Criteria	The variance should change smoothly across the image with no abrupt changes and no visible artefacts
Frequency	Acceptance test Annual test

#### B.6.5 Noise Decomposition using Variance

Aim	To quantify the relative contribution of electronic (additive), quantum and structure (multiplicative) noise sources to total noise (variance)
Reference	<ol style="list-style-type: none"> <li>1. Monnin P, Bosmans H, Verdun FR, Marshall NW. Comparison of the polynomial model against explicit measurements of noise components for different mammography systems. Phys Med Biol. 2014;59(19)</li> <li>2. Marshall NW, Kotre CJ, Robson KJ, Lecomber AR. Receptor dose in digital fluorography: A comparison between theory and practice. Phys Med Biol. 2001;46(4).</li> <li>3. Mackenzie A, Honey ID. Characterization of noise sources for two generations of computed radiography systems using powder and crystalline photostimulable phosphors. Med Phys [Internet]. 2007;34(8):3345-57. Available from: <a href="http://doi.wiley.com/10.1118/1.2750973">http://doi.wiley.com/10.1118/1.2750973</a></li> </ol>
Instrumentation	Dosimeter, validated software for calculation of parameters, filters (1 mm or 2 mm Cu or 21 mm Al)
Procedure	Use the image series acquired for the response function (preferably a fluoroscopy sequence as this is likely to have the largest contribution of electronic noise).

Evaluation	<ol style="list-style-type: none"> <li>1) Measure the variance in a 5 x 5 mm ROI at the centre of the FoV.</li> <li>2) Do this for all the series acquired i.e., all the IR-IAK/image levels.</li> <li>3) Plot variance as a function of IR-IAK /image</li> <li>4) Fit a 2<sup>nd</sup> order polynomial curve to the variance, weighting the variance data points by 1/(IR-IAK/image)<sup>2</sup> when performing the curve fit. In this model, total variance is the sum of variance due to electronic, quantum and structure noise sources.             <math display="block">\sigma^2 = \sigma_e^2 + \sigma_q^2 + \sigma_s^2</math> <math display="block">\sigma^2 = e + q \text{ IRIAK} + s \text{ IRIAK}^2</math> </li> <li>5) Record the fit coefficients for electronic (e), quantum (q) and structure noise (s) (variance) – track these coefficients over the lifetime of the Image detector.</li> <li>6) Using the fit coefficients, calculate the electronic, quantum and structure variance at each IR-IAK level.</li> <li>7) For each IR-IAK level, calculate the fraction of variance for each source (e, q and s) compared to the total variance. Quantum noise should form the largest fraction of total image noise at the standard clinical IRIAK/image for the imaging mode tested.             <ol style="list-style-type: none"> <li>a. Electronic noise is dominant from an IR-IAK /image given by e/q</li> <li>b. Structure noise is dominant from an IR-IAK /image given by q/s</li> </ol> </li> <li>8) Repeat the curve fitting for other imaging modes (fluoroscopy, cardiac imaging, and series imaging) if tested.</li> </ol>
Pass/Fail Criteria	There should be a simple relationship between variance and IR-IAK; variance should be described by the three noise components. At typical IR-IAK /image for each imaging mode, quantum variance should form >50% of total variance.
Frequency	Commissioning: Fluoroscopy, Cardiac or Series Modes (using the relevant response function) Annual: Fluoroscopy mode.

### B.6.6 Noise Power Spectrum (NPS)

Aim	To assess the magnitude of noise power as a function of spatial frequency
Reference	<ol style="list-style-type: none"> <li>1. Granfors PR, Aufrichtig R, Possin GE, Giambattista BW, Huang ZS, Liu J, et al. Performance of a 41x41 cm<sup>2</sup> amorphous silicon flat panel x-ray detector designed for angiographic and R&amp;F imaging applications. Med Phys. 2003;30(10):2715-26.</li> <li>2. Dobbins JT, Samei E, Ranger NT, Chen Y. Intercomparison of methods for image quality characterization. II. Noise power spectrum. Med Phys [Internet]. 2006;33(5):1454. Available from: <a href="http://doi.wiley.com/10.1118/1.2188819">http://doi.wiley.com/10.1118/1.2188819</a></li> </ol>
Instrumentation	Dosimeter, validated software for calculation of parameters, filters (1 mm or 2 mm Cu or 21 mm Al)
Procedure	<ol style="list-style-type: none"> <li>1) The images obtained for the response function are used for the NPS calculation.</li> <li>2) Select the IR-IAK /level for which the NPS will be calculated: this IR-IAK /image should match the value used clinically for the imaging mode selected. This IR-IAK/image should be used for NPS evaluation throughout the lifetime of the detector unless there is a large change in the IR-IAK/image used clinically.</li> </ol>
Evaluation	<ol style="list-style-type: none"> <li>1) To calculate the NPS, select the image sequence acquired at the relevant IR-IAK level.</li> <li>2) Extract a large region from the image centre (e.g. 576 x 576 from a 1024 x 1024 image).</li> <li>3) It is typical in NPS algorithms to remove large area intensity trends that are present in the region used to calculate the NPS, a process often referred to as 'de-trending'. One means of achieving this is to fit a 2D polynomial surface to this region and then subtracting this 2D surface from the region</li> <li>4) Extract NPS ROIs of 128 x 128 pixels from this large region in a half-overlapping pattern and apply the NPS algorithm to these ROIs (Dobbins et al., 2006).</li> <li>5) Once the 2D NPS has been calculated, obtain 1D sections of the NPS along the 0° and 90° Fourier axes, corresponding to the horizontal and vertical directions across the detector. The NPS should be sectioned, 7 bins on each side of the axis, but the on-axis NPS values should be excluded.</li> <li>6) Normalise the NPS: divide by mean (linearized pixel value)<sup>2</sup> of the region used for the NPS analysis. Most software will do this automatically or give this as an option.</li> <li>7) Record the NNPS at 0.5 mm<sup>-1</sup> and 2 mm<sup>-1</sup> (or 1.5 mm<sup>-1</sup> for a binned mode)</li> <li>8) At the Commissioning stage consider assessing the NPS at the additional IR-IAK levels i.e., 1/3.2 and 3.2 times the normal value for the Imaging Mode chosen.</li> </ol>

Evaluation	Note: NNPS is likely to be subject to the influence of lag which will reduce NNPS compared to a measurement made without the presence of lag. This lag can originate within the Image detector (the X-ray converter layer and the pixels) or may also include some form of applied post processing (frame averaging or recursive temporal filtering).
Pass/Fail Criteria	Record the normalised NPS (NNPS) at 0.5 mm <sup>-1</sup> and 2 mm <sup>-1</sup> (or 1.5 mm <sup>-1</sup> for a binned mode). NNPS at these frequencies should be within ±15% of the baseline value Annual test
Frequency	Commissioning: Fluoroscopy, Cardiac or Series Modes (using the relevant response function) Annual test: Fluoroscopy mode.

## B.7. IMAGE QUALITY

### B.7.1 Signal-to-noise ratio rate, $SNR^2_{rate}$

Aim	To estimate Signal-to-noise ratio <sup>1</sup> rate $SNR^2_{rate}$ using a model observer
Reference	<ol style="list-style-type: none"> <li>1. Tapiovaara, M. J. (1993) SNR and noise measurements for medical imaging: II. Application to fluoroscopic x-ray equipment. <i>Phys. Med. Biol</i>, 38, pp. 1761-1788.</li> <li>2. Tapiovaara, M. J. (2003) Objective measurement of image quality in fluoroscopic x-ray equipment: FluoroQuality. STUK-A196 / MAY 2003.</li> <li>3. Tapiovaara M.J. and Sandborg M How should low-contrast detail detectability be measured in fluoroscopy? <i>Medical Physics</i> 31(9) 2564-2576, (2004) doi: 10.1118/1.1779357</li> <li>4. Tesselaar, E. and Sandborg, M. (2016) Assessing the usefulness of the quasi-ideal observer for quality control in fluoroscopy. <i>Radiation Protection Dosimetry</i>, 169(1), pp. 360-364. doi: 10.1093/rpd/ncv434.</li> <li>5. Elgström, H., Tesselaar, E. and Sandborg, M. (2021) Signal-to-noise ratio rate measurements in fluoroscopy for quality control and teaching good radiological technique. <i>Radiation Protection Dosimetry</i>, 195(3-4), pp. 407-415. doi: 10.1093/rpd/ncaa222.</li> </ol>

<sup>1</sup> Please note that the signal in B.7.1 is really a difference between the signal behind the test object and the signal in the background beside the test object. It could therefore be denoted SDNR, but in order to keep the same notation as in references 1-5 we use SNR.

Instrumentation	<p>Patient simulating material</p> <p>Setup 1: PMMA or equivalent slabs from 5 to 30 cm (at least 30 x 30 cm<sup>2</sup> area)</p> <p>Setup 2: Cu sheets of a range of thicknesses e.g., 0.5, 1, 2, 3 mm thick etc, large enough to cover the whole x-ray beam at the collimator</p> <p>TIQ test object</p> <p>One or more small, well-defined target(s) are needed that can be added/removed from the tissue simulating phantom without moving the phantom.</p> <p>Size: 1 to 10 mm effective diameter</p> <p>Composition: e.g., aluminium, iron, iodine simulating material, a stent, bone simulating material.</p> <p>Thickness: sufficient to generate a signal that is clearly visible over a range of patient phantom thicknesses.</p> <p>Software</p> <p>Software (MATLAB-script) to compute <math>SNR^2_{rate}</math> can be obtained (for non-commercial use) from the EFOMP website. The software must not be used on patients as it is not a medical device.</p>
-----------------	---

Procedure	<p><u>TIQ using scattering phantom and ‘system’ geometry (setup 1)</u></p> <ol style="list-style-type: none"> <li>1) Establish how many fluoro images the system can store from a single run (consult the system manual). Approximately 1000 images are recommended. If only a smaller number of images can be stored, then several sequences should be acquired and appended during the analysis. Make sure not to include the first images that are used to stabilise the acquisition.</li> <li>2) Remove the mattress and align the patient simulating phantom with the central beam axis, select the fluoroscopy mode or acquisition program to be tested, FoV, source-image distance (SID), and table height.</li> <li>3) Place the detail test object at the required position within the FoV e.g., on top of the PMMA. See Figure 3b.</li> <li>4) Perform an initial fluoroscopy sequence so the system selects the x-ray factors for the TIQ phantom.</li> <li>5) Record the air kerma-area product (<math>P_{KA}</math>) before the image sequence.</li> <li>6) Perform the imaging and store the image sequence. Record the acquisition parameters: program/mode, pulse rate, tube voltage, tube current, pulse width, spectral pre-filter, etc. or consult the DICOM header or structured report information.</li> <li>7) Record the air kerma-area product (<math>P_{KA}</math>) after the image sequence and the fluoroscopy run time (t). Compute the <math>P(t)_{KA}</math> by <math>(P(t)_{KA} - P(t)_{KA})/t</math>.</li> <li>8) Remove the detail test object, repeat the fluoroscopy sequence to acquire the signal absent images and store the image sequence. Ensure the system selects the same kV, mA, added filtration etc. as used for the signal present sequence. This step is not required if background ROIs are extracted next to the detail(s) in the signal present sequence.</li> <li>9) Repeat for other imaging protocols and FoVs as needed.</li> </ol> <p><u>TIQ using ‘detector’ geometry (setup 2)</u></p> <ol style="list-style-type: none"> <li>1) Position the test object detail directly on the x-ray detector housing with the x-ray tube positioned at the top (Figure 3a). This method is suited for mobile C-arm systems but could also be used for fixed installations. Use 2 mm copper sheet mounted on the x-ray beam collimator instead of PMMA to attenuate the beam to match that for a normal-sized patient. Use 0.5 mm Cu for mini-C-arms.</li> <li>2) Follow steps 4-9 from Setup 1 to compute the <math>SNR_{rate}^2</math> for the ‘detector’ setup</li> </ol>
	<p>Compute the <math>SNR_{rate}^2</math> and associated uncertainty using the Matlab-analysis software. Typical uncertainty is 4-7% (<math>1 \pm</math> standard deviation) using 1024 images in a sequence.</p>
Pass/Fail Criteria	$SNR_{rate}^2$ should be within $\pm 20\%$ of the baseline value for the acquisition program and dose mode measured at Commissioning
Frequency	Commissioning Annual test (one clinically relevant set-up)

### B.7.2 Threshold-contrast detail detectability (TCDD) – Statistical method

Aim	To estimate TCDD in the form of $C_{TSM}$ using the statistical method
Reference	1. Paruccini, N. et al. (2021) ‘A single phantom, a single statistical method for low-contrast detectability assessment’, Physica Medica, 91(October), pp. 28-42. doi: 10.1016/j.ejmp.2021.10.007
Instrumentation	<p>Patient simulating material PMMA or equivalent slabs from 5 to 30cm (at least 30 x 30 cm<sub>2</sub> area) Cu sheets of a range of thicknesses e.g., 0.5, 1, 2, 3 mm thick etc and large enough to cover the whole x-ray beam at the collimator.</p> <p>TIQ test object An aluminium plate of size 3 cm x 3 cm and thickness <math>0.5 \pm 0.02</math> mm thick, of purity 99.9%. A step wedge with 5 steps, with thickness ranging from 0.25 to 1.25 mm in <math>0.25 \pm 0.01</math> mm steps, each step has x-y size 0.6 cm x 0.8 cm. The step wedge is used to convert contrasts defined in pixel values to equivalent Aluminium (mm).</p> <p>Software Software can be obtained from LCD-lab.org for non-commercial use. The software must not be used on patients as it is not a medical device.</p>

Procedure	<p><u>TIQ using scattering phantom and 'system' geometry</u></p> <ol style="list-style-type: none"> <li>1) Remove the mattress and select the fluoroscopy mode or acquisition program to be tested, FoV.</li> <li>2) Place the patient simulating material on the table and the statistical method test object on top of the phantom or on the entrance side (see Figure 3b).</li> <li>3) Adjust table height so that the scattering phantom is at the system isocenter.</li> <li>4) Adjust SID so there is a 5 cm gap between PMMA phantom and detector housing.</li> <li>5) Once setup, perform an initial fluoroscopy sequence so the system selects the x-ray factors for the TIQ phantom.</li> <li>6) Perform fluoroscopy or series acquisition in order to obtain at least 30 images for the TIQ analysis.</li> <li>7) Save the fluoroscopy images.</li> <li>8) Transfer the images and compute <math>C_{TSM}</math></li> </ol> <p><u>TIQ using 'detector' geometry</u></p> <ol style="list-style-type: none"> <li>1) Position the test object detail directly on the x-ray detector housing with the x-ray tube positioned at the top (Figure 3a). This method is suited for mobile C-arm systems but could also be used for fixed installations.</li> <li>2) Select the fluoroscopy mode or acquisition program to be tested, FoV, source-image distance, and SID (this is normally fixed on a mobile C-arm).</li> <li>3) Add copper sheets at the x-ray tube collimator until x-ray factors (kV, mA, ms, focus, pre-filter etc) match those for a normal-sized patient.</li> <li>4) Record the x-ray factors.</li> <li>5) Perform fluoroscopy or series acquisition in order to obtain at least 30 images for analysis. Save the fluoroscopy images.</li> <li>6) Repeat other imaging protocols and FoVs as needed.</li> <li>7) Transfer the images and compute <math>C_{TSM}</math></li> </ol>
Evaluation	<p>Analysis can be carried out with the dedicated software. Alternatively, the following steps should be implemented.</p> <ol style="list-style-type: none"> <li>1) Define a main ROI of <math>120 \times 120</math> pixels within a large aluminium region.</li> <li>2) Extract a series of smaller ROIs (sub-ROIs) with a binning size starting from <math>2 \times 2</math> pixels.</li> <li>3) For a given sub-ROI size (<math>d \times d</math>), calculate the means of all the sub-ROIs (<math>\bar{x}</math>), generate the histogram of the mean values and take the standard deviation of this distribution (<math>\sigma_x</math>).</li> <li>4) Calculate the threshold contrast for the statistical method (<math>C_{TPV}</math>) in terms of pixel values, defined using the 95% confidence level as:             <math display="block">C_{TPV}(d) = 3.29 \sigma_x(d)</math> </li> <li>5) Repeat for the range of sub-ROI sizes, e.g., from <math>2 \times 2</math> to <math>24 \times 24</math></li> <li>6) Convert the raw threshold contrast values to Aluminium thickness equivalent. Measure the mean pixel value in each step of the Al step wedge and plot against Al thickness. Apply a linear regression between mean pixel value and Al thickness for each image in the series and record the slope (<math>m</math>). Calculate the threshold contrast for the statistical method (<math>C_{TSM}</math>) in terms of Al (mm) as:             <math display="block">C_{TSM}(d) = C_{TPV}(d) * m</math> </li> </ol> <p>where <math>m</math> is the slope from the fit of MPV and Al (mm)</p> <ol style="list-style-type: none"> <li>7) A minimum of 25 sub-ROIs should be extracted for each sub-ROI size to give a minimum level of precision for the measurement.</li> </ol>
Pass/Fail Criteria	$C_{TSM}$ should be within $\pm 20\%$ of the baseline value for the imaging protocol /dose mode.
Frequency	Commissioning Annual test

### B.7.3 Threshold-contrast detail detectability (TCDD) – CHO readout

Aim	To estimate TCDD ( $C_{TCHO}$ ) using a CHO readout of the Leeds C-D test objects
Reference	<ol style="list-style-type: none"> <li>Bertolini, M. et al. (2019) 'Characterization of GE discovery IGS 740 angiography system by means of channelized Hotelling observer (CHO)', Physics in Medicine and Biology. IOP Publishing, 64(9). doi: 10.1088/1361-6560/ab144c.</li> <li>Favazza, C. P. et al. (2015) 'Implementation of a channelized Hotelling observer model to assess image quality of x-ray angiography systems', Journal of Medical Imaging, 2(1), p. 015503. doi: 10.1117/1.JMI.2.1.015503.</li> <li>Ortenzia, O. et al. (2020) 'Radiation dose reduction and static image quality assessment using a channelized hotelling observer on an angiography system upgraded with clarity IQ', Biomedical Physics and Engineering Express. IOP Publishing, 7(2). doi: 10.1088/2057-1976/ab73f6.</li> </ol>
Instrumentation	<p><u>Patient simulating material</u>          PMMA or equivalent slabs from 5 to 30 cm (at least 30 x 30 cm<sup>2</sup> area)          Cu sheets of a range of thicknesses e.g., 0.5, 1, 2, 3 mm thick and large enough to cover the whole x-ray beam at the collimator.</p> <p><u>TIQ test object</u>          Use the available TO (e.g., Leeds TO10 or TO12 for fluoroscopy and angiography, or Leeds TO16 or TO20 only for angiography acquisitions). Detail diameters from rows from 4.0 mm to 0.35 mm diameter should be used for the analysis.</p> <p><u>Software</u>          Software (MATLAB-script) to compute the contrast detail curves can be obtained (for non-commercial use) from the EFOMP website.</p>
Procedure	<p><u>TIQ using scattering phantom and 'system' geometry</u></p> <ol style="list-style-type: none"> <li>Approximately 400 images are required for the CHO calculation. If the system can only store a smaller number of images, then acquisitions should be repeated and the images added together in the analysis to improve the precision.</li> <li>Remove the mattress and select the fluoroscopy mode or acquisition program to be tested, FoV, SID.</li> <li>Place the patient simulating material on the table and the Leeds test object e.g., on top of the phantom (see Figure 3b). Adjust couch height so that the scattering phantom is at the system isocentre.</li> <li>Once setup, perform an initial fluoroscopy sequence so the system selects the x-ray factors for the TIQ phantom.</li> <li>Perform the fluoroscopy and store the image sequence.</li> <li>Remove the test object from the beam and repeat the same fluoroscopy sequence for the same length of time and store the image sequence for the signal absent images. Check that the imaging system selects the same settings (kV, mA, added filtration etc.) as for the sequence with test object, otherwise substitute the Leeds TO with a blank slab with the same attenuation. This step can be omitted if the background ROIs are extracted from positions near the targets (discs) in the test object image.</li> <li>Repeat for other imaging protocols and FoVs as needed.</li> <li>Transfer the images and compute <math>C_{TCHO}</math></li> </ol> <p><u>TIQ using 'detector' geometry</u></p> <ol style="list-style-type: none"> <li>Position the Leeds test object detail directly on the x-ray detector housing with the x-ray tube positioned at the top (Figure 3a). This method is suited for mobile C-arm systems but could also be used for fixed installations.</li> <li>Select the fluoroscopy mode or acquisition program to be tested, FoV, SID.</li> <li>Add copper sheets at the x-ray tube collimator until x-ray factors (kV, mA, ms, focus, pre-filter etc) match those for a normal-sized patient. Record the x-ray factors.</li> <li>Once setup, perform an initial fluoroscopy sequence so the system selects the x-ray factors for the TIQ phantom.</li> <li>Perform fluoroscopy in order to obtain at least 400 images for analysis. Save the fluoroscopy images.</li> <li>Repeat for other imaging protocols and FoVs if needed.</li> <li>Transfer the images and compute <math>C_{TCHO}</math></li> </ol>

Evaluation	Analysis can be carried out with the dedicated software.
Pass/Fail Criteria	$C_{TCHO}$ should be within $\pm 20\%$ of the baseline value for the imaging protocol/dose mode.
Frequency	Commissioning Annual test

#### B.7.4 Threshold-contrast detail detectability (TCDD) - CHO readout

Aim	To estimate (TCDD $C_{TCHO}$ ) using a CHO readout of the Leeds C-d test objects
Reference	<ol style="list-style-type: none"> <li>Cohen, G., McDaniel, D. L. and Wagner, L. K. (1984) 'Analysis of variations in contrast-detail experiments', Medical Physics, 11(4), pp. 469-473;</li> <li>Marshall, N. W. et al. (1992) 'Analysis of variations in contrast-detail measurements performed on image intensifier-television systems', Physics in Medicine and Biology, 37(12), pp. 2297-2302.</li> <li>Launders, J. H. et al. (1995) 'Update on the recommended viewing protocol for FAXIL threshold contrast detail detectability test objects used in television fluoroscopy', British Journal of Radiology, 68(805), pp. 70-77.</li> <li>Tapiovaara, M. J. (1997) 'Efficiency of low-contrast detail detectability in fluoroscopic imaging.', Medical physics, 24(5), pp. 655-64. Available at: <a href="http://www.ncbi.nlm.nih.gov/pubmed/9167156">http://www.ncbi.nlm.nih.gov/pubmed/9167156</a>.</li> <li>Tapiovaara, M. J. and Sandborg, M. (2004) 'How should low-contrast detail detectability be measured in fluoroscopy?', Medical Physics, 31(9), p. 2564. doi: 10.1118/1.1779357.</li> </ol>
Instrumentation	<p><u>Patient simulating material</u></p> <p>PMMA or equivalent slabs from 5 to 30cm (at least 30 x 30 cm<sup>2</sup> area) Cu sheets of a range of thicknesses e.g., 0.5, 1, 2, 3 mm thick etc and large enough to cover the whole x-ray beam at the collimator.</p> <p><u>TIQ test object</u></p> <p>Use a suitable contrast detail test object (e.g., Leeds TO10 for fluoroscopy and TO12, TO16 or TO20 for fluoroscopy and angiography).</p>
Procedure	<p><u>TIQ using scattering phantom and 'system' geometry</u></p> <ol style="list-style-type: none"> <li>Remove the mattress and select the fluoroscopy mode or acquisition program to be tested, FoV, SID.</li> <li>Place the patient simulating material on the table and the Leeds test object e.g., on top of the phantom or at the entrance side (see Figure 3b). Adjust couch height so that the scattering phantom is at the system isocenter.</li> <li>Perform an initial fluoroscopy sequence so the system selects x-ray factors.</li> <li>Perform the imaging fluoroscopy</li> <li>Use a consistent viewing protocol such that the number of discs seen is maximised and visually score the images.</li> <li>The result can be left as a 'number of discs'.</li> <li>Repeat for other imaging protocols and FoVs as needed</li> </ol> <p><u>TIQ using 'detector' geometry</u></p> <ol style="list-style-type: none"> <li>Position the Leeds test object detail directly on the x-ray detector housing with the x-ray tube positioned at the top (Figure 3a). This method is suited for mobile C-arm systems but could also be used for fixed installations.</li> <li>Select the fluoroscopy mode or acquisition program to be tested, FoV, distance and SID.</li> <li>Add copper sheets at the x-ray tube collimator until x-ray factors (kV, mA, ms, focus, pre-filter etc) match those for a normal-sized patient. Record the x-ray factors.</li> <li>Once setup, perform an initial fluoroscopy sequence so the system selects the x-ray factors for the TIQ phantom.</li> <li>Perform fluoroscopy</li> <li>Use a consistent viewing protocol such that the number of discs seen is maximised and visually score the images.</li> <li>The result can be left as a 'number of discs'.</li> <li>Repeat for other imaging protocols and FoVs as needed.</li> </ol>
Evaluation	Record the number of details and compare with previous evaluations.
Pass/Fail Criteria	NA
Frequency	Commissioning Annual test



### B.7.5 Limiting spatial resolution (LSR)

Aim	To estimate limiting spatial resolution with a line pair test object
Reference	1. Albert, M. et al. (2002) 'Aliasing effects in digital images of line-pair phantoms', (August), pp. 1716-1718. doi: 10.1118/1.1493212.
Instrumentation	<p><u>Patient simulating material</u> PMMA or equivalent slabs from 5 to 30cm (at least 30 x 30 cm<sup>2</sup> area).</p> <p><u>LSR test object</u> A suitable line pair test object</p>
Procedure	<p><u>LSR using scattering phantom and 'system' geometry</u></p> <ol style="list-style-type: none"> <li>1) Remove the mattress</li> <li>2) Select the most commonly used fluoroscopy mode, then select the relevant PMMA thickness and FoV then set the SID.</li> <li>3) Place the patient simulating material on the table and the line pair test object on top of the phantom, in the centre or at the entrance side (see Figure 3b). Adjust couch height so that the scattering phantom is at the system isocentre.</li> <li>4) The line pair patterns should be positioned at approximately 45° to the pixel matrix.</li> <li>5) Perform an initial fluoroscopy sequence so the system can select the relevant x-ray factors.</li> <li>6) Perform the fluoroscopy imaging, fix the viewing conditions, and visually score the images</li> <li>7) Repeat for a number of PMMA thicknesses, fluoroscopy modes, and FoVs.</li> </ol> <p><u>LSR using 'detector' geometry</u></p> <ol style="list-style-type: none"> <li>1) Position the line pair test object detail directly on the x-ray detector housing with the x-ray tube positioned at the top (Figure 3a). The bar patterns should be positioned at an angle of approximately 45° to the pixel matrix. This method is suited for mobile C-arm systems but could also be used for fixed installations. Do not place additional Cu filtration at the x-ray tube.</li> <li>2) Select the largest FoV and the fluoroscopy mode or acquisition program to be tested</li> <li>3) Perform fluoroscopy, fix the viewing conditions, and visually score the test object images.</li> <li>4) Repeat for the other FoVs.</li> <li>5) Calculate the limiting spatial resolution</li> </ol>
Evaluation	Visual scoring
Pass/Fail Criteria	<p>For 'detector' geometry:</p> <ul style="list-style-type: none"> <li>- the LSR should not differ from the baseline values by more than 25%</li> <li>- the LSR should be compared against national regulations where they exist</li> </ul>
Frequency	<p>Acceptance test (detector geometry)</p> <p>Commissioning (system geometry and detector geometry)</p> <p>Annual test (system geometry for FPD, system geometry and detector geometry for XRII)</p>



## SECTION C – REFERENCES

Abbey, C. K. and Barrett, H. H. (2001) 'Human- and model-observer performance in ramp-spectrum noise : effects of regularization and object variability', *Journal of the Optical Society of America A*, 18(3), pp. 473–488.

Albert, M. et al. (2002) 'Aliasing effects in digital images of line-pair phantoms', (August), pp. 1716–1718. doi: 10.1118/1.1493212.

American College of Radiology. ACR-AAPM (2016). 'Technical Standard for Diagnostic Medical Physics Performance Monitoring of Fluoroscopic Equipment'. Available at: <https://www.acr.org/-/media/ACR/Files/Practice-Parameters/fluoro-equip.pdf?la=en>. (Accessed 25 March 2020)

Andersson, J. et al. (2021) 'Estimation of patient skin dose in fluoroscopy: summary of a joint report by AAPM TG357 and EFOMP', *Medical Physics*, 48(7), pp. e671–e696. doi: 10.1002/mp.14910.

Barrett, H. H. et al. (1993) 'Model observers for assessment of image quality.', *Proceedings of the National Academy of Sciences of the United States of America*, 90(21), pp. 9758–65. Available at: <http://www.pubmedcentral.nih.gov/articlerender.fcgi?artid=47653&tool=pmcentrez&rendertype=abstract>.

Barrett, H. H. and Myers, K. J. (2003) *Foundations of Image Science*. Wiley.

Båth, M. and Månsson, L. G. (2007) 'Visual grading characteristics (VGC) analysis: a non-parametric rank-invariant statistical method for image quality evaluation.', *The British journal of radiology*, 80(951), pp. 169–76. doi: 10.1259/bjr/35012658.

Bednarek DR, Barbarits J, Rana VK, Nagaraja SP, Josan MS, Rudin S. Verification of the performance accuracy of a real-time skin-dose tracking system for interventional fluoroscopic procedures. *Proc SPIE–Int Soc Opt Eng* 2011;7961: 796127\_1.

Bertolini, M. et al. (2019) 'Characterization of GE discovery IGS 740 angiography system by means of channelized Hotelling observer (CHO)', *Physics in Medicine and Biology*. IOP Publishing, 64(9). doi: 10.1088/1361-6560/ab144c.

Boone, J. . et al. (1993) 'A survey of fluoroscopic exposure rates: AAPM Task Group No. 11 Report', *Medical Physics*, 20(3), pp. 789–94.

Bordier C, Klausz R, Desponds L. Patient dose map indications on interventional X- ray systems and validation with Gafchromic XR-RV3 film. *Rad Prot Dosim* 2015; 163:306–18.

Burgess, A. E. (2011) 'Visual perception studies and observer models in medical imaging', *Seminars in Nuclear Medicine*. Elsevier Inc., 41(6), pp. 419–436. doi: 10.1053/j.semnuclmed.2011.06.005.

Carmichael, J. H. E. et al. (1996) *European guidelines on quality criteria for diagnostic radiographic images* EUR 16260 EN.

Chao, E. H. et al. (2000) 'A Statistical Method of Defining Low Contrast Detectability. In: Oak Brook, editor. *Radiol. Soc. North Am., 2000.*', *Radiology*.

Cohen, G., McDaniel, D. L. and Wagner, L. K. (1984) 'Analysis of variations in contrast-detail experiments', *Medical Physics*, 11(4), pp. 469-473.

Cowen, A. R., Haywood, J. M., et al. (1987) 'A set of X-ray test objects for image quality control in digital subtraction fluorography. I: Design considerations.' *The British Journal of Radiology*, 60(718), pp. 1001-9.

Cowen, A. R., Workman, A., et al. (1987) 'A set of X-ray test objects for image quality control in digital subtraction fluorography. II: Application and interpretation of results.' *The British Journal of Radiology*, 60(718), pp. 1011-8.

Cunningham IA. Applied Linear-Systems Theory. In: Jacob Beutel, editor. *Medical Imaging Volume 1 Physics and Psychophysics*. Bellingham: SPIE - The International Society for Optical Engineering; 2000. p. 79-156.

Dabin J et. al. Accuracy of skin dose mapping in interventional cardiology: Comparison of 10 software products following a common protocol. *Physica Medica* 2021 82 279-294

Dance, D. R. et al. (2014) *Diagnostic Radiology Physics: A Handbook for Teachers and Students*, *Diagnostic Radiology Physics: A Handbook for Teachers and Students*. Vienna, Austria: International Atomic Energy Authority (IAEA).

Doerfler, A. et al. (2015) 'Flat-Panel Computed Tomography (DYNA-CT) in Neuroradiology. From High-Resolution Imaging of Implants to One-Stop-Shopping for Acute Stroke', *Clinical Neuroradiology*, 25, pp. 291-297. doi: 10.1007/s00062-015-0423-x.

Dobbins III, James T., Ergun, David L., Rutz, Lois, Hinshaw, Dean A., Blume, Hartwig, Clark DC. DQE(f) of four generations of computed radiography acquisition devices. *Med Phys*. 1995;22(10):1581-93.

Dobbins JT, Samei E, Ranger NT, Chen Y. Intercomparison of methods for image quality characterization. II. Noise power spectrum). *Med Phys* [Internet]. 2006; 33(5):1454. Available from: <http://doi.wiley.com/10.1118/1.2188819>

Eckstein, M. P., Abbey, C. K. and Bochud, F. O. (2000) 'A Practical Guide to Model Observers for Visual Detection in Synthetic and Natural Noisy Images', in Beutel, J., Kundel, H. L., and Van Metter, R. L. (eds) *Handbook of Medical Imaging, Volume 1. Physics and Psychophysics*. SPIE, Bellingham, WA, pp. 595-628.

Elgström, H., Tesselaar, E. and Sandborg, M. (2021) 'Signal-to-noise ratio rate measurements in fluoroscopy for quality control and teaching good radiological technique', *Radiation Protection Dosimetry*, 195(3-4), pp. 407-415. doi: 10.1093/rpd/ncaa222.

European Commission (2012) RP 162. Criteria for Acceptability of medical radiological equipment used in diagnostic radiology, nuclear medicine and radiotherapy, *Radiation Protection 162*. doi: 10.2768/22561.

Fahrig, R. et al. (2021) 'Flat-panel cone-beam CT in the clinic: history and current state', *Journal of Medical Imaging*, 8(05), pp. 1-40. doi: 10.1117/1.jmi.8.5.052115.

Favazza, C. P. et al. (2015) 'Implementation of a channelized Hotelling observer model to assess image quality of x-ray angiography systems', *Journal of Medical Imaging*, 2(1), p. 015503. doi: 10.1117/1.JMI.2.1.015503.

Gallas, B. D. and Barrett, H. H. (2003) 'Validating the use of channels to estimate the ideal linear observer.' *Journal of the Optical Society of America. A, Optics, image science, and vision*, 20(9), pp. 1725–38. Available at: <http://www.ncbi.nlm.nih.gov/pubmed/12968645>.

Gardavaud F, Tavolaro S, Gussenmeyer-Mary N, Cornelis F, Boudgh`ene F. PeakSkin Dose evaluation for vascular clinical procedures in interventional radiology: a comparison between three computation numerical solutions. *Phys Med* 2018; 56

Granfors, P. R. et al. (2003) 'Performance of a 41×41 cm<sup>2</sup> amorphous silicon flat panel x-ray detector designed for angiographic and R&F imaging applications', *Medical Physics*, 30(10), pp. 2715–2726.

Green, D. M. and Swets, J. A. (1966) *Signal detection theory and psychophysics*. John Wiley.

Habib Geryes B, Hadid-Beurrier L, Waryn MJ, Jean-Pierre A, Farah J. Benchmarking the DACS-integrated Radiation Dose Monitor (R) skin dose mapping software using XR-RV3 Gafchromic (R) films. *Med Phys* 2018; 45:4683–92.

Hay, G. A. et al. (1985) 'A set of X-ray test objects for quality control in television fluoroscopy.' *The British Journal of Radiology*, 58(688), pp. 335–344.

He, X. and Park, S. (2013) 'Model Observers in Medical Imaging Research', *Theranostics*, 3(10), pp. 774–786. doi: 10.7150/thno.5138.

de las Heras Gala, H. et al. (2017) 'Quality control in cone-beam computed tomography (CBCT) EFOMP-ESTRO-IAEA protocol (summary report)', *Physica Medica*, 39, pp. 67–72. doi: 10.1016/j.ejmp.2017.05.069.

Hiles, P. and Starritt, H. (1996) *IPEM Report 32 (II) Measurement of the performance characteristics of diagnostic x-ray systems used in medicine: x-ray image intensifier television systems*. York, UK.

Holm, T. and Moseley, R. D. (1964) 'The Conversion Factor for Image Intensifiers', *Radiology*, 82(January), pp. 898–904. doi: 10.1148/82.5.898.

IEC 62220-1-3 (2008) *Medical electrical equipment - Characteristics of digital X-ray imaging devices - Part 1-3: Determination of the detective quantum efficiency - Detectors used in dynamic imaging*. Geneva, Switzerland.

IAEA. *Dosimetry in diagnostic radiology: an international code of practice*. — Vienna: International Atomic Energy Agency, 2007. p.; 24 cm. — (Technical reports series, ISSN 0074-1914; no. 457) STI/DOC/-10/457 ISBN 92-0-115406-2.

[https://www-pub.iaea.org/MTCD/Publications/PDF/TRS457\\_web.pdf](https://www-pub.iaea.org/MTCD/Publications/PDF/TRS457_web.pdf)

International Atomic Energy Agency (2018) 'Radiation Protection and Safety in Medical Uses of Ionizing Radiation', IAEA Safety Standards Series No. SSG-46, IAEA, Vienna. Available at: <https://www.iaea.org/publications/11102/radiation-protection-and-safety-in-medical-uses-of-ionizing-radiation>

ICRU Rep. No. 54.' (1996). Bethesda, MD.

IEC 60601-2-43:2022. *Medical electrical equipment - Part 2-43: Particular requirements for the basic safety and essential performance of X-ray equipment for interventional procedures*

IEC 60601-2-54: 2022 (. Medical electrical equipment - Part 2-54: 'Particular requirements for the basic safety and essential performance of X-ray equipment for radiography and radioscopy.

IEC 62220-1-1: 2015. Medical electrical equipment - Characteristics of digital X-ray imaging devices - Part 1-1: Determination of the detective quantum efficiency - Detectors used in radiographic imaging.

IEC 62220-1-2: 2007. Medical electrical equipment - Characteristics of digital X-ray imaging devices - Part 1-1: Determination of the detective quantum efficiency - Detectors used in mammography.

IEC 62220-1-3: 2008. Medical electrical equipment - Characteristics of digital X-ray imaging devices - Part 1-3: Determination of the detective quantum efficiency - Detectors used in dynamic imaging.

IPEM (2005) Recommended standards for the performance testing of diagnostic x-ray imaging systems, IPEM Report No. 91. York, UK.

Jones AK & Pasciak AS 2011, Calculating the peak skin dose resulting from fluoroscopically guided interventions. Part I: Methods, *Journal of Applied Clinical Physics* 12 402

Jones, A. K. et al. (2014) 'Medical imaging using ionizing radiation: Optimization of dose and image quality in fluoroscopy', *Medical Physics*, 41(1), pp. 014301-1-26. doi: 10.1118/1.4835495.

Kyprianou IS, Rudin S, Bednarek DR, Hoffmann KR. Generalizing the MTF and DQE to include x-ray scatter and focal spot unsharpness: Application to a new microangiographic system. *Med Phys*. 2005;32(2):613.

Launders, J. H. et al. (1995) 'Update on the recommended viewing protocol for FAXIL threshold contrast detail detectability test objects used in television fluoroscopy', *British Journal of Radiology*, 68(805), pp. 70-77.

Lin, P. J. P. et al. (2022) 'AAPM Task Group Report 272: Comprehensive acceptance testing and evaluation of fluoroscopy imaging systems', *Medical Physics*, 49(4), pp. e1-e49. doi: 10.1002/mp.15429.

Lin, P. J. P., Goode, A. R. and Corwin, F. D. (2022) 'Review and investigation of automatic brightness/dose rate control logic of fluoroscopic imaging systems in cardiovascular interventional angiography', *Radiological Physics and Technology*. Springer Singapore, 15(1), pp. 6-24. doi: 10.1007/s12194-022-00649-3.

Lundh, C. et al. (2021) 'A model for evaluating the use of imaging in image-guided interventional procedures - Possible implications on optimisation of radiation protection', *Radiation Protection Dosimetry*, 195(3-4), pp. 139-144. doi: 10.1093/rpd/ncab040.

Mackenzie, A. et al. (2010) IPEM Report 32 (Part VII) Measurement of the performance characteristics of diagnostic x-ray systems: digital imaging systems. York, UK.

Malchair F et. al. 2020 Review of skin dose calculation software in interventional cardiology. *Physica Medica* 80 75-83

Mackenzie A, Doshi S, Doyle P, Hill A, Honey I, Marshall NW, et al. IPEM Report 32 (Part VII) Measurement of the performance characteristics of diagnostic x-ray systems: digital imaging systems. York, UK; 2010.

Mackenzie A, Honey ID. Characterization of noise sources for two generations of computed radiography systems using powder and crystalline photostimulable phosphors. *Med Phys* [Internet]. 2007;34(8):3345-57. Available from: <http://doi.wiley.com/10.1118/1.2750973>

Malusek A, Helmrot E, Sandborg M, Grindborg J-E and Alm Carlsson G In-situ calibration of clinical built-in KAP meters with traceability to a primary standard using a reference KAP-meter. *Phys. Med. Biol.* 59, 7195–7210 (2014), doi:10.1088/0031-9155/59/23/7195

Marshall, N. W. et al. (1992) 'Analysis of variations in contrast-detail measurements performed on image intensifier-television systems', *Physics in Medicine and Biology*, 37(12), pp. 2297–2302.

Marshall, N. W. et al. (2001) 'Receptor dose in digital fluorography: A comparison between theory and practice', *Physics in Medicine and Biology*, 46(4). doi: 10.1088/0031-9155/46/4/325.

Marshall NW, Mackenzie A, Honey ID. Quality control measurements for digital x-ray detectors. *Phys Med Biol.* 2011;56(4).

Menzel, H.-G., Schibilla, H. and Teunen, D. (1999) European Guidelines on Quality Criteria for Computed Tomography European Guidelines on Quality Criteria, Eur 16262 En.

Metz, C. E. (1986) 'ROC Methodology in Radiologic Imaging', *Investigative Radiology*, 21, pp. 720–733.

Monnin P, Bosmans H, Verdun FR, Marshall NW. Comparison of the polynomial model against explicit measurements of noise components for different mammography systems. *Phys Med Biol.* 2014;59(19).

National Council on Radiation Protection and Measurements (2010) 'Radiation Dose Management for Fluoroscopically-Guided Interventional Medical Procedures, NCRP Report No. 168'. National Council on Radiation Protection and Measurements, Bethesda, Maryland.

NEMA (2018) 'NEMA Standards Publication XR 27-2013 (R2018) X-ray Equipment for Interventional Procedures User Quality Control Mode'. National Electrical Manufacturers Association (NEMA), Virginia, USA.

Official Journal of the European Union (2014) 'European Council Directive 2013/59/Euratom on basic safety standards for protection against the dangers arising from exposure to ionising radiation and repealing directives 89/618/Euratom, 90/641/Euratom, 96/29/Euratom, 97/43 Euratom and 2003/122/Euratom'. OJ of the EU. L13;57:1-73 Available at: <https://eur-lex.europa.eu/LexUriServ/LexUriServ.do?uri=OJ:L:2014:013:0001:0073:EN:PDF> . (Accessed 14 Mar 2020)

Paruccini, N. et al. (2021) 'A single phantom, a single statistical method for low-contrast detectability assessment', *Physica Medica*, 91(October), pp. 28–42. doi: 10.1016/j.ejmp.2021.10.007.

Rose, A. (1948) 'The sensitivity performance of the human eye on an absolute scale', *J. Opt. Soc. Am.*, 38, pp. 196–208.

Samei E, Ranger NT, Dobbins JT, Chen Y. Intercomparison of methods for image quality characterization. I. Modulation transfer function. *Med Phys.* 2006;33(5):1454–65

Shepard, S. J. (2002) Quality Control in Diagnostic Radiology AAPM Report 72, Report of Task Group #12 Diagnostic X-ray Imaging Committee.

Smedby, O. and Fredrikson, M. (2010) 'Visual grading regression: analysing data from visual grading experiments with regression models.', *The British journal of radiology*, pp. 1–9. doi: 10.1259/bjr/35254923.

Stevens, G. (2021) Dynamic X-ray Imaging Systems Used in Medicine. York, UK.

Tapiovaara, J. (1993) 'SNR and noise measurements for medical imaging: II. Application to fluoroscopic x-ray equipment', *Phys. Med. Biol.*, 38, pp. 1761–1788. <https://iopscience.iop.org/article/10.1088/0031-9155/38/12/006/pdf>

Tapiovaara, M. (2003) Objective measurement of image quality in fluoroscopic x-ray equipment: FluoroQuality, STUK-A196 / MAY 2003. Tapiovaara, M. J. (1997) 'Efficiency of low-contrast detail detectability in fluoroscopic imaging.', *Medical physics*, 24(5), pp. 655–64. Available at: <http://www.ncbi.nlm.nih.gov/pubmed/9167156>.

Tapiovaara, M. J. and Sandborg, M. (2004) 'How should low-contrast detail detectability be measured in fluoroscopy?', *Medical Physics*, 31(9), p. 2564. doi: 10.1118/1.1779357.

Tapiovaara, M. J. and Wagner, R. F. (1993) 'SNR and noise measurements for medical imaging: I. A practical approach based on statistical decision theory', *Physics in Medicine and Biology*, 38(1), pp. 71–92. doi: 10.1088/0031-9155/38/1/006.

Tesselaar, E. and Sandborg, M. (2016) 'Assessing the usefulness of the quasi-ideal observer for quality control in fluoroscopy', *Radiation Protection Dosimetry*, 169(1), pp. 360–364. doi: 10.1093/rpd/ncv434.

Toroi P, Komppa T and Kosunen A 2008 A tandem calibration method for kerma-area product meters. *Phys. Med. Biol.* 53 4941–58, DOI 10.1088/0031-9155/53/18/006

Vedantham, S. et al. (2004) 'Solid-state fluoroscopic imager for high-resolution angiography : Physical characteristics of an 8 cm × 8 cm experimental prototype Solid-state fluoroscopic imager for high-resolution angiography : Physical characteristics of an 8 cm × 8 cm experimental p', 1462. doi: 10.1118/1.1750992.

Villa, R. et al. (2019) 'Model observers for Low Contrast Detectability evaluation in dynamic angiography: A feasible approach', *Physica Medica*, 64(June), pp. 89–97. doi: 10.1016/j.ejmp.2019.06.015.

Worrall, M. et al. (2020) 'IPEM Topical Report: An evidence and risk assessment based analysis of the efficacy of quality assurance tests on fluoroscopy units - Part II; Image quality', *Physics in Medicine and Biology*. IOP Publishing, 65(22), p. 195011. doi: 10.1088/1361-6560/abb92.

## SECTION D – APPENDICES

### D.1. Appendix 1. Radiation Safety Procedures

The performance evaluation of fluoroscopic systems should include a radiation safety survey to determine whether the radiological medical equipment, the practical techniques and the ancillary equipment are complying with the national radiation control regulations, based on the European Basic Safety Standards (BSS). A summarised list of BSS requirements for fluoroscopes and interventional radiology equipment is shown in the table below.

---

#### **Summary of BSS Requirements applicable to Fluoroscopy/Angiography Systems**

*All fluoroscopy equipment has a device that automatically controls the dose rate, using an image intensifier or equivalent device (flat panel detector) {Art. 60. 3. (a)}.*

*All equipment used for interventional radiology has a device or software that informs the operators at the end of the procedure, of relevant parameters for assessing the patient dose. In addition, equipment installed after 6 February 2018 has the capacity to transfer this information to the examination record. {Art. 60. 3. (a)}*

*Interventional radiology equipment installed after 6 February 2018 has also a device or a feature informing the practitioner of the quantity of radiation produced by the equipment during the procedure. {Art. 60. 3 (d)}*

*Image acquisition protocols, at least for the most common interventional procedures, will be reviewed to assess if “patient doses from interventional radiology are kept as low as reasonably achievable consistent with obtaining the required medical information, taking into account economic and societal factors”. {Art. 56. 1.}*

*Diagnostic reference levels have been established and are used for adult and paediatric interventional radiology procedures. {Art. 56. 2.}*

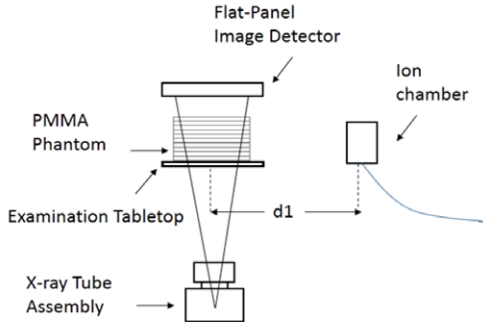
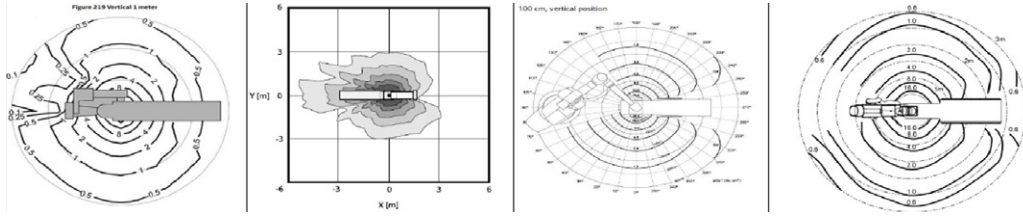
*A medical physics expert is involved in all dosimetry {Art 58 (d) (ii) & Art 61. 1. (c)} and radiation safety assessments, liaising with the radiation protection expert as appropriate {Art 83}.*

---

Medical physicists can replace this list with the corresponding requirements in their national regulations.

The radiation safety survey can consist of a review of image acquisition protocols, staff radiation doses and any relevant documentation such as previous safety reports; a visual inspection to check for equipment integrity and ease of motions; verification of interlock functions, such as collision alerts, and stray (leakage plus scatter) radiation measurements around the fluoroscope using the maximum air kerma rate and the largest field size. The extent and depth of the survey will depend on whether it is performed at acceptance testing and commissioning or during a periodic equipment performance evaluation.

Stray radiation measurements

References	See Section A.6
Instrumentation	<p>Procedure 1:</p> <ul style="list-style-type: none"> <li>- PMMA 30x30x40 cm<sup>3</sup> slab phantom.</li> <li>- Calibrated survey meter or large volume ionisation chamber and electrometer with kerma rate and integrated modes.</li> <li>- Stand to hold the ion chamber in air.</li> </ul>
Procedure	<p><u>Procedure 1 (Hand-held survey meter or ion chamber on a stand)</u></p> <p>Set up the phantom perpendicular to the x-ray beam and position the measurement device at various distances around the phantom, in the locations where the interventionalist(s) stand(s) and where the auxiliary staff monitor the procedure's technical parameters and the patient's vital signs. Typical measurement distances are 50 cm away from the centre of the phantom and 20 cm above and below the table at 20 cm from the edge of the phantom. Turn on the fluoroscope using the maximum field size. Record the settings given by the AEC (kV, mA, pulse width, filtration) and the values of air kerma rate or ambient dose equivalent (depending on how the instrument is calibrated) which are read by the survey meter or ion chamber in the different positions.</p> <p><i>Figure Appendix 1-1, below, shows a diagram of a simple set-up.</i></p> 
Evaluation	<p>Assuming that the leakage component of the secondary radiation is negligible compared with the scatter radiation, the measured Air Kerma Rates may be compared with the iso-scatter plots found in the Manufacturer's IUF/Accompanying Documents, by normalising to the same technique settings. An illustration of such plots is shown in Figure Appendix 1-2. Below.</p> 
Pass/Fail Criteria	The measurement conditions and the resulting values should be recorded for future tests.
Frequency	At acceptance testing and when a major system component such as the x-ray tube has been replaced.

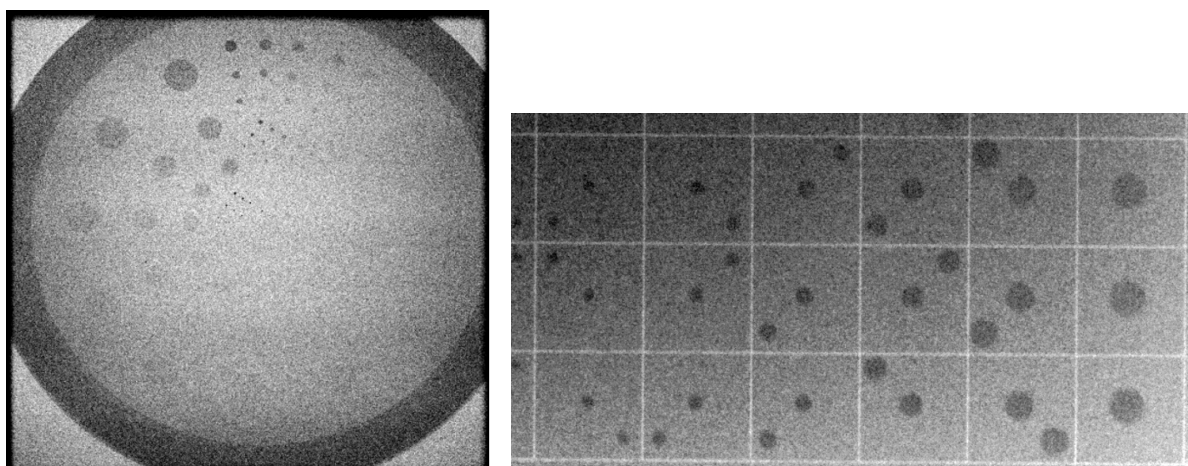


## D.2. Appendix 2. Phantoms

The most common means currently of evaluating technical image quality in QC testing is with test objects, where the parameters assessed are usually low-contrast detectability and limiting spatial resolution.

### **Threshold-contrast detail detectability (TCDD) test objects**

Threshold low contrast detail detectability (TCDD) is assessed using threshold contrast-detail test objects, which have a long history in the evaluation of imaging devices, including screen/film, XRII and TV camera tubes since the 1950's (Rose, 1948; Burger, 1950; Hay et al., 1985; Cowen, Workman, et al., 1987; Thijssen, 1993; Karssemeijer and Thijssen, 1996). These test objects are usually arranged in a homogeneous background and generate a set of stimuli with varying diameter and contrast. For each detail diameter, the visibility falls systematically until the disc is no longer visible. The job of the observer is to determine the last stimulus considered visible for each diameter and the contrast of this stimulus is defined as the threshold contrast (CT). The stimulus for which this occurs depends on the signal to noise ratio (SNR) in the image and the system parameters that influence this will depend on how the test object is imaged. For example, if the test objects are placed at the detector input plane (~'detector' geometry), at some prescribed x-ray energy then the most influential parameters will be x-ray detector exposure rate used and the DQE of the x-ray detector (Cowen, Haywood, et al., 1987). TCDD results can therefore be used as an overall measure of technical imaging performance, as quantified by the SNR or SDNR, of either the imaging system or the x-ray detector, depending on how the TCDD test object is imaged.



*Figure Appendix 2-1 a) image of Leeds TO12 TCDD test object, an example of “count to the last visible disc” design; b) CDRAD test object, an example of an alternative forced choice design (4-AFC here).*

### **TCDD types, metric for the test object score and test object composition**

TCDD test objects generally have a detail plate, typically made of PMMA or Aluminium, that contains the details used to generate the stimuli. These plates can be imaged with a stack of (typical) patient simulating material, so that the system selects x-ray imaging parameters relevant to patient imaging. This is usually PMMA blocks but a few millimetres of Cu or Al can also be used. Many test objects follow the initial design described by Albert Rose (Rose, 1948) and generate circular signals of varying diameter against a homogeneous background, using either discs of varying thickness or holes of different depths drilled into the plate. When imaged, this generates a set of signals whose contrast and therefore visibility falls until the disc is no longer visible. As discussed above the arrangement of the discs across will be different depending on the readout method envisioned. Some test objects, for example CDRAD (Thijssen, 1993) have a disc randomly positioned in a corner of each square together with a disc at the square, enabling the use of both multiple

alternative forced choice (MAFC) and 'count until the last disc' readout methods. A range of different TCDD test objects are available from different suppliers. Details of test object design and composition, where available, are given in Table Appendix 2-1.


It is important to consider the output value produced by the test object, as this will be used to express the image quality score. For test objects that use holes of different depths in PMMA or Aluminium to generate signals, such as CDRAD, CDDISC or the Gammex model 151, the image quality score can be given as hole depth (mm). Expressed like this, then the image quality score is effectively test object specific and comparing between systems requires the same test object to be used. This is useful for longitudinal testing against a baseline but cannot be used to set a typical performance standard for a common procedure unless physicists all use the same test object. It might be possible to convert this to a threshold contrast for a given beam quality via calibration measurements (Aufrechtig, 1999) but this is difficult to achieve for fluoroscopy, given the range of possible factors that can be selected by these systems. A further difficulty is scatter adiation, where the scatter fraction is very sensitive to the geometry.

An alternative approach is to use a detail plate in a low scatter geometry, as done with the Leeds test objects. The specific materials used for discs in these test objects are not specified. Instead, tables of radiation contrasts are supplied with the test objects for tube voltages between 65 kV and 80 kV and added copper filtration (1.0, 1.5 and 2.0 mm copper). Successive diameters in the Leeds test objects change by a factor of  $\sqrt{2}$ , while for a given diameter there is a factor of  $\sqrt{2}$  change in contrast between successive discs. For a quantum noise limited system, a factor of 2 increase in detector exposure should visualise one extra disc at each diameter (Rose, 1948). These objects are calibrated to produce a defined range of contrasts under low scatter beam qualities at specific energies (Hay et al., 1985). By accounting for the energy used in the measurement and imaging under low scatter conditions, an absolute limiting threshold contrast for the x-ray detector can be estimated. If a typical performance level can be established for an imaging mode at some x-ray detector input exposure rate, then reference curves can be formed and used for comparison (Evans, 2004). However, used like this, the influence of spectral selection of the imaging system and anti scatter rejection technique on target detectability is not assessed.

A further consideration regarding test object composition is the recent introduction of contrast to noise ratio (CNR) imaging modes on fluoroscopy and angiography systems (Dehairs, Bosmans and Marshall, 2019; Werncke et al., 2021a, 2021b). In these modes, the elemental composition of the target can be specified and based on this information, the AEC selects x-ray factors that maximise the visibility of objects with this composition. Examples can be iodine, carbon dioxide or barium used as contrast agent materials, iron used in guidewires, and platinum or tantalum used in stent markers (Dehairs, Bosmans and Marshall, 2019; Werncke et al., 2021b). Evaluation of material specific imaging modes with test objects containing targets of a different elemental composition may give inconsistent or unexpected results and may have reduced relevance when trying to predict system performance when imaging patients (Lin, Goode and Corwin, 2022). Some test objects are available with specific elemental contrasts, for example NEMA XR21-2000 detail plate contains cylindrical holes filled with different areal densities of iodine to generate contrast targets (Balter et al., 2001).

**Table Appendix 2-1.** Some of the TCCD test objects available

Name	Design	Base plate thickness/ composition	# Details	Detail Diameters (mm)	Detail thicknesses/ hole depth	Analysis software?	Image/ diagram
Artinis CDDISC	MAFC/ Count to last disc	10 mm PMMA	240	Cylindrical holes: 0.3, 0.5, 0.6, 0.8, 1.0, 1.3, 1.6, 2.0, 2.5, 3.2, 4.0, 5.0, 6.3, 8.0 In exponential steps	Cylindrical holes: 0.3, 0.5, 0.6, 0.8, 1.0, 1.3, 1.6, 2.0, 2.5, 3.2, 4.0, 5.0, 6.3, 8.0 In exponential steps	No	
Artinis CDRAD	MAFC/ Count to last disc	10 mm PMMA	225	Cylindrical holes: 0.3, 0.5, 0.6, 0.8, 1.0, 1.3, 1.6, 2.0, 2.5, 3.2, 4.0, 5.0, 6.3, 8.0	Cylindrical holes: 0.3, 0.5, 0.6, 0.8, 1.0, 1.3, 1.6, 2.0, 2.5, 3.2, 4.0, 5.0, 6.3, 8.0	Artinis CD Analyser; calculation method not specified	
CIRS Ra-diography Fluoroscopy QA Phantom Model 903	Count to last disc	Aluminium layer (30 x 70 x 9.53 mm)	24	Discs, 5.6, 4.0, 2.8, 2.0	6 depths, 0.38 to 1.52 mm	No	
Gammex LC Resolution QC Tool (model 151)	Count to last disc	Al block, (L x W x H) 180 x 180 x 13 mm	100	0.58 to 7.93 mm	0.13 to 2.29 mm	No	
Leeds TO10	Count to last disc	10 mm thick PMMA, diameter	108	Discs, 11.1, 7.9, 5.6, 4.0, 2.8, 2.0, 1.4, 1.0, 0.70, 0.50, 0.35, 0.25	14 thicknesses, thickness and composition not specified, contrast range 0.011 to 0.954 @ 70 kV, 1 mm Cu	AutoPIA calculation method not specified	
Leeds TO12	Count to last disc	10 mm PMMA, diameter	108	Discs, 11.1, 7.9, 5.6, 4.0, 2.8, 2.0, 1.4, 1.0, 0.70, 0.50, 0.35, 0.25	17 thicknesses, thickness and not specified, composition not specified, contrast range 0.0043 to 0.954 @ 70 kV, 1 mm Cu	AutoPIA calculation method not specified	
Leeds TO20	Count to last disc	10 mm PMMA, diameter	144	Discs, 11.1, 7.9, 5.6, 4.0, 2.8, 2.0, 1.4, 1.0, 0.70, 0.50, 0.35, 0.25	20 thickness, thickness not specified, composition not specified, contrast range 0.0016 to 0.954 @ 70 kV, 1 mm Cu	AutoPIA calculation method not specified	
DIN 6868-15 e.g. PTW NORM RAD/ FLU or Pro-Project Pro-Fluo 150	Count to last disc	Various e.g. 310 x 310 mm, thickness 30 mm PMMA with 1.5 mm Cu	8	Discs, 10 mm	8 thicknesses (contrasts 0.9% to 9.4%)	On-line data logging available e.g. at Pro-Project.pl	

NEMA XR21 - 2000 cardiac phantom	Count to last disc	25 mm PMMA	32	Disc/cylinder targets, 4, 3, 2, 1 mm	Iodine embedded in epoxy, 20, 10, 5 and 2.5 mg/cm <sup>2</sup>	No	
----------------------------------	--------------------	------------	----	--------------------------------------	--	----	---

### **Line pair test objects**

A test object measurement of limiting spatial resolution is made using a line pair test object, which consists of lines separated by certain spacing, corresponding to a spatial frequency, cut into a thin lead test object. The lines are grouped by spatial frequency and the last spatial frequency group that can be resolved is defined as the limiting or threshold resolution. In fact, the test object generates  $\square$ -square waves, which include a fundamental sinusoidal wave for each spatial frequency group.

The line pair test object gives an estimate of the highest spatial frequency that is transmitted through the imaging system (provided this fundamental frequency exists in the test object). As with the TCDD, the factors influencing the limiting spatial resolution depend on the position of the test object when imaged. When positioned at the detector input plane, the x-ray detector is the determining factor. For detector tests, a high dose rate (without saturation) and low energy to limit the influence of noise and contrast (signal) on the result. Flat panel detectors have a fixed pixel spacing, with binning or interpolation applied in some FOVs, and the limiting resolution will generally follow the Nyquist frequency i.e.,  $N_y = 1/(2.p)$  where p is the pixel spacing. This is the case provided that visual bias is not limiting the measurement i.e. the test object is sufficiently magnified at the display stage when being scored. Limiting spatial resolution of the x-ray detector is a useful routine test for XR/II-TV based fluoroscopy systems where XR/II focus can change due to faults or drift in the focusing voltages.


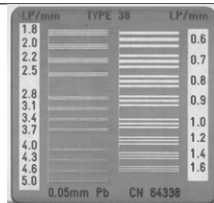
When the test object is positioned at the patient position, geometric blurring from the x-ray tube will also influence the result and in fact noise and x-ray contrast could also have some influence on the result. Used like this, the line pair test becomes a system sharpness test.

Again, visual reading is often used when scoring this test object, even though digitally stored images are generally available now via a fluoroscopy store function. Some caution is required when visually scoring a line pair test object acquired on digital image receptors as aliasing can generate additional patterns within a given line pair frequency (Albert et al., 2002). Should digital images be available without re-binning or downsampling, then the square wave contrast transfer function can be calculated, which gives a quantitative estimate of sharpness and can be used as an alternative to an MTF measurement (Droegge and Morin, 1982). It should be noted that measurement of the MTF gives a more complete and robust evaluation of detector sharpness.

### **Line pair test object phantoms**

The most commonly used line pair test objects are manufactured by Hüttner Röntgenteste (DE) (Table Appendix 2-2), where line pairs are cut into a thin Pb sheet. Different Pb sheet thicknesses are available, from 0.01 mm Pb to 0.1 mm Pb, with 0.1 mm Pb being a common thickness. There is a 12% change in spatial frequency between each spatial frequency group in these test objects. The Type 18 and Type 38 phantoms are often included in test objects designed by other test object manufacturers. Hüttner Type 18 is used in the Leeds TOR18 FG. Hüttner Type 38 (or a version of this test object) is used in the Leeds Fluoro 4, the PTW/Freiburg NORMI 13, the RaySafe Pro-Fluoro 150, the Pro-Fluo 150 from Pro-Project and the NEMA XR-21 test objects.

**Table Annex 2-2.** Hüttner line pair test objects

Name	Base plate Composition / thickness	# line pair groups	Line pair frequencies	Scoring software	Image/diagram
Hüttner type 18	Pb/ 0.01 mm to 0.1 mm	21	0.5 lp/mm to 5.0 lp/mm	No	
Hüttner type 18	Pb/ 0.01 mm to 0.1 mm	20	0.6 lp/mm to 5.0 lp/mm	No	

### Digital subtraction angiography (DSA)

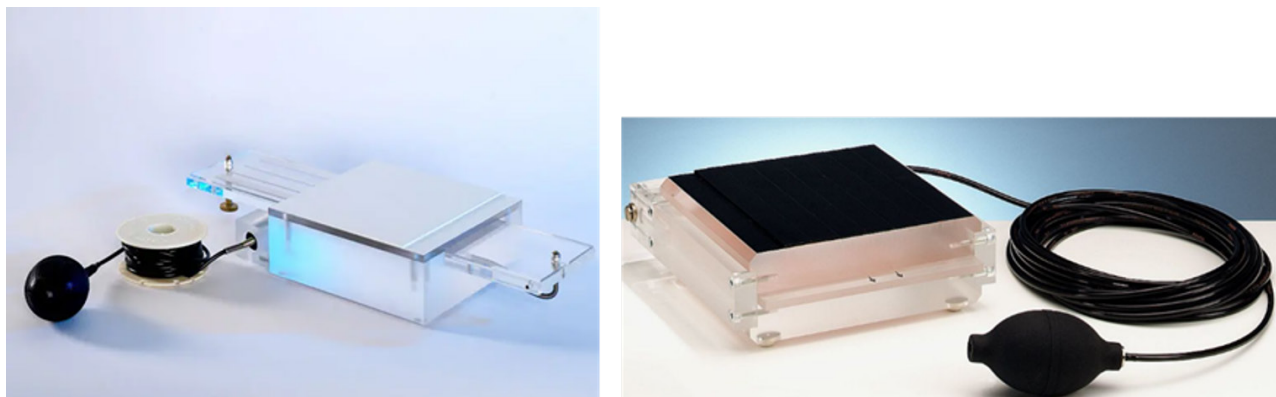
Digital subtraction angiography (DSA) is an imaging mode designed to improve the visualisation of contrast within blood vessels by removing overlying structures. The technique involves the injection of an iodine-based contrast agent in the vessel of interest. Image acquisition starts just prior to the injection and continues until sufficient contrast has been delivered to visualise the vessel or arterial/venous structure. A mask image is defined using one of the images acquired before the contrast is introduced and this image is subtracted from subsequent images in the sequence. If the patient does not move then overlying structures common to both images cancel out leaving only the difference between the mask and the later images i.e. the filled vessel containing the iodine contrast. A logarithmic transform is applied to the images before the subtraction is performed, as this stops the modulation of the filled vessel by the signal intensities in the overlying anatomy. Subtracting two images that contain uncorrelated (quantum) noise increases the variance of the noise in the resulting (subtracted) image by a factor of 2 and therefore DSA modes often have increased exposure/image to reduce noise. Other options to control noise in the subtracted images include image processing and the use of a higher exposure/image for the mask images.

Evaluation of these imaging modes is more complicated than for non-subtracted imaging. A phantom containing a blank mask is positioned in the FOV, the DSA is started and the blank mask removed and replaced by a detail plate containing objects or details of interest. Clearly, manipulation of the test objects in the primary beam and close to the presence of a scattering object must be done carefully.

A number of TIQ test objects are available for testing DSA modes. Leeds test objects supply the TO20 TCDD (Cowen, Haywood, et al., 1987; Cowen, Workman, et al., 1987), which has a similar layout and covers the same diameter ranges as TO10 and TO12 but can be used to test smaller contrasts, with 144 discs in total. The discs are not made from iodine or iodine simulating material. The Leeds test objects have linear and logarithmic step wedges for testing the accuracy and reproducibility of DSA system look up tables. The now defunct IEC standard 61223-3-3 described a DSA performance testing phantoms which are still produced e.g. X-Check DSA test object (PTW), QUART DSA phantom (QUART), Leeds DSA 8/54 test object (see Figure Appendix 2-3). The test object has a 57 mm thick PMMA body with a 10 mm slot for a 9.5 mm thick PMMA slider. This slider contains aluminium strips 10 mm in diameter with thicknesses of 0.05, 0.1, 0.2 and 0.4 mm, simulating



iodine contrast concentration of 5 to 10 mg/ml for vascular diameters of 1 to 4 mm. There is also a copper step wedge, with 7 steps from 0.2 to 1.4 mm Cu, to test dynamic range and the logarithmic look up table (LUT) applied in DSA mode. These test objects feature a pneumatic hand pump for safe movement of the mask and detail plates during the DSA run.



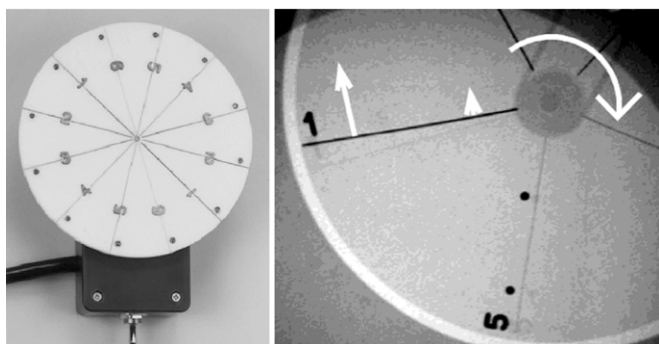
*Figure Appendix 2-2. Examples of DSA test objects designed to meet the previous IEC Standard IEC 61223-3-3 (left) Quartz (DE) DSA test object (right) PTW -Check DSA test object.*

Tests of DSA performance are currently not included in this QC protocol but may be added in the future. One could question the value of an explicit test of DSA modes, and whether these modes could be tested by applying a standard TIQ method to acquire a DSA sequence and then evaluating the images without applying the subtraction. A potential problem with this is that DSA modes tend to use a higher exposure/image, which means that system structured (fixed pattern) noise is multiplied more strongly into the image and this can limit the measured threshold contrast (Kume et al., 1986; Marshall et al., 2001). This could potentially bias the result and underestimate the TIQ score for the DSA modes. An explicit evaluation of a commonly used DSA mode especially given that aspects such as noise reduction and increased exposure/image for the mask could influence TIQ and eventually clinical image quality. Physicists can apply one of the four TCDD methods described (Section 4.1) however some of these methods have not been validated for DSA imaging. Furthermore, DSA modes typically operate at between 2 and 4 images/second, meaning that Methods 1 and 3, requiring the acquisition of 400 or 1000 images respectively, are not practical options.

### **Temporal/motion test objects**

Given that fluoroscopy and angiography devices are designed to image moving structures it is surprising that so few test objects have been designed and implemented to evaluate the dynamic performance of these systems. An exception is the work by Guibelalde et al ((Guibelalde et al., 2001, 2004; Kotre, Marshall and Guibelalde, 2005) where a programmable moving platform was used to study the influence of motion on test object scores in dynamic imaging systems. Difficulty in scoring a moving test object visually may account for the sparse work on this topic, as digital images were unavailable on early fluoroscopy units. A second problem is designing a test object with relevant motion and targets and relating the results to clinical performance, a problem with TIQ test objects in general.

A rotating spoke test object has been developed (Model L-629, Ludlum Medical Physics, USA), which is described for use in the NEMA XR-21 cardiac phantom (Balter et al., 2001). A circular acrylic disk of diameter ~14 cm contains 12 steel wires arranged in a spoke pattern at 30° intervals, along with 6 lead dots at the end of each wire. The wire diameters range from 0.13 mm to 0.56 mm. The disk is rotated at 30 revolutions per minute (RPM) in order to simulate the motion of guidewires etc. Details of how to evaluate the phantom are not given and there are no published papers reporting application of this test object or giving typical values.



*Figure Appendix 2-3. The Ludlum rotating spoke test object (left) An x-ray image of the test object showing the presence of lag (the lower, faint line next to Line 1 in this image) (Balter et al., 2001).*

Another option is to use a platform to move a test object at some velocity, a method that has been applied to the measurement of the MTF (Friedman and Cunningham, 2008; Dehairs et al., 2017; Monnin et al., 2021). Leeds Test Objects supply a moving platform (MOTUS) that can be programmed for speeds between 0 and 7.5 cm/s with a distance range of 5 cm.

This report does not describe an explicit assessment of the temporal imaging performance of fluoroscopy using test objects, however it is recognized that this is a very important aspect of system performance, especially for cardiac imaging systems. Updates of this work may include such an evaluation.



**EFOMP**

EUROPEAN FEDERATION OF ORGANISATIONS FOR MEDICAL PHYSICS

# QUALITY CONTROL OF DYNAMIC X-RAY IMAGING SYSTEMS

**EFOMP PROTOCOL**

VERSION 01. 2024